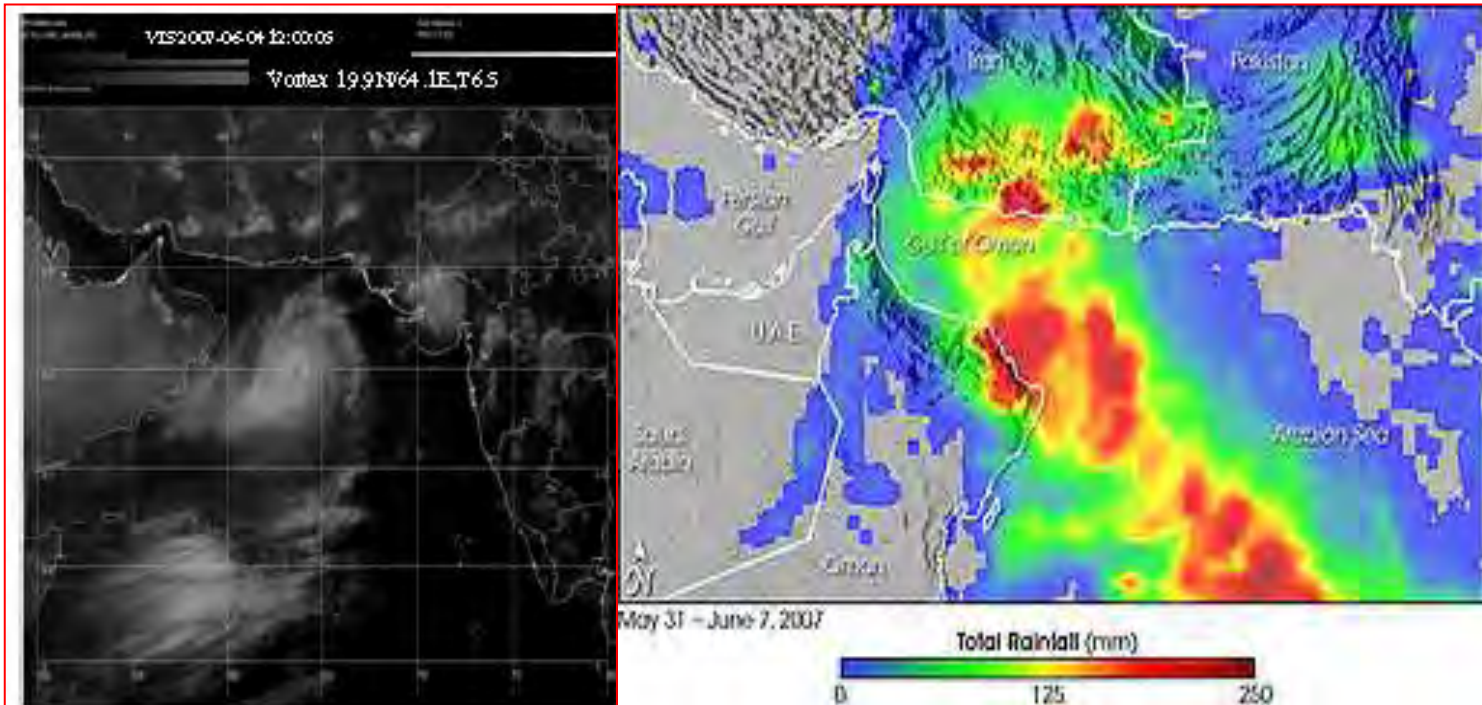




GOVERNMENT OF INDIA
INDIA METEOROLOGICAL DEPARTMENT

IMD MET. MONOGRAPH No:
CYCLONE WARNING DIVISION No. 08/2011

A Report on the Super Cyclonic Storm “GONU” during 1-7 June, 2007



Satellite imagery of „GONU’ for 04 June, 2007

Total rainfall around the gulf of Oman between
31 May and 7 June, 2007.

**AJIT TYAGI, B.K.BANDYOPADHYAY, M.MOHAPATRA,
SUMAN GOEL, NARESH KUMAR, A.B.MAZUMDAR, MEDHA KHOLE.**

CYCLONE WARNING DIVISION
OFFICE OF THE
DIRECTOR GENERAL OF METEOROLOGY
INDIA METEOROLOGICAL DEPARTMENT

NEW DELHI
FEBRUARY-2011

A Report on the Super Cyclonic Storm “GONU” during 1-7 June, 2007

**AJIT TYAGI,
B.K.BANDYOPADHYAY,
M.MOHAPATRA,
SUMAN GOEL,
NARESH KUMAR,
MEDHA KHOLE.
A.B.MAZUMDAR,**

CYCLONE WARNING DIVISION

**OFFICE OF THE
DIRECTOR GENERAL OF METEOROLOGY
INDIA METEOROLOGICAL DEPARTMENT
NEW DELHI**

PREFACE

First ever super cyclone "GONU" over the Arabian Sea (1-7 June 2007) crossed Oman coast near Muscat on 5 June as a very severe cyclonic storm. It then emerged into Gulf of Oman and had a second landfall over Iran on 6 June as a cyclonic storm. It was second landfalling cyclone over Iran after 1898. The system was mainly detected and tracked by satellite, as there was no radar along the Oman coast.. The intensity of the system remained unpredicted by most of the Numerical Weather Prediction (NWP) Models. It posed a challenge to the NWP and other conventional, synoptic and statistical methods to predict the intensity of such a super cyclone. Considering all the above mentioned characteristic features, a meteorological monograph has been brought out. Many features of the super cyclonic storm 'GONU' like genesis, intensification movement, landfall and disastrous weather have been discussed. The monitoring and prediction aspects of this cyclone by the synoptic and thermodynamic observations, satellite observations, dynamical parameters and NWP models and their limitations are examined and discussed. The grey areas requiring more research and investigation are highlighted. It will be useful in monitoring and forecasting and further research studies of such systems in future

Many research and observational inputs were received from Oman Meteorological Department and Satellite & Computer Division at IMD Head Quarter (HQ), which are highly appreciated and duly acknowledged. I also thank to Mr. M.G. Mittal, Mr. Kalu Ram, Mr. R.P. Sharma , Mr. D.P. Nayak and Mrs. Monica Sharma of Cyclone Warning Division for their valuable contribution to bring out this meteorological monograph on cyclone, „GONU’

February 2011

Ajit Tyagi

Director General of Meteorology

INDIA METEOROLOGICAL DEPARTMENT
DOCUMENT AND DATA CONTROL SHEET

1	Document title	A Report on the Super Cyclonic Storm "GONU" during 1-7 June, 2007
2	Document type	Technical Report
3	Issue No.	Cyclone Warning Division Report No. 8/2011
4	Issue date	21.02.2011
5	Security Classification	Unclassified
6	Control Status	Uncontrolled
7	Document type	Scientific Report
8	No. of Pages	83
9	No. Figures	35
10	No. of reference	60
11	Distribution	Unrestricted
12	Language	English
13	Authors	Ajit Tyagi, B. K. Bandyopadhyay M. Mohapatra, Suman Goel, Naresh Kumar, A. B. Mazumdar, Medha Khole,
14	Originating Division/Group	Cyclone Warning Division, New Delhi
15	Reviewing and Approving Authority	Director General of Meteorology, India Meteorological Department
16	End users	Operational Forecaster, Disaster Manager and Researcher
17	Abstract	The first ever super cyclone "GONU" over the Arabian Sea (1-7 June 2007) crossed Oman coast near Muscat on 5 June as a very severe cyclonic storm. It then emerged into Gulf of Oman and had a second landfall over Iran on 6 June as a cyclonic storm. It was second landfalling cyclone over Iran after 1898. The system was mainly detected and tracked by satellite, as there was no radar along the Oman coast.. The intensity of the system remained unpredicted by most of the Numerical Weather Prediction (NWP) Models. It posed a challenge to the NWP and other conventional, synoptic and statistical methods to predict the intensity of such a super cyclone. Considering all the above mentioned characteristic features, a meteorological monograph has been brought out. Many features of the super cyclonic storm 'GONU' like genesis, intensification movement, landfall and disastrous weather have been discussed. The monitoring and prediction aspects of this cyclone by the synoptic and thermodynamic observations, satellite observations, dynamical parameters and NWP models and their limitations are examined and discussed. The grey areas requiring more research and investigation are highlighted. It will be useful in monitoring and forecasting and further research studies of such systems in future
18	Key words	Tropical Cyclone, Gonu, Track, Intensity, Landfall, Arabian Sea

CONTENTS

	Page No.
Abstract	1
1. Introduction	2-6
2. Life history of cyclone “GONU”	6
3. Weather and damage due to cyclone „GONU’ in	6-9
3.1. Oman	6-8
3.2. Iran	8-9
4. Data and Methodology	9-11
4.1 Synoptic and thermodynamic observations	10
4.2 Dynamical parameters	10
4.3 Satellite imageries and its derived products.	10
4.4 Performance of NWP models	10
4.5 Climate change aspects	11
5 Results and discussion	11-60
5.1 Synoptic features	12-22
5.2 Dynamical parameters	22-32
5.3 Thermodynamic Parameters:	32-38
5.4 Satellite observed features	39-60
6. Features observed through other satellites	61-63
7. Performance of dynamical and statistical models	63-65
8. Performance of RSMC, New Delhi	65-68
9. Climate Change aspects	68-77
9.1 Cyclonic disturbances landfalling over Arabia-Africa:	69-70
9.2 Interannual and Interdecadal variation	70-73
9.3 Current Understanding of the Impact of Climate Change on Tropical Cyclone Activity	74-76
9.4. Scenario over the north Indian Ocean	76-77
10. Conclusions and suggestions	77-78
Acknowledgements	79
References	79-82

ABSTRACT

The super cyclonic storm "GONU" (1-7 June 2007) developed over the Arabian Sea during onset phase of the southwest monsoon. It first crossed Oman coast near Muscat on 5 June as a very severe cyclonic storm caused loss of lives and properties due to heavy rain leading to flood, gale wind leading to structural damages and storm surge leading to coastal inundation and flooding. This cyclone was very unique in its nature as it was the first ever super cyclone over the Arabian Sea as per the recorded history of India Meteorological Department (IMD). After its landfall over Oman, it emerged into Gulf of Oman, moved in northwesterly direction had a second landfall over Iran on 6 June as a cyclonic storm. It was second landfalling cyclone over Iran after 1898. It also caused loss of lives and properties in Iran. The system was mainly detected and tracked by satellite, as there was no radar along the Oman coast. The genesis and movement of this cyclone though could be predicted by various numerical weather prediction models with reasonable accuracy. However, the intensity of the system remained unpredicted by most of the models. It posed a challenge to the NWP modelling and other conventional, synoptic and statistical methods to predict the intensity of such a super cyclone though the super cyclone intensity was short.

Considering all the above mentioned characteristic features, a meteorological monograph has been brought out. Many features of the super cyclonic storm 'GONU' like genesis, intensification movement, landfall and associated disastrous weather analysis have been discussed. The monitoring and prediction aspects of this cyclone by the synoptic and thermodynamic observations, satellite observations, dynamical parameters and numerical weather prediction models and their limitations have been critically examined and discussed. The critical grey areas requiring more research and investigation have been highlighted. The augmentation in observational network and types of observations required to monitor and predict such systems are also suggested in this meteorological monograph. It will be useful not only in monitoring and forecasting of such systems in future but also for taking up further research studies.

Key Words: Tropical cyclone, Gonu, north Indian Ocean, Track, Intensity

1. Introduction

A super cyclonic storm, „**GONU**’ developed over the Arabian Sea during 1-7 June 2007. The maximum wind speed associated with the storm was 127 knots. A comparison of the most powerful tropical cyclones developing over different Ocean basins is given below:

Ocean basin:	Cyclone	Lowest estimated central pressure (ECP)
Arabian Sea:	Cyclone GONU (2007)	920 hPa
Bay of Bengal:	Orissa cyclone (1999)	912 hPa
Northeast Pacific:	Hurricane LINDA (1997)	902 hPa
North central Pacific:	Hurricane LOKE (2006)	915 hPa
South Pacific:	Cyclone ZOE (2002)	890 hPa
West Pacific:	Typhoon TIP (1979)	870 hPa
Southwest Indian Ocean:	Cyclone GAFILO (2004)	895 hPa
Australia:	Cyclone LNIGO (2003)	900 hPa
North Atlantic:	Hurricane WILMA (2005)	882 hPa

It indicates that Arabian Sea generally experiences less intense cyclone compared to other Ocean basins. Compared with the most intense cyclone over the Bay of Bengal, cyclone **GONU**’ was slightly less intense than Orissa Supper Cyclone of October 1999.

The system caused loss of life and property in Oman and Iran due to heavy rainfall, strong winds and storm surge. Gale winds with speed of 100 kmph were recorded at Muscat at the time of landfall. About 50 persons died and estimated damage to property was about \$4.2 billion in Oman. The number of human deaths was 28 and loss of property was \$ 215 million over Iran. The special features of **GONU**’ are as follows:

- It was the first ever super cyclonic storm developed over the Arabian Sea as per recorded history of IMD (2008).
- The maximum intensification of the system took place between 1500 UTC of 03 June and 1500 UTC of 04 June where the T-number changed from 3.5 (severe cyclonic storm) to 6.5 (super cyclonic storm). The 24 hours change in T number during this period was 3.0 against the normal rate of intensification of T 1.0 Hence, it was a rapidly intensifying cyclone.
- The super cyclone intensity lasted for a few hours (6 hours during 1500 to 2100 UTC of 04 June 2007) as the system gradually weakened from 2100 UTC of 04 June even though the system was over the sea.
- The super cyclonic storm, **GONU** made two landfalls first over Oman and the second over Iran. This was the second landfalling cyclonic storm for Iran after 4 June 1898 (IMD, 2008).

The system was mainly detected and tracked by satellite, as there was no radar along Oman coast. At present, IMD utilises the Dvorak technique of subjective assessment based on satellite (Dvorak, 1975, 1984) and environmental conditions for estimating the intensity. Some kind of check lists have been devised to work out the likely intensity changes (IMD, 2003). Higher sea surface temperatures (SSTs) (more than 26.5°C), a deep lower level moist layer, absence of strong vertical wind shear, increase in vorticity over the area, are favourable criteria for intensification of a tropical low to a cyclonic storm and further intensification (Gray, 1992 and Frank, 1977). The satellite based monitoring and prediction of intensification were reviewed by Kelkar (1997) and further updated by Kalsi (2006) and Bhatia et al., (2006). According to them, new developments like derivation of cyclone parameters in terms of ocean surface wind fields by scatterometer more frequently and rapid scan observations by the satellites, use of water vapour imagery with better resolutions and other derived products like outgoing Long wave Radiation (OLR) can immensely help in not only monitoring and prediction of intensity but also in improving the Numerical Weather Prediction (NWP) model performance. According to Shea (2009), the depth of thermocline layer and hence the ocean thermal energy play a dominant role for intensification. According to him, ocean thermal energy of more than 100 KJ in the thermocline layer is favourable for intensification into a very severe cyclonic storm. The detailed review of the synoptic and thermodynamic characteristics associated with the intensification/decay of the cyclonic storm over the north Indian Ocean are presented by Krishna Rao (1997). The review of the dynamical characteristics of intensification is given by Mohanty and Gupta (1997). A review of the prediction of tropical cyclone characteristics by NWP models is presented by Prasad (1997) and has been updated by Rama Rao et. al (2007). However, the intensity change at present is not properly captured in the NWP models (Rama Rao, et al., 2007). The genesis and movement of the cyclone **GONU** though could be predicted by various NWP models, with reasonable accuracy, the intensity of the system remained unpredicted by most of the models. It posed a challenge to the NWP modelling as well as other conventional, synoptic and statistical methods to predict the intensity accordingly though the period of super cyclone intensity was short. Further, in view of the development of first ever super cyclone, **GONU** over the Arabian Sea, questions were raised about likely impact of climate change on tropical cyclone over the Arabian Sea.

Considering all the above, an in-depth study has been undertaken to analyse various features of the super cyclonic storm, **GONU** like genesis, intensification, movement, landfall and associated disastrous weather. The monitoring and prediction aspects of this cyclone by the synoptic and thermodynamic observations, satellite observations, dynamical parameters and numerical weather prediction models and their limitations have been critically examined and discussed. The critical grey areas requiring more research and investigation have been highlighted. A brief life history and damages due to the cyclonic storm, **GONU** are presented in section 2 and 3 respectively. The data and method of analysis used in the study are discussed in section 4. The results

and discussions are presented in section 5. The broad conclusions and suggestions are presented in section 6.

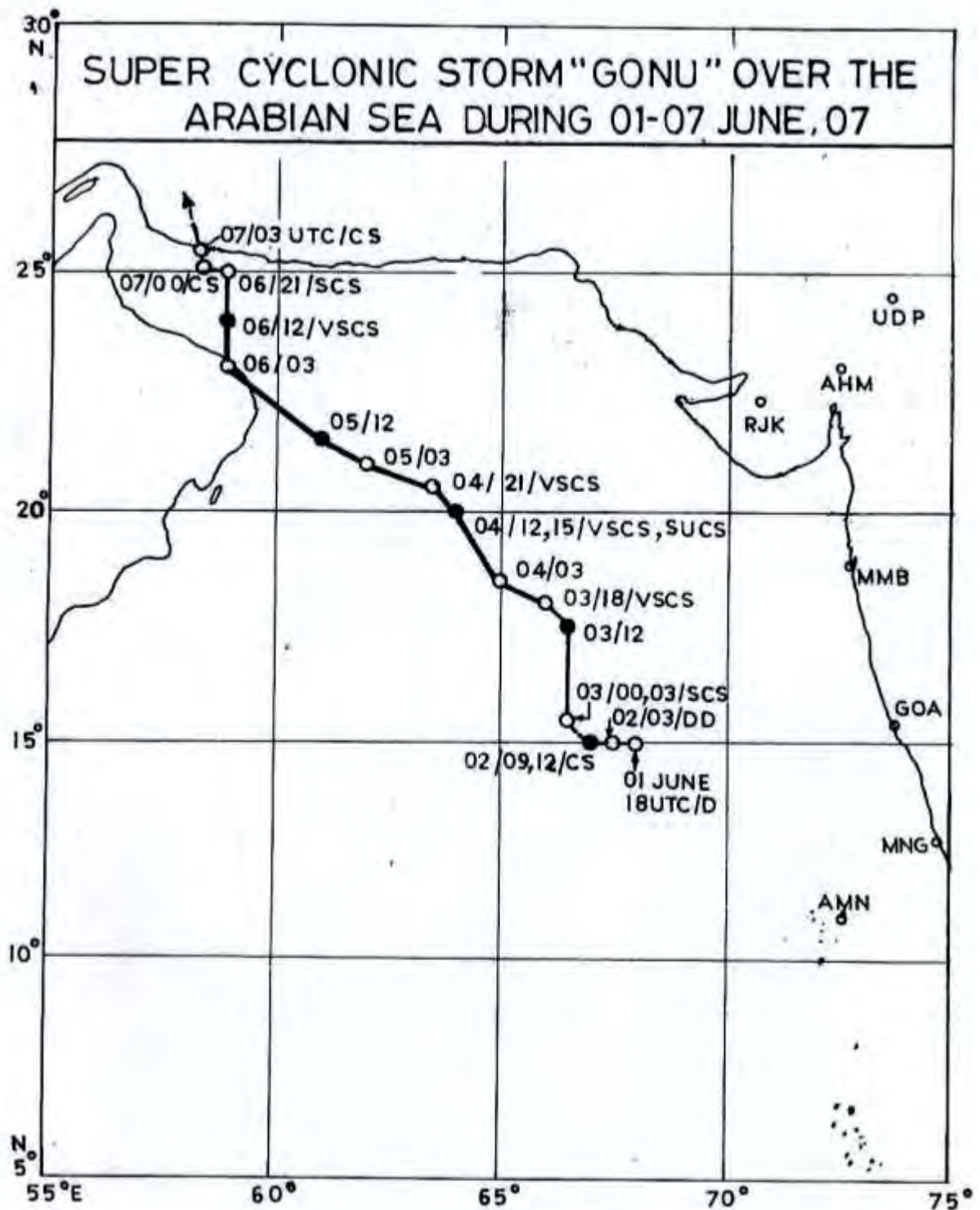


Fig.1. Track of super cyclonic storm "GONU"

Table-1: Best track positions and other parameters of Super cyclonic storm “GONU” over the Arabian Sea during 01-07, June 2007

Date	Time (UTC)	Centre lat. ^o N/ long. ^o E	C.I. No.	Estimated Central Pressure (hPa)	Estimated Maximum Sustained Surface Wind (kt)	Estimated Pressure drop at the Centre (hPa)	Grade
01-06-2007	1800	15.0/68.0	1.5	1002	25	4	D
	2100	15.0/68.0	1.5	1002	25	4	D
02-06-2007	0000	15.0/68.0	1.5	1002	25	4	D
	0300	15.0/67.5	2.0	1000	30	5	DD
	0900	15.0/67.0	2.5	998	35	8	CS
	1200	15.0/67.0	3.0	992	45	10	CS
	1500	15.0/67.0	3.0	992	45	10	CS
	1800	15.0/67.0	3.0	992	45	10	CS
	2100	15.0/66.5	3.0	992	45	10	CS
03-06-2007	0000	15.5/66.5	3.5	988	55	16	SCS
	0300	15.5/66.5	3.5	988	55	16	SCS
	0600	16.0/66.5	3.5	988	55	16	SCS
	0900	16.5/66.5	3.5	988	55	16	SCS
	1200	17.5/66.5	3.5	988	55	16	SCS
	1500	17.5/66.5	3.5	988	55	16	SCS
	1800	18.0/66.0	4.0	980	65	22	VSCS
	2100	18.0/66.0	4.0	980	65	22	VSCS
04-06-2007	0000	18.5/65.0	4.5	974	77	30	VSCS
	0300	18.5/65.0	5.0	960	90	40	VSCS
	0600	19.0/64.5	5.5	952	102	52	VSCS
	0900	19.5/64.5	6.0	934	115	66	VSCS
	1200	20.0/64.0	6.0	934	115	66	VSCS
	1500	20.0/64.0	6.5	920	127	80	SUCS
	1800	20.5/63.5	6.5	920	127	80	SUCS
	2100	20.5/63.5	6.0	935	115	66	VSCS
05-06-2007	0000	20.5/63.0	6.0	936	115	66	VSCS
	0300	21.0/62.0	6.0	936	115	66	VSCS
	0600	21.5/61.5	5.5	950	102	52	VSCS
	0900	21.5/61.0	5.5	950	102	52	VSCS
	1200	21.5/61.0	5.0	960	90	40	VSCS
	1500	22.0/61.0	4.5	970	77	30	VSCS
	1800	22.0/60.5	4.5	970	77	30	VSCS
	2100	22.5/60.5	4.5	970	77	30	VSCS
06-06-2007	0000	22.5/59.5	4.5	970	77	30	VSCS
	VSCS crossed northeast Oman coast near Muscat between 0200-0300 UTC of 6 June.						
	0300	23.0/59.0	4.5	970	77	30	VSCS
	0600	23.5/59.5	4.5	970	77	30	VSCS
	0900	23.5/59.5	4.5	970	77	30	VSCS
	1200	24.0/59.0	4.5	970	77	30	VSCS

	1500	24.0/59.0	4.5	970	77	30	VSCS
	1800	24.5/59.0	4.0	978	65	22	VSCS
	2100	25.0/59.0	3.5	984	55	16	SCS
07-06-2007	0000	25.0/59.0	3.0	988	45	10	CS
	0300	25.5/58.5	3.0	988	45	10	CS
	The cyclonic storm crossed Makaran (Iran) coast near Lat. 58.0 ⁰ E between 0300 - 0400 UTC of 7 June.						

2. Life history of cyclone “GONU”

Cyclone **-GONU**” developed from a low pressure area over eastcentral Arabian Sea on 31 May 2007 in association with the southwest monsoon surge. It concentrated into a depression over the same area and then into a cyclonic storm **-GONU**” at 1200 UTC of 1 June. Thereafter, it moved in a north-northwesterly direction and intensified into a severe cyclonic storm at 0300 UTC and a very severe cyclonic storm at 1800 UTC of 3 June. It further intensified into a super cyclonic storm at 1500 UTC of 4 June. Thereafter, it moved in a west-northwesterly direction and started weakening gradually due to relatively colder SST and increasing vertical wind shear. It crossed Oman coast near lat. 22.5⁰N as a very severe cyclonic storm between 0200-0300 UTC of 6 June. After crossing Oman coast, it emerged into the Gulf of Oman, weakened gradually and moved in a north-northwesterly direction. It made second landfall over Iran coast near long. 58.5⁰ E between 0300 and 0400 UTC of 7 June as a cyclonic storm. Moving in the same direction, it weakened gradually and it was seen as a well marked low pressure area over Iran and neighbourhood on 8 June 2007. The track of the system is shown in Fig. 1. The best track parameters are shown in Table-1 (RSMC, 2008).

3. Weather and damage due to cyclone „GONU’

3.1. Oman

About seven hours before passing near the northeastern Oman coastline, Cyclone **GONU**’ began affecting the country with strong winds and heavy precipitation, with rainfall totals reaching 610 mm (24 inches) near the coast. The rainfall in the region is shown in Fig 2.. The estimated wind and wave height are shown in Fig.3

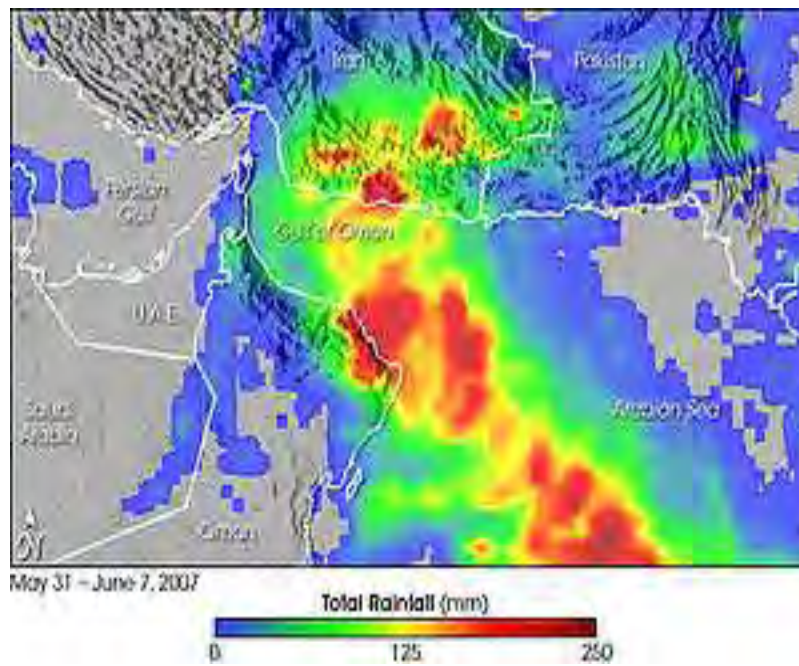


Fig.2 Total rainfall around the gulf of Oman between 31 May and 7 June, 2007.

The red areas show where rainfall exceeded 200 mm (8 inches).

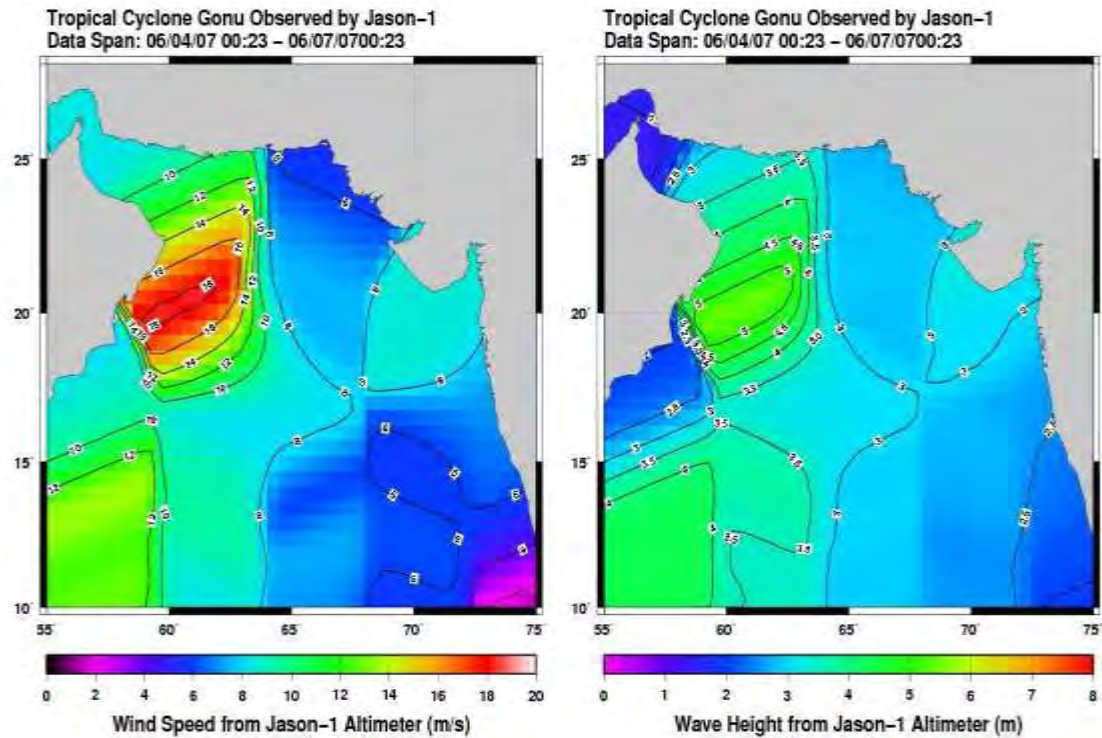


Fig.3. Estimated wind speed and wave height in association with cyclone, GONU

GONU produced strong waves along much of the coastline,http://en.wikipedia.org/wiki/Cyclone_Gonu - cite note-gn60507-48 leaving many coastal roads flooded. Strong winds knocked out power and telephone lines across the eastern region of the country, leaving thousands isolated until the lines were repaired. The cyclone caused extensive damage along the coastline, including the city of Sur and the village of Ras al Hadd at the easternmost point of the Omani mainland. In Muscat, winds reached 100 km/h (62 mph) and uprooted electrical poles, leaving the capital city without power. Strong waves and heavy rainfall flooded streets and some buildings. The liquefied natural gas terminal in Sur, which handles 10 million tonnes of gas each year, was badly hit by the storm and could not be operated. According to the Oman News Agency, the cyclone killed 49 people in the country. Around 20,000 people were affected, and damage in the country was estimated at around \$4 billion (2007 USD), ranking it as the worst natural disaster on record in Oman. The Muscat International Airport reopened after three days of closure. The production of desalinated water was interrupted, as both of Oman's desalination plants failed. The first, Ghubrah, lost supplies of natural gas, halting production; while the second, Barka, sustained damaged switchgear due to flooding. These plants provide water to Muscat's 631,000 residents and surrounding areas. The country lost an estimated \$200 million (2007 USD) in oil exports.http://en.wikipedia.org/wiki/Cyclone_Gonu - cite note-61 The waves in the coastline were reported to be 10 m (32 ft) high, which destroyed about a dozen fishing boats. About 300 boats were moved from the water or emptied of equipment, and overall damage to the port of Fujairah was reported as severe. The port of Fujairah reopened on June 7. A boat sank near the port of Fujairah, leaving its ten passengers missing.

3.2. Iran

Upon striking Iran, **GONU** caused moderate to heavy rainfall, including 74 mm (2.91 inches) in the city of Chabahar. Winds reached 111 km/h in gust which caused power outages and damaged some homes made of clay; the power outage led to some fires across the city of Chabahar. The rainfall flooded at least 40 houses, and resulted in the temporary closure of several major roads. Cyclone **GONU** produced a storm tide of 2 m (6.5 ft) in some locations, with many homes near the coastline receiving damage. In Bandar-e-gaz, heavy rainfall overflowed a river, killing three people in a vehicle caught in the water. Flooding from the rainfall also destroyed a dam in Nikshahr County. Throughout the country, the cyclone caused 23 deaths, including 20 from drowning; damage in Iran was estimated at 2 billion (IRR)/ \$216 million (USD). Some photographs (Fig 4a and 4b) show the devastation due to GONU in Muscat



Fig. 4(a) Damage in Muscat in association with cyclone „GONU’



Fig.4(b) Damage in Muscat in association with cyclone „GONU’

4. Data and Methodology

To analyse various characteristics of **GONU**, the best track data of RSMC, New Delhi (RSMC, 2008) have been considered. The system was tracked by

INSAT and hence all the INSAT observations and derived satellite products have been considered to analyse the characteristics of the system. In addition, the synoptic analyses and NWP model analyses available from different centres have been considered. The genesis, intensification, movement and dissipation of the super cyclonic storm, **GONU**, are analysed by considering the synoptic, thermodynamic & dynamic parameters during 30 May to 7 June 2007. The details of the data used and the methodology are discussed in Sec. 4.1-4.5.

4.1 Synoptic and thermodynamic observations

The following synoptic and thermodynamic parameters over Indian Region are analysed to find out the capability of synoptic and thermodynamic parameters to monitor and predict genesis, intensification/decay and movement of super cyclone, **GONU**:

- (i) Mean sea level pressure and geopotential thickness
- (ii) 24-hours pressure change
- (iii) Pressure departure from normal
- (iv) Surface and upper air winds
- (v) Sea Surface temperatures
- (vi) Relative humidity, moisture flux and precipitable water

4.2 Dynamical parameters

The following dynamical parameters during 30 May to 7 June 2007 are analysed based on LAM analysis of IMD:

- (i) Relative vorticity and vorticity advection
- (ii) Convergence/divergence
- (iii) Vertical wind shear of horizontal wind
- (iv) Vertical velocity

4.3 Satellite imageries and its derived products.

The characteristics of the cyclone, **-GONU** are analysed by hourly INSAT imageries and derived products during 30 May – 7 June, 2007. The monitoring and prediction capabilities of satellite technique in the case of such a super cyclone are verified by analyzing the following:

- (i) INSAT- Kalpana-I imageries
- (ii) Cloud top temperatures
- (iii) Cloud motion vectors in lower, middle and upper troposphere
- (iv) Water vapour derived winds
- (v) Outgoing long wave radiation (OLR)
- (vi) Quantitative Précipitation Estimate (QPE)

4.4 Performance of NWP models

IMD operationally runs three regional models, Limited Area Model (LAM), MM5 model and Quasi-Lagrangian Model (QLM) for short range prediction. The

MM5 model is run at the horizontal resolution of 45 km with 23 sigma levels in the vertical and the integration is carried up to 72 hours over a single domain covering the area between lat. 30 ° S to 45 ° N long. 25 ° E to 125 ° E. Initial and boundary conditions are obtained from the NCEP Global Forecast System (NCEP GFS) readily available on the Internet at the resolution of 1 ° x1 ° lat./long. The boundary conditions are updated at every six hours interval. The LAM is integrated up to 48 hours at the horizontal resolution of 0.75 ° x0.75 ° lat/long with 16 sigma levels in the vertical over the same domain using the initial and boundary conditions provided by T-80 Global operational model run at NCMRWF. The model is also made flexible to run with NCEP GFS outputs as initial and boundary conditions. The QLM model (resolution 40 km, 18 levels) is used for cyclone track prediction in case of cyclone situation in the Arabian Sea or Bay of Bengal. IMD also makes use of NWP products prepared by some other operational NWP Centres like, National Centre for Medium Range Weather Forecasting (NCMRWF) T-254 model, European Centre for Medium Range Weather Forecasting (ECMWF) , United Kingdom Met Office (UKMO model) etc. The performance of all the available NWP models have been verified and discussed.

4.5 Climate change aspects

To study the climate change aspect, the data on frequency, intensity and track of cyclone over the Arabian Sea has been collected from cyclone e-Atlas developed by IMD (2008). For the purpose of analysis, depression and deep depression have been considered as a single category. Similarly severe cyclonic storm, very severe cyclonic storm and super cyclonic storm have been considered as a single category. Hence, the frequencies of cyclonic disturbances have been analyzed in three categories, viz (1) depression/deep depression (D), (2) cyclonic storm (C) and (3) severe cyclonic storm and above (S). The annual and decadal average, coefficient of variation (CV) and linear trend coefficients of the frequencies of above categories of cyclonic disturbances have been calculated and analyzed. Also, the annual average and linear trend coefficients of the total frequencies of cyclonic storms (C+S) and total cyclonic disturbances (D+C+S) have been analyzed. The trend in the track of cyclonic disturbances moving towards Arabia- Africa has also been analysed.

5. Results and discussion

The synoptic observations and various weather charts are analysed and presented in section. 5.1. The analysis of various dynamical parameters are presented and discussed in section 5.2. The thermo-dynamical parameters are analysed and discussed in section 5.3. The Satellite observations are presented in section 5.4. The various NWP model forecasts are analysed and presented in section 5.5. The verification of operational forecasts issued by RSMC, New Delhi is presented in section 5.6. The climate change aspects in view of development

of first ever super cyclone, **GONU** over the Arabian Sea is analysed and discussed in section 5.7.

5.1 Synoptic features

The mean sea level pressure and surface wind are presented and discussed in section 5.1.1. The 24-hours pressure change and pressure departure from normal are analysed and presented in section 5.1.2. The upper winds over Indian region are analysed and discussed in section 5.1.3. The LAM analysis of pressure, wind and geopotential heights are presented and discussed in section 5.1.4.

5.1.1. Mean Sea Level Pressure and Surface Wind

The characteristics of outer core circulation and the radius of the outer most closed isobars are generally considered for estimating suggest the intensity of a cyclone. Filling cyclones are seen to have a larger and a stronger outer core circulation. According to Weatherford and Gray (1988), both these measures are poorly related to intensity. However, as the data from ships of opportunity and the Buoy data were very meagre during the life period of **GONU**, the outer core circulation could not be properly estimated. But the coastal observations indicated the formation of a low pressure area over eastcentral Arabian Sea on 31 May, in association with an active east-west shear zone.

The shape of **GONU** was almost circular through out its life period except on a few occasions when it was elliptical. Based the radii of outer most closed isobar, the size of **GONU** has been estimated and same is given in Table -2. From the Table it is found that the size of GONU varied between 500 to 900 km. It was maximum (911 km) during the Super cyclone stage.

Table -2: Estimated size of cyclone ,GONU'

Date	Time (UTC)	Position of outermost Isobar ($^{\circ}$ N/ $^{\circ}$ S)	Distance between a & b, c & d (km)	Average (km)
2.6.07	12	a. 17.8/67.0	644	644
		b. 12.0/67.0		
		c. 15.0/64.0	644	
3.6.07	03	a. 15.5/63.1	750	736
		b. 15.5/70.1	722	
		c. 18.7/66.5		
	12	d.12.2/66.5	522	499
		a. 15.9/64.9		
		b. 19.5/68.5	477	
		c. 18.8/64.7		
		d.16.5/68.5		

4.6.07	03	a. 22.5/61.5 b. 17.3/66.8	800	671
		c. 20.5/66.5 d. 16.9/63.0	544	
	12	a. 23.0/61.5 b. 16.0/66.0	909	911
		c. 22.5/66.0 d. 17.0/60.0	913	
5.6.07	03	a. 23.8/62.0 b. 18.4/62.0	600	637
		c. 21.0/65.0 d. 21.0/58.5	674	
	12	a. 24.8/61.0 b. 18.8/61.0	667	618
		c. 21.5/63.8 d. 21.5/58.3	569	
6.6.07	03	a. 24.5/59.0 b. 20.2/58.5	481	445
		c. 23.0/61.0 d. 23.0/57.0	409	
	12	a. 26.0/60.0 b. 18.5/57.5	872	689
		c. 23.0/62.2 d. 24.5/57.0	506	
7.6.07	03	a. 29.5/59.0 b. 24.0/58.5	613	524
		c. 27.0/61.0 d. 27.0/56.0	435	
		Average		637

5.1.2. Upper winds

The upper winds based on synoptic observations over the region for the three representative levels of 500 and 200 hPa are shown in Fig.5. Like the isobaric analysis, the wind pattern at 850 hPa suggested the existence of an active east-west shear zone in lower tropospheric levels (not shown). The associated cyclonic circulation extended upto mid-tropospheric levels from 30 May 2007 onwards. The coastal winds suggested gradual intensification of the system from 0000 UTC to 1200 UTC of 30 May. The associated cyclonic circulation extended upto mid-tropospheric level. The system lay to the south but close to the ridge throughout its life period. It also interacted with the environment as the upper tropospheric ridge moved northwards with northward movement of the system. According to Srinivasan and Ramamurthy (1973), as the storm reaches sub-tropical ridge line, the westward movement of the storm slows down. According to their study, in 80% of the occasions, the storm moves in a

west-northwesterly direction, if it is 3° or more to the south of the ridge line. When the centre is near the ridge line, there is a pre-pondered northerly motion. Hence, the cyclone “**GONU**” moved according to the steering concept endorsing the earlier findings. The study further confirms that the steering current is represented by the wind flow over the storm area at a sufficiently higher level where the storm circulation disappears.

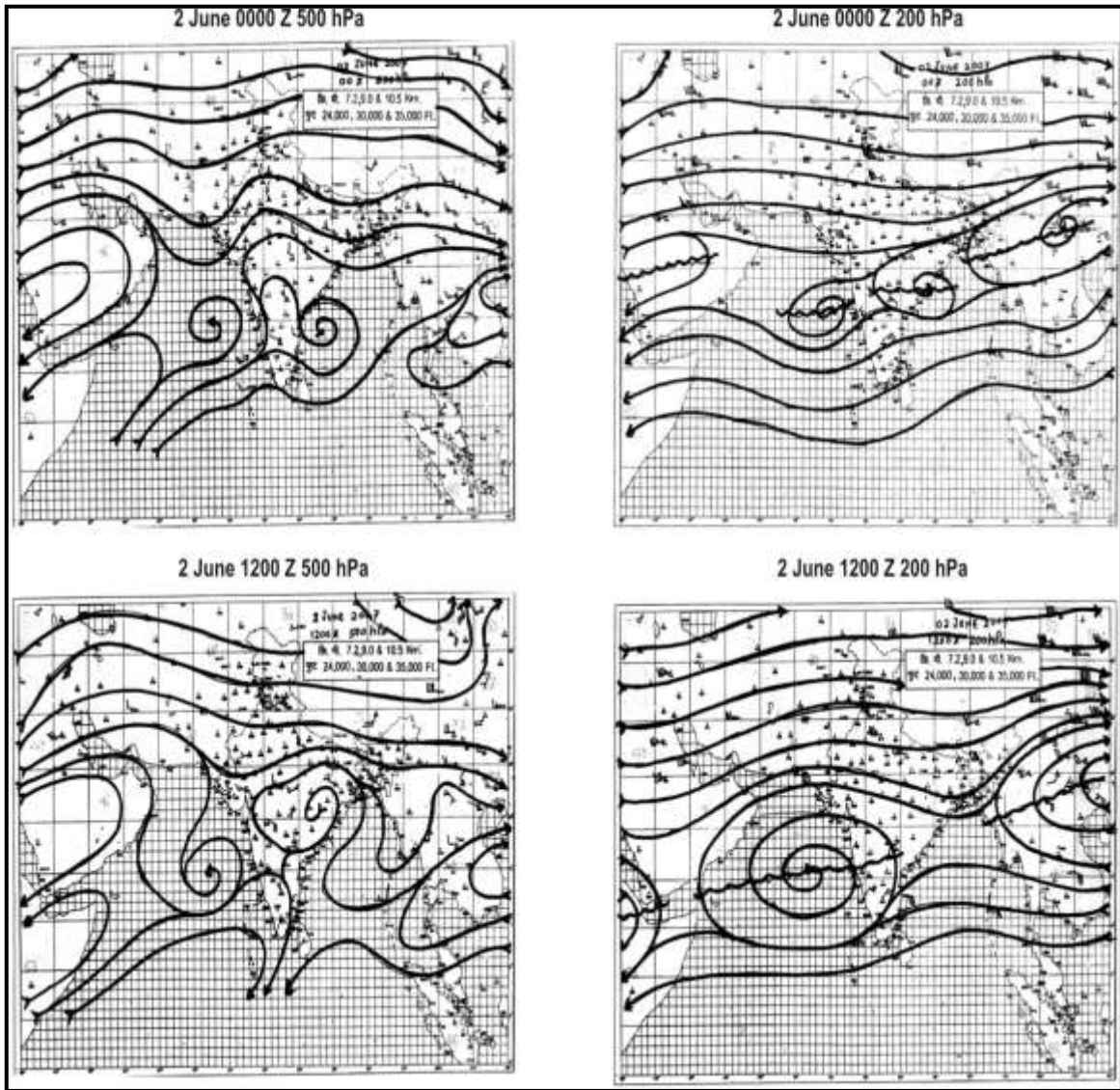


Fig 5(a) Stream line analysis of 500 and 200 hPa levels at 0000 and 1200 UTC of 2 June, 2007.

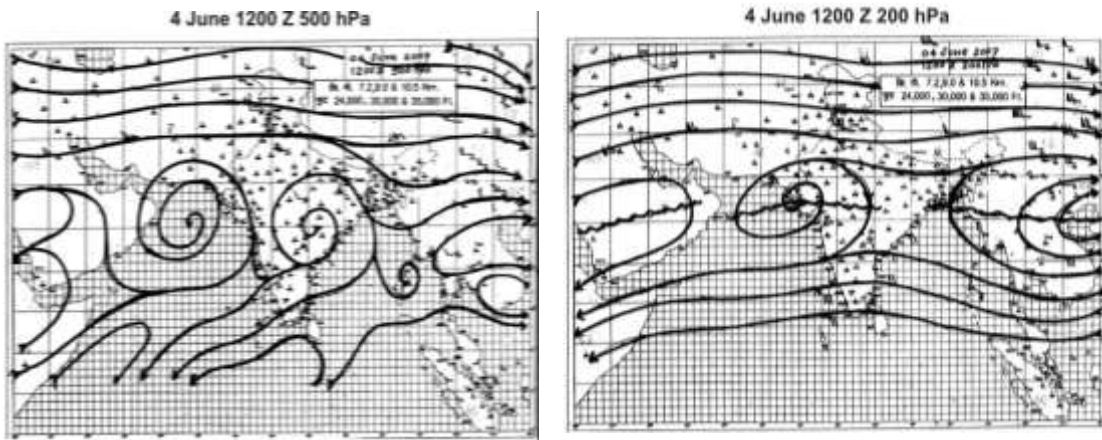


Fig. 5(b) Stream line analysis of 500 and 200 hPa levels at 1200 UTC of 4 June, 2007.

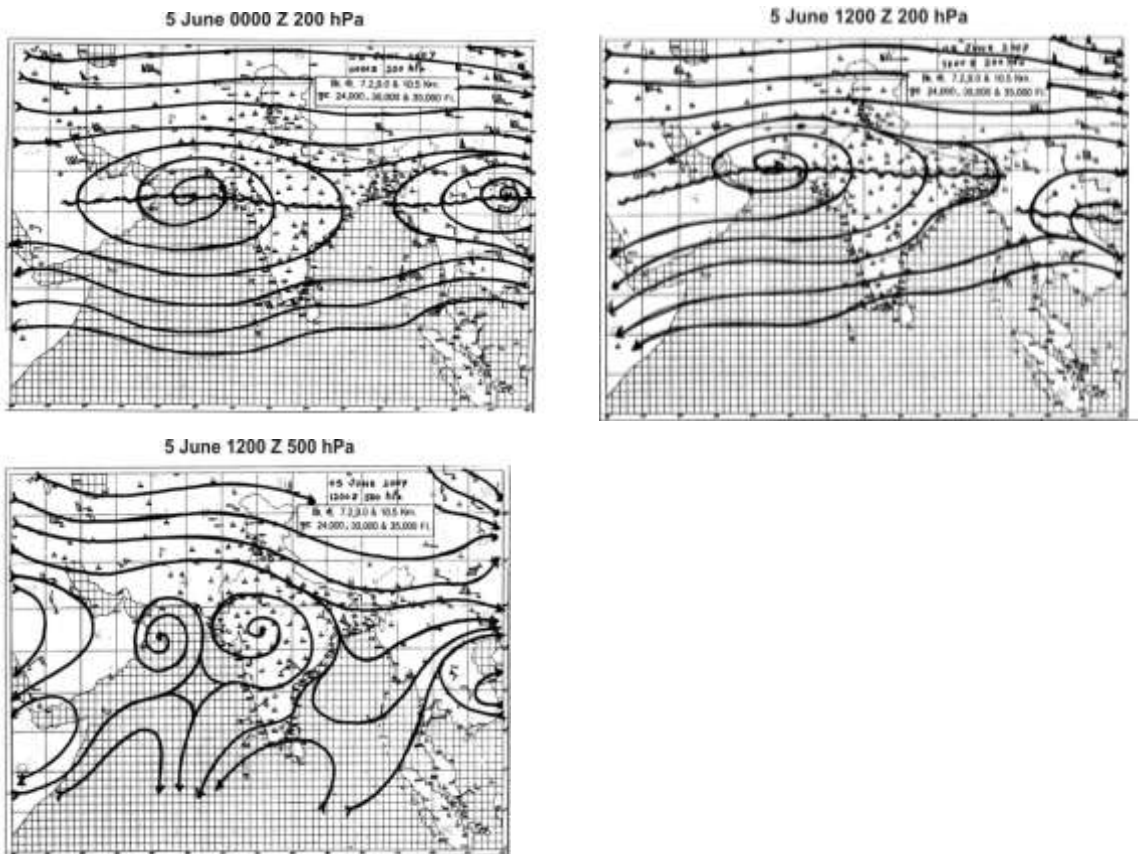


Fig. 5(c) Stream line analysis of 500 and 200 hPa levels at 0000 & 1200 UTC of 5 June, 2007.

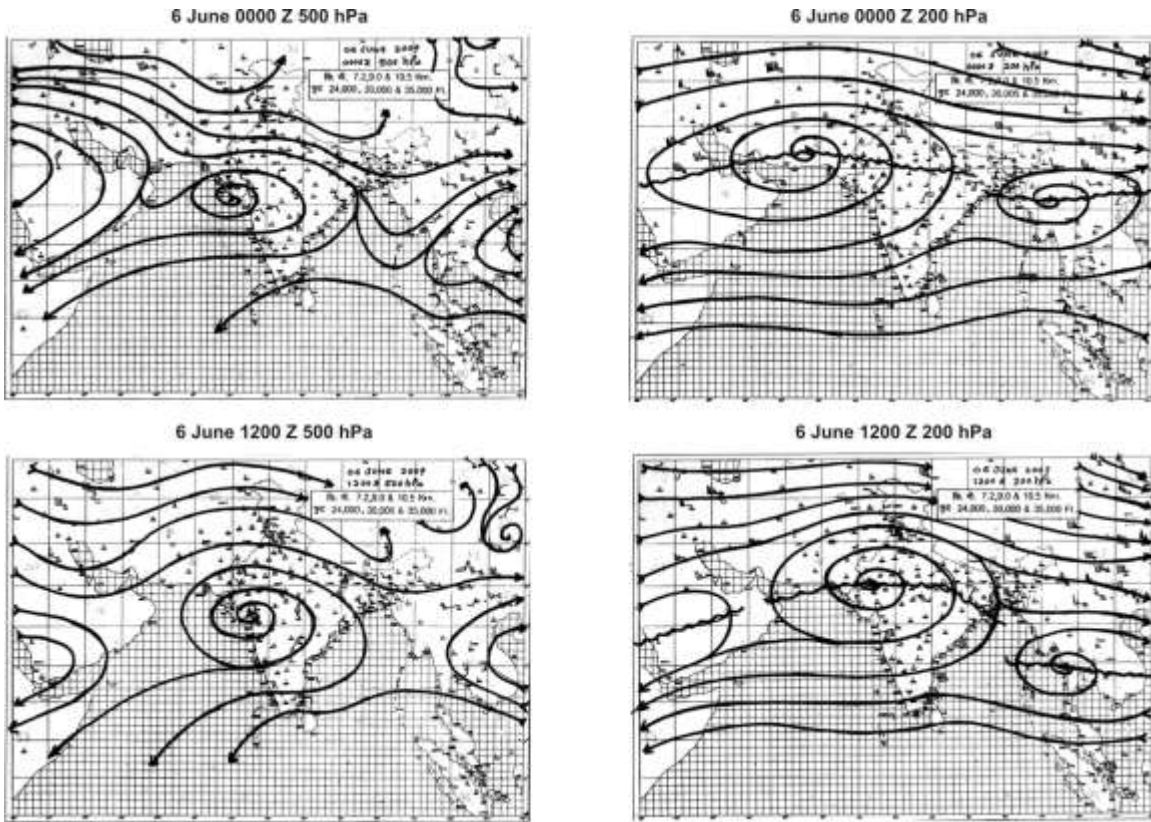


Fig. 5(d) Stream line analysis of 500 and 200 hPa levels at 0000 & 1200 UTC of 6 June, 2007.

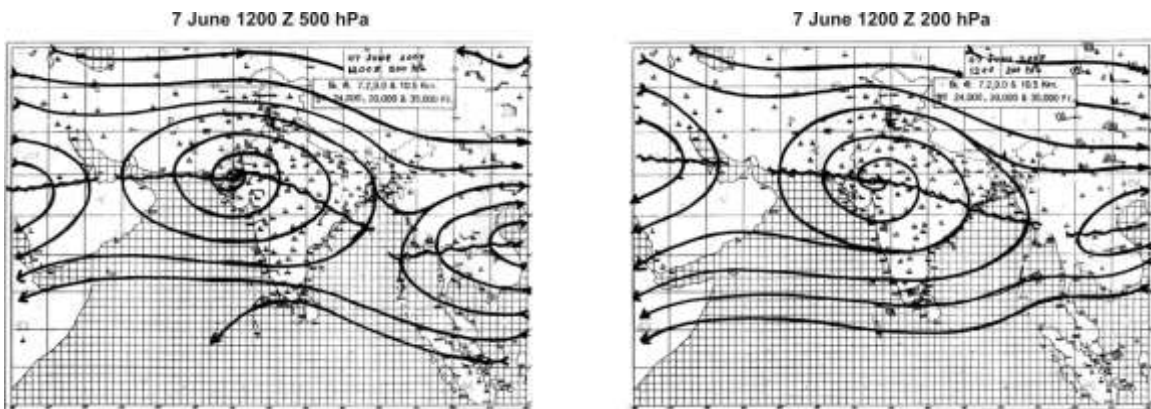


Fig. 5(e) Stream line analysis of 500 and 200 hPa levels at 1200 UTC of 7 June, 2007.

5.1.3 LAM analysis of pressure and wind:

The mean sea level pressure and wind at three representative levels of 850, 500 and 200 hPa at 0000 UTC of 30 and 31 May 2007 are shown in fig.6&7. As per IMD criteria, the system lay as an extended low pressure area at 0000 UTC of 30 and as a well marked low at 0000 UTC of 31 May. The cyclonic circulation extended upto mid-tropospheric levels prior to genesis. The wind speed was about 10 knots at 850 hPa level. Considering upper tropospheric wind at 200 hPa level, the ridge line lay to the north but close to of the circulation centre suggesting north-northwestward movement of the system. Hence, the analysis fields of the LAM clearly reflected the genesis, and movement of the system with reduced intensity. The discrepancies in the LAM analysis are primarily due to the sparse data assimilation over the cyclone region.

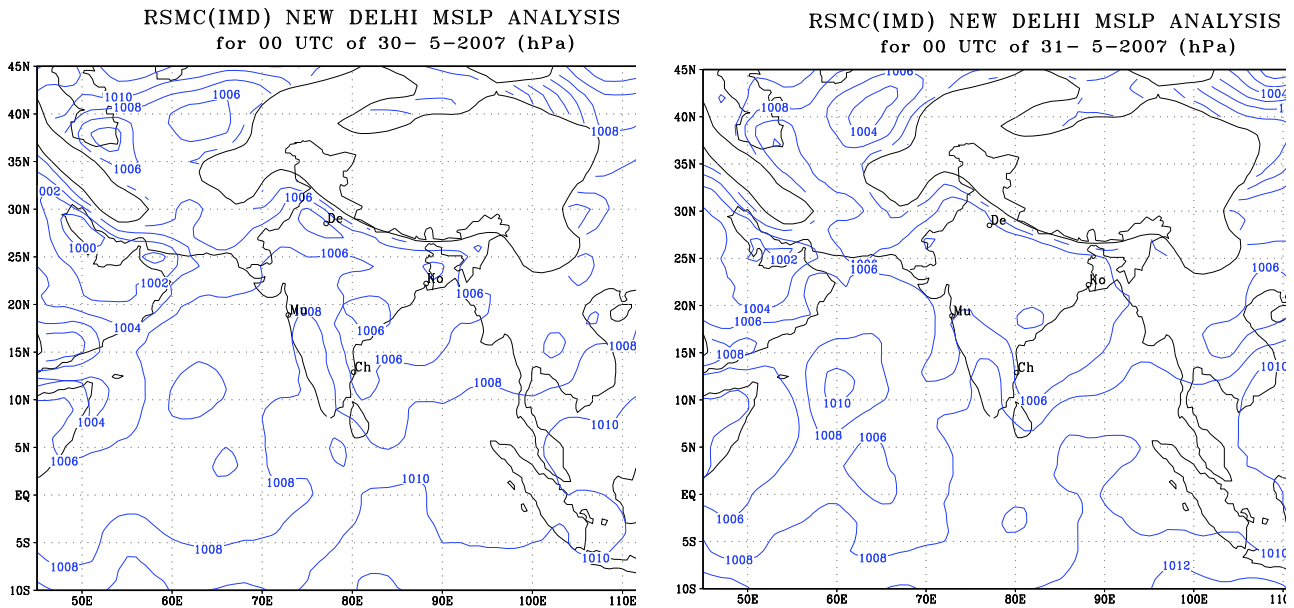


Fig. 6(a) LAM analysis of MSLP at 0000 UTC of 30 and 31 May depicted the genesis of Cyclone "GONU"

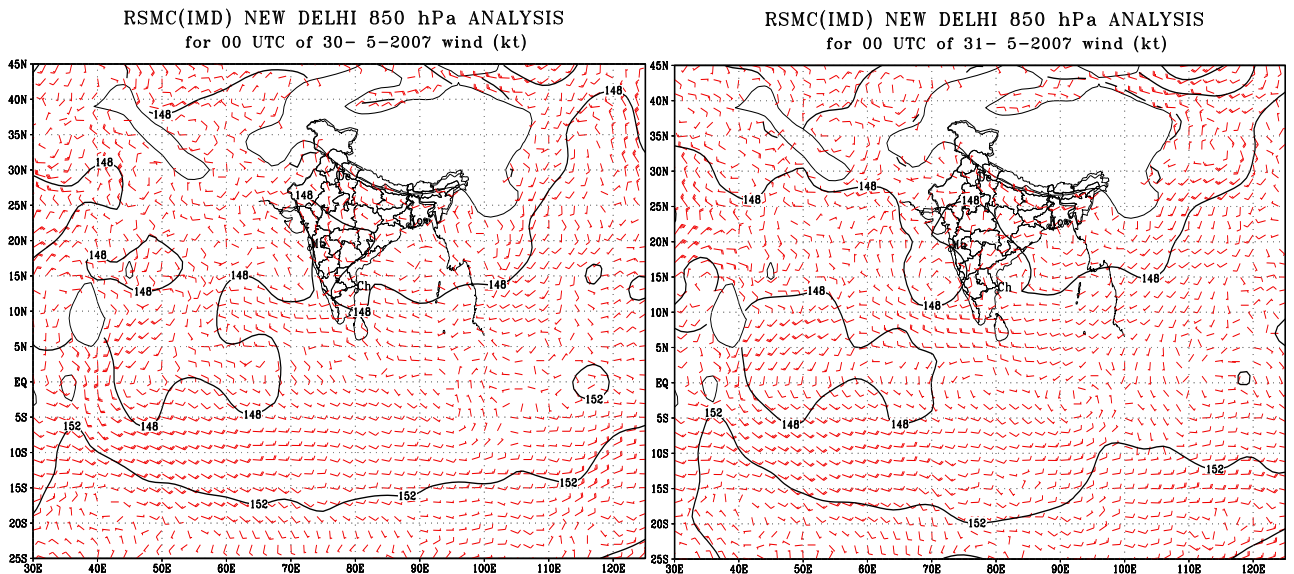


Fig. 6(b) LAM analysis of 850 hPa level wind at 0000 UTC of 30-31 May, 2007

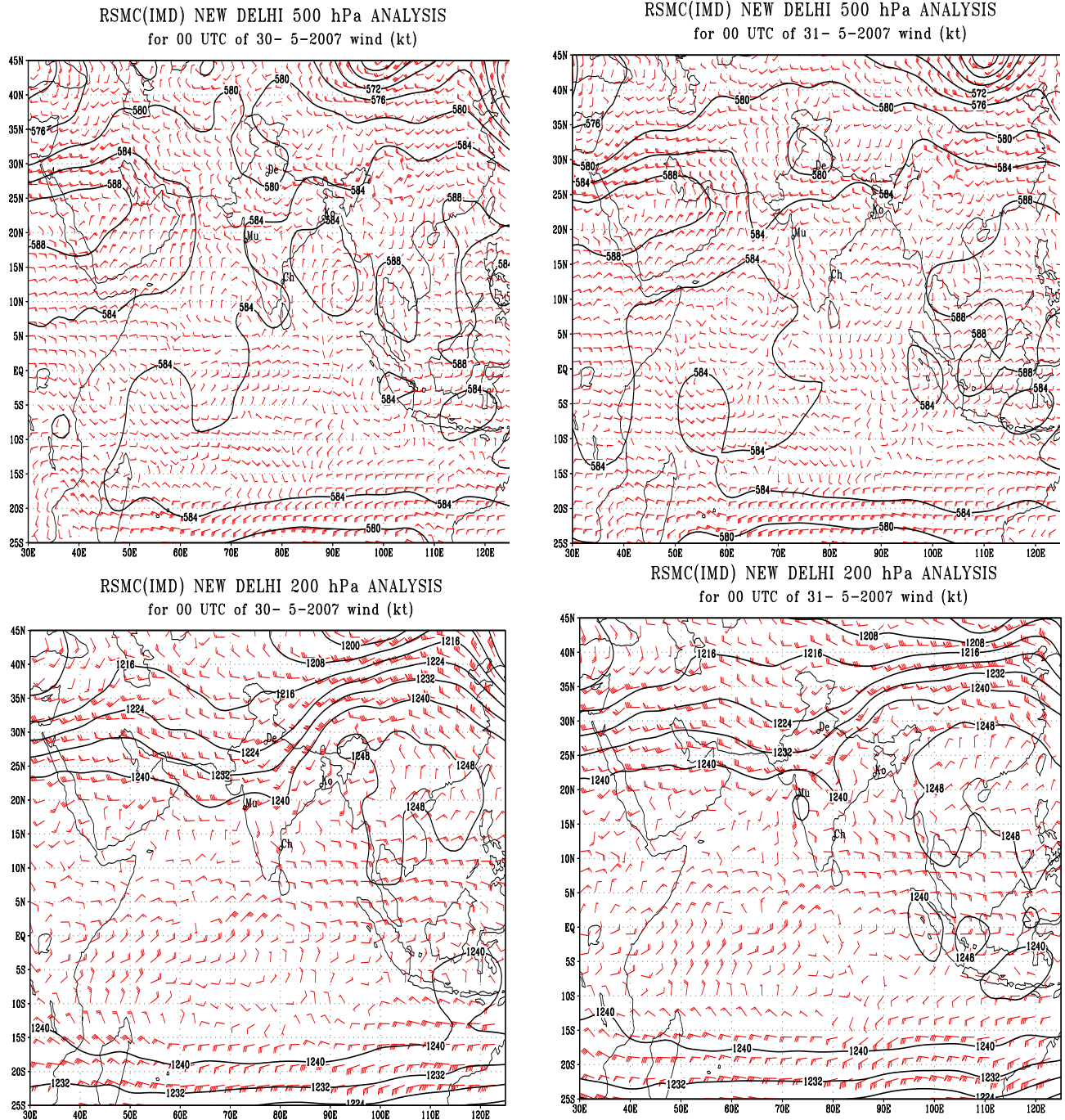


Fig. 6(c) LAM analysis of 500 hPa and 200 hPa level wind at 0000 UTC of 30 & 31 May 2007

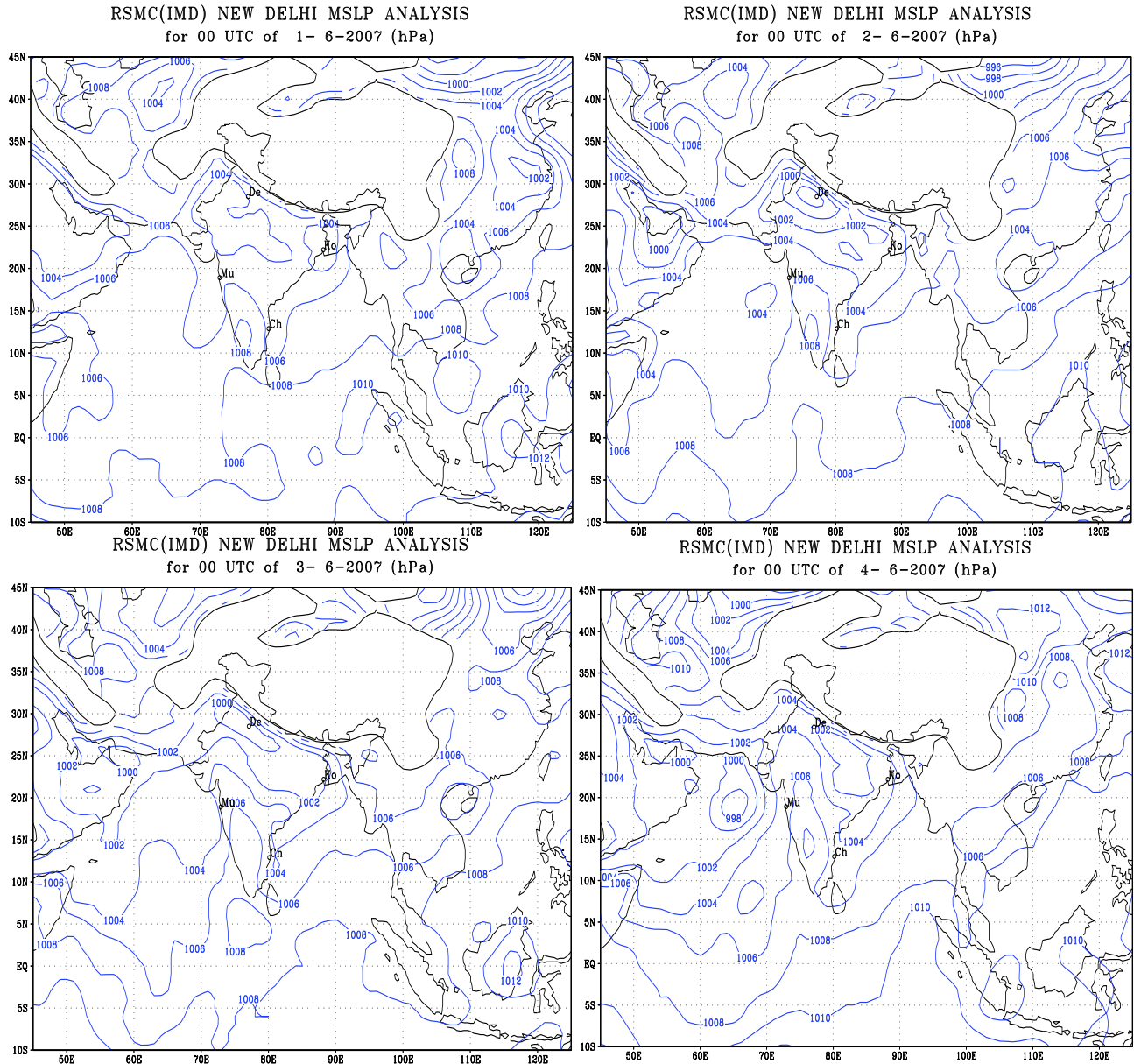


Fig. 7(a) LAM analysis of MSLP during 1-4 June 2007.

To examine the intensification of the system upto super cyclone stage, the LAM analysis of MSLP and wind in representative levels during 1-4 June 2007 are shown in Fig. 7. The intensity of the system could not be preferring reflected in the LAM analysis. However, wind at 850 hPa level gradually increased indicating intensification of the system. Comparing the actual intensity based on Dvork's technique (Table-1), the wind speed was highly underestimated by the LAM. Similar was the case with other operational models of IMD. However, ECMWF analysis was better in estimating the intensity of the system (not shown). It may be due better resolution, physics and data assimilation in the ECMWF model. Regarding the movement, the LAM analysis

indicated north-northwestward movement during the period. The analysis at 500 hPa level indicated northeastward movement on 4 June against the continuous northwestward movement. The upper tropospheric ridge at 200 level hPa shifted northward during the life period of the system like the actual upper tropospheric ridge.

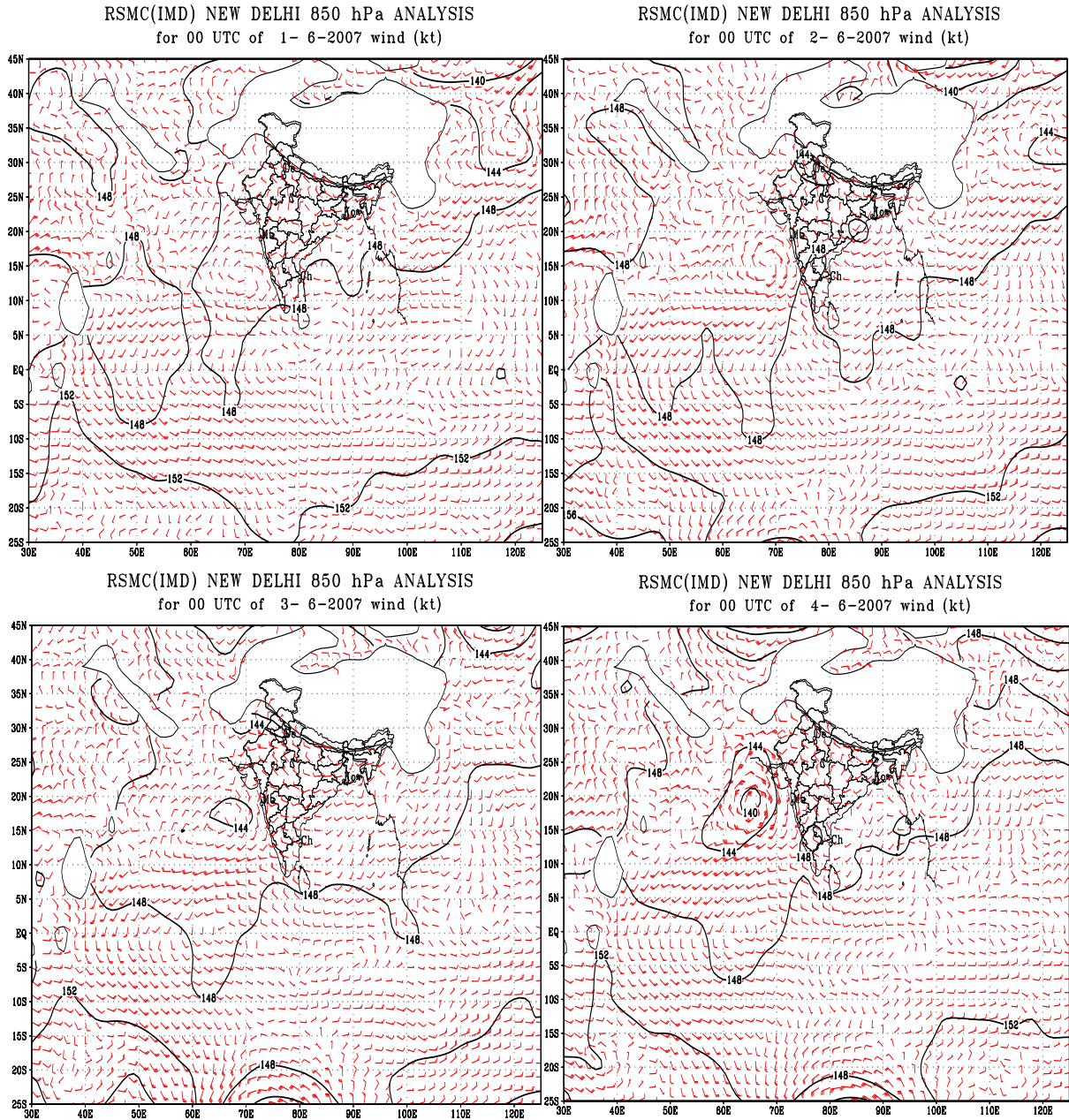
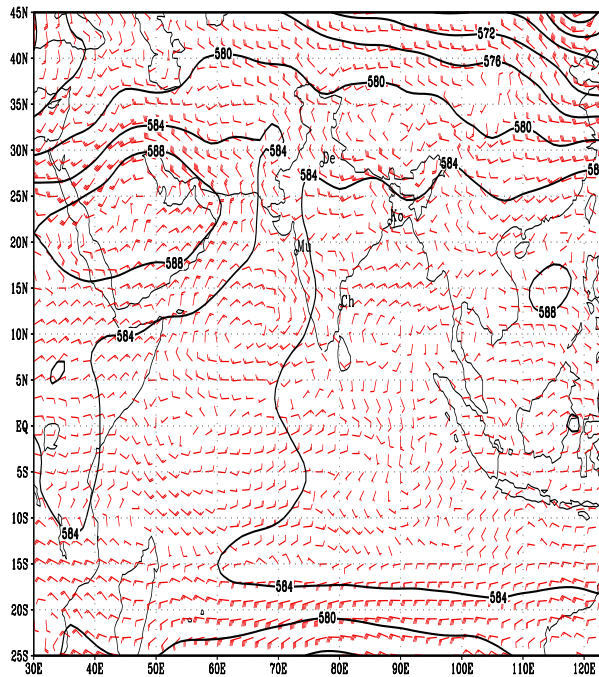
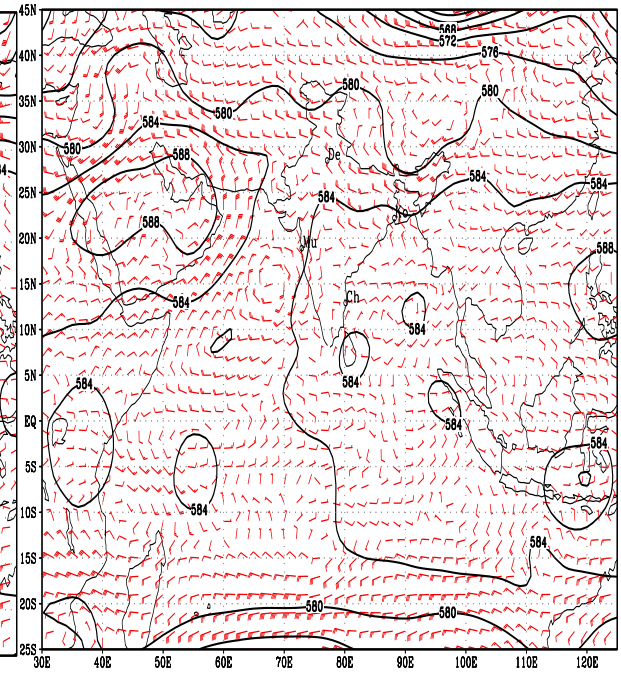


Fig. 7(b) LAM analysis of wind at 850 hPa during 1-4 June 2007.

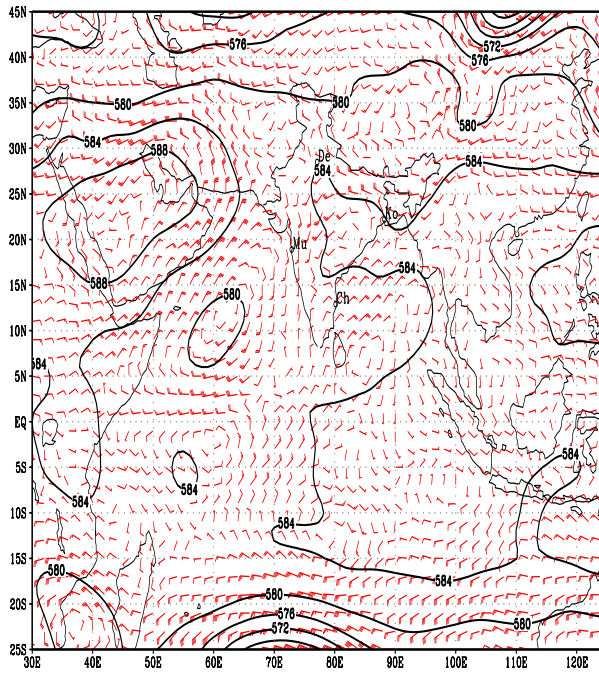
RSMC(IMD) NEW DELHI 500 hPa ANALYSIS
for 00 UTC of 1- 6-2007 wind (kt)



RSMC(IMD) NEW DELHI 500 hPa ANALYSIS
for 00 UTC of 2- 6-2007 wind (kt)



RSMC(IMD) NEW DELHI 500 hPa ANALYSIS
for 00 UTC of 3- 6-2007 wind (kt)



RSMC(IMD) NEW DELHI 500 hPa ANALYSIS
for 00 UTC of 4- 6-2007 wind (kt)

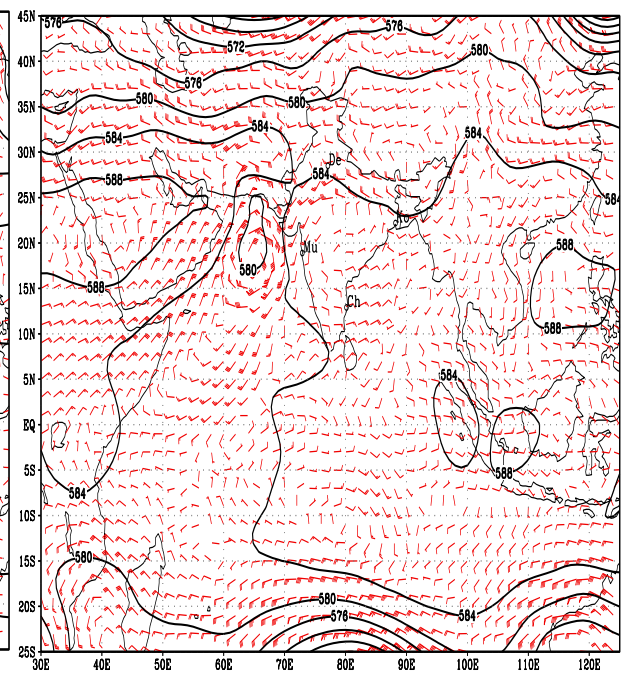


Fig 7(c) LAM analysis of wind at 500 hPa level during 1-4 June 2007.

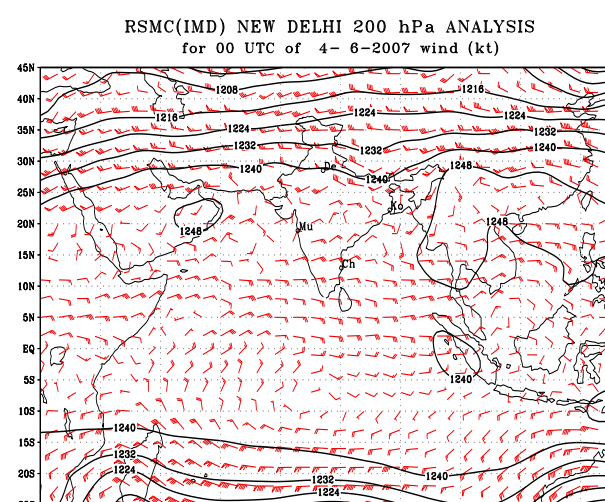
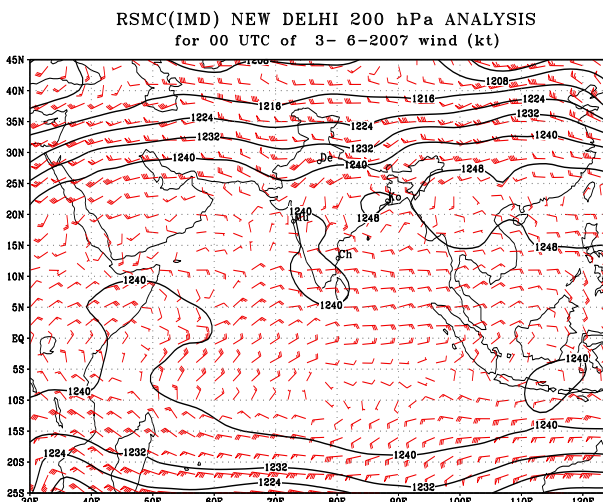
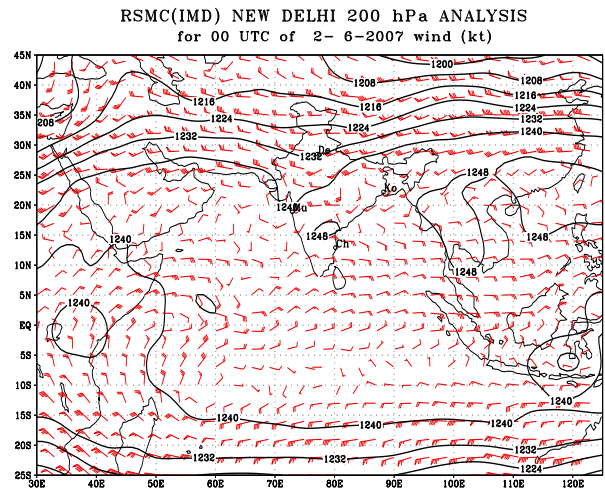
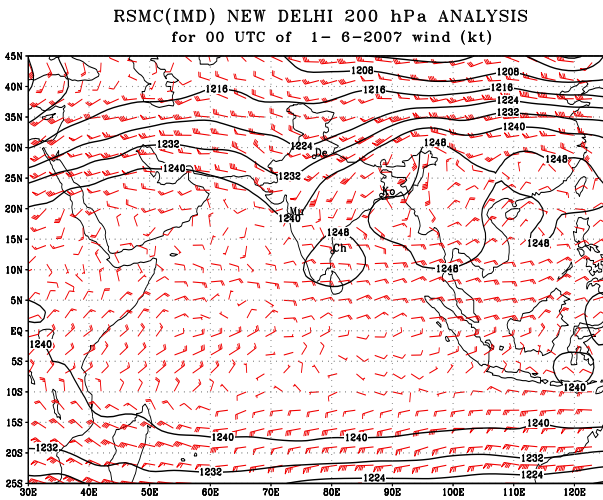


Fig. 7(d) LAM analysis of wind at 200 hPa Level during 1-4 June 2007.

5.2 Dynamical parameters

The vorticity, divergence and vorticity advection over the region are presented and analysed in section 5.2.1. The vertical wind shear and vertical velocity over the region are analysed and discussed in section 5.2.2 and 5.2.3 respectively.

5.2.1 Vorticity, divergence and vorticity advection

The low level relative vorticity and divergence over Indian region at 850 hPa levels at 0000 UTC during 30-31 May 2007 (Genesis period) as obtained from LAM analysis are shown in Fig. 8. The same during the intensification period (1-4 June) are shown in Fig. 9. The vorticity advection at 850 hPa level based on LAM analysis during genesis and intensification stages are shown in Fig. 10 and Fig. 11. The low level relative vorticity was slightly positive over the southeast and adjoining eastcentral Arabian Sea on 30 May. It gradually increased and became significantly positive with higher values over eastcentral Arabian Sea at 0000 UTC of 31 May. It then rapidly increased and became maximum on 4 June. It then decreased rapidly (not shown)

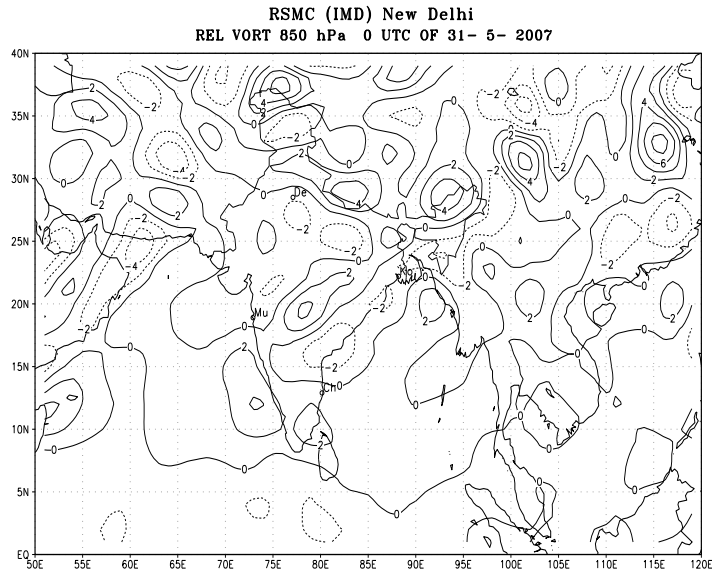
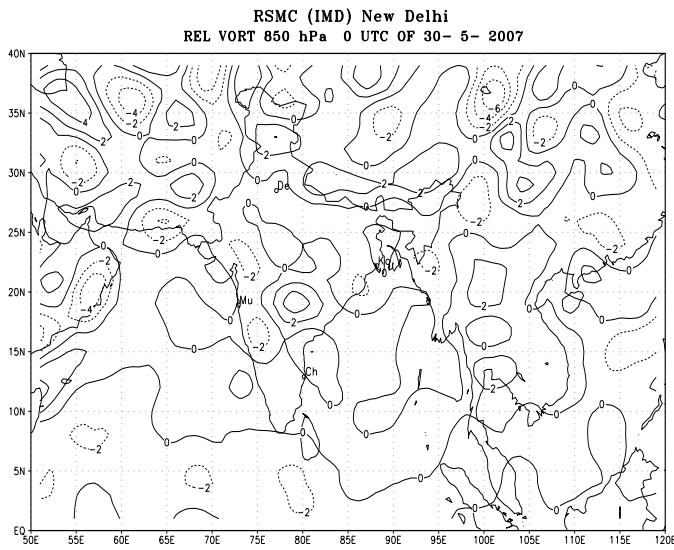


Fig. 8(a). Relative vorticity at 850 hPa level during genesis period of the system (30-31May) according to LAM analysis.

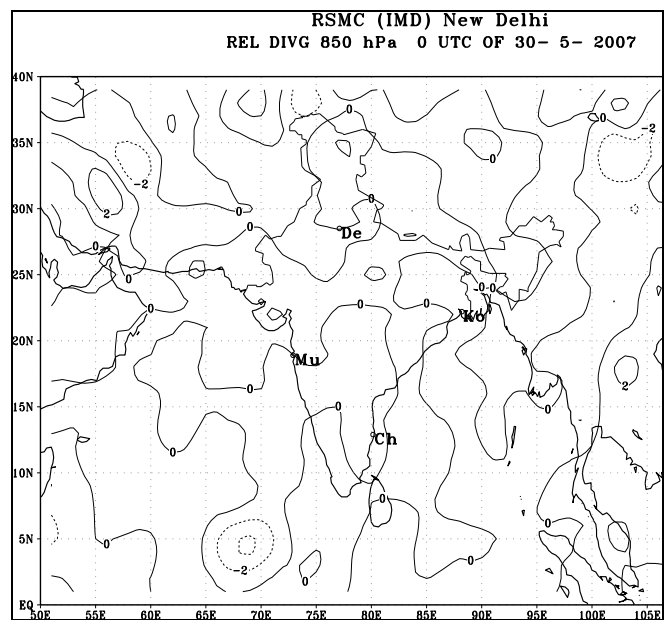
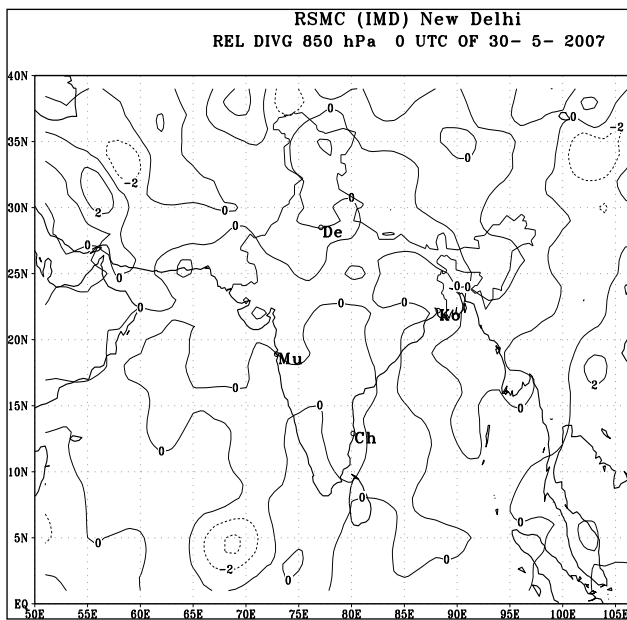


Fig.8(b) Relative divergence at 850 hPa level during genesis period of the system (30-31 May) according to LAM analysis.

The spatial and temporal distributions of vorticity in the lower levels were in agreement with the trend in the intensity and movement of the system with minor variation. There was only one maxima in positive vorticity to the north-northwest of system centre. This was in agreement with the rainfall distribution, though the centres of maxima in rainfall and low level vorticity differed in their locations. As the location of maximum positive vorticity indicates the likely

movement of the system, the vorticity field in this case helped in forecasting the north-northwesterly movement of the system.

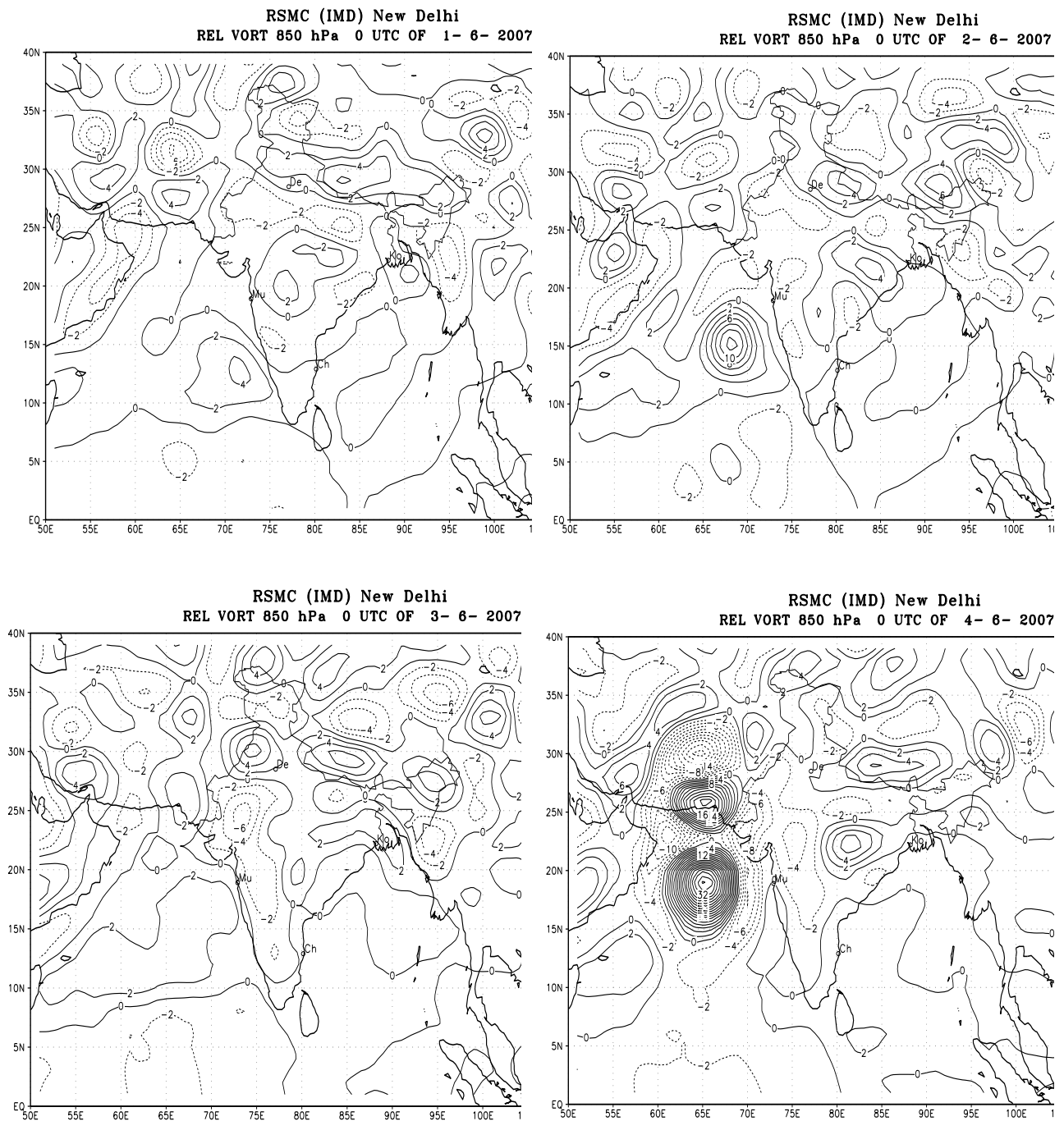


Fig. 9(a) Relative vorticity at 850 hPa level during intensification phase of the system (1-4 June) according to LAM analysis.

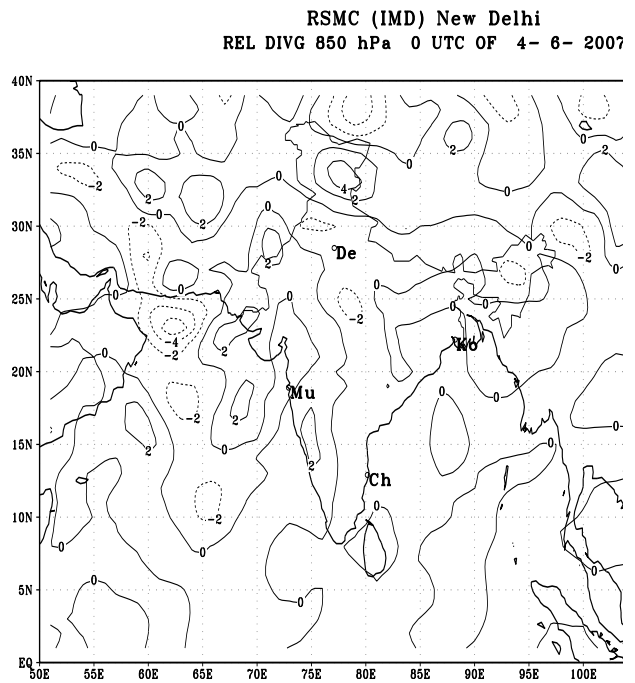
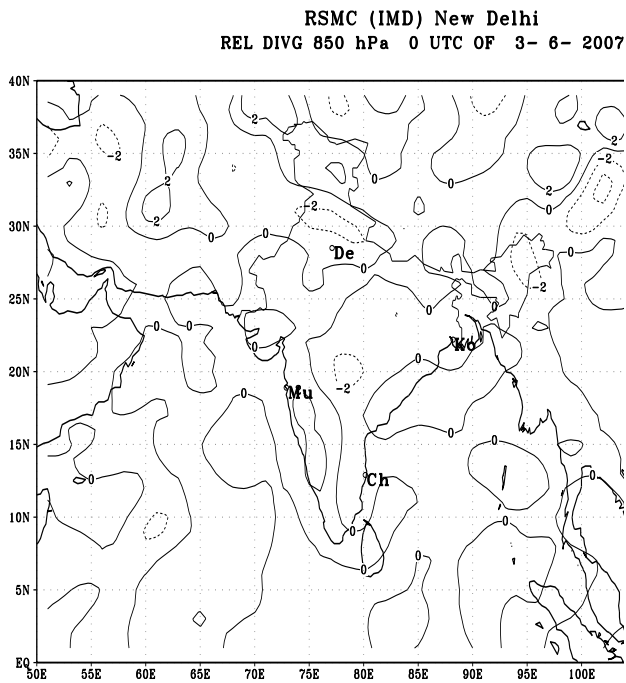
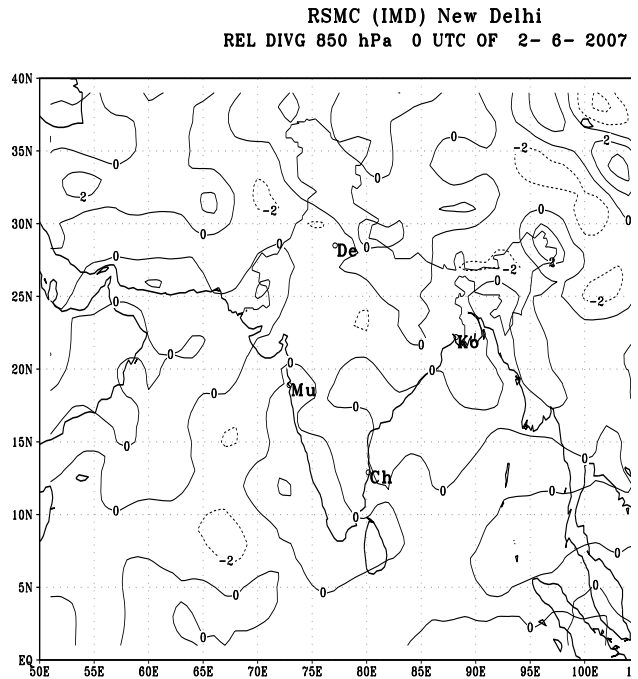
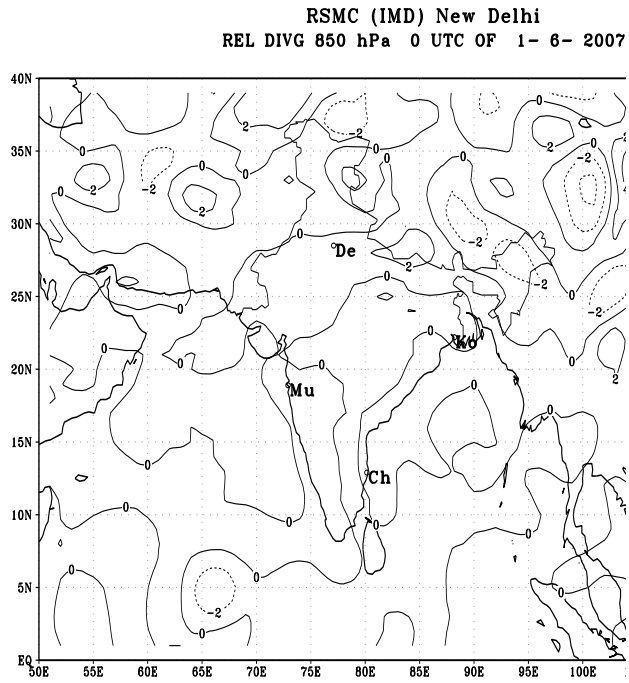


Fig. 9(b). Relative divergence at 850 hPa level during intensification phase of the system (1-4 June) according to LAM analysis.

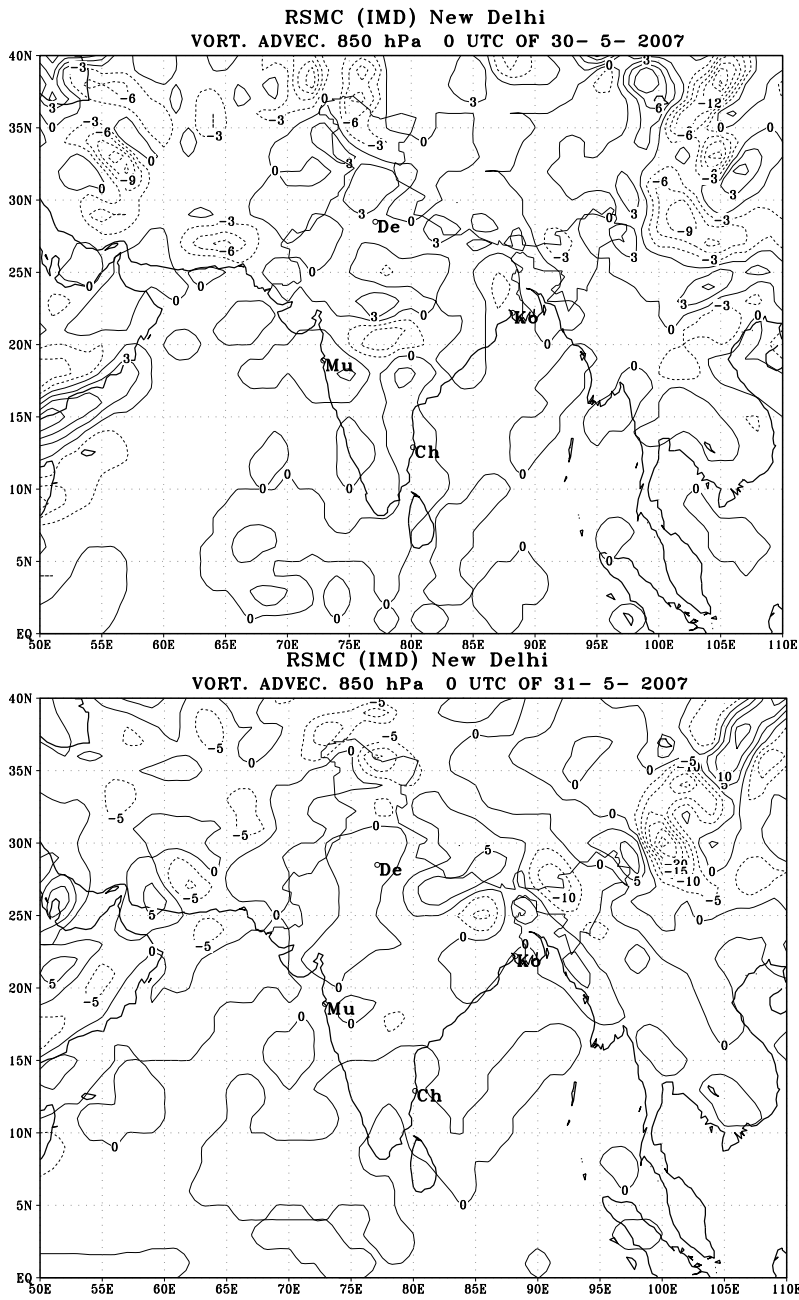


Fig. 10. Vorticity advection at 850 hPa level according to LAM analysis during genesis period (30-31 May 2007)

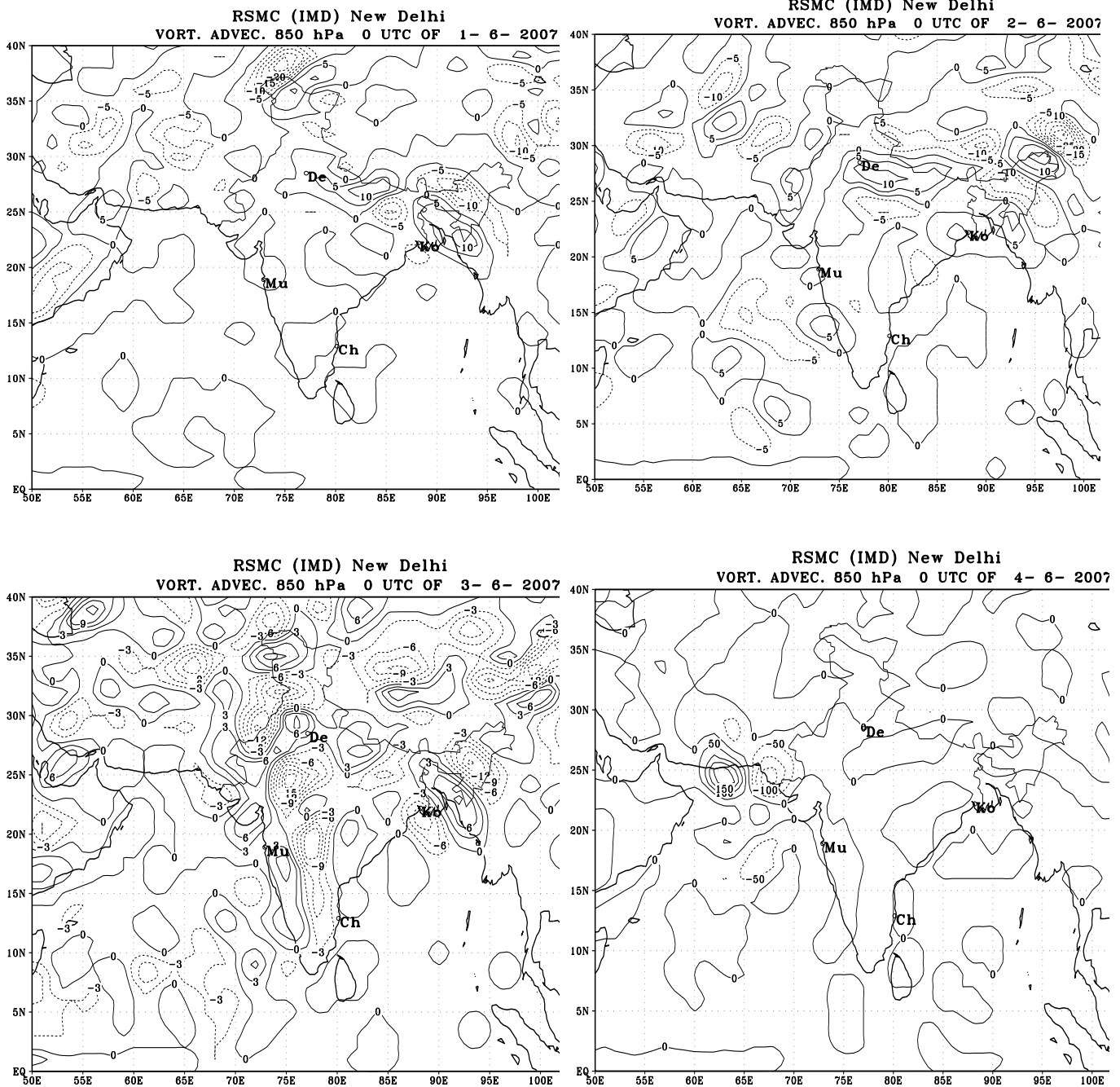


Fig.11. Vorticity advection at 850 hPa level according to LAM analysis during intensification period (1-4 June 2007)

According to Mc Bride (1995), the low level vorticity in developing cloud clusters is twice that in non-developing disturbances. In a developing tropical disturbance, the effect of intense convection is to generate a convergent low

level wind field as air flows towards convection. This convergence produces an increase in relative vorticity. Unlike the vorticity field, the divergence/convergence field was not very pronounced over the storm region as shown in Fig. 8(b) and 9(b).

According to the barotropic vorticity equation, (Holton, 1979), the barotropic vorticity depends on the (a) advection of relative vorticity (b) advection of earth vorticity and (c) vorticity change due to divergence or convergence, when the tilting, solenoidal and frictional effects are neglected in the above equation. At the first approximation, the maximum cyclonic vorticity is at the centre and decreases with increasing radius. Hence, if the cyclone is moving in a given direction, the local rate of change of cyclonic vorticity must also increase in the same direction. As the tropical cyclones generally respond like a protected symmetric vortex in a uniform, non-interacting wind flow, the motion of the storm is governed by the advection of relative vorticity. The flow simply advects the vortex along with it.

5.2.2 Vertical wind shear

The vertical wind shear of horizontal winds between 850 and 200 hPa levels over Indian region at 0000 and during 30-31 May (Genesis period), according to LAM analysis are shown in Fig.12. The vertical wind shear over the system field was about 10 knots during the genesis period which is favourable for genesis and intensification. During intensification phase the wind shear slightly increased and they were about 15-20 kt on 1 June and 15-25 on 2 June. It again decreased to 10-15 knots on 3 June and increased to 20-30 knots on 4 June (Fig. 13). It indicates that, though the wind shear was favourable during genesis, it was not so during intensification into super cyclone stage. It may be mentioned that the intensity was maximum at 1500 UTC of 4 June. Thus, the analysis suggests that the system intensified into a super cyclone inspite of high vertical wind shear which is intriguing and needs further research to understand the role of vertical wind shear. There was anti-cyclonic shear over the region which gradually moved from northwest Peninsula India (near Mumbai) on 31 May towards southwest during 1-2 June and towards northwest on 3 June. It moved northward on 4 June. A close examination of the system centre and the ridge line on the vertical wind shear showed that the system lay just to the south of the ridge line on these days. Hence, there was north-northwestward movement of the system. Earlier studies (Krishna Rao, 1997) also suggested that the vertical wind shear could be used as a precursor for the movement of the cyclonic storms.

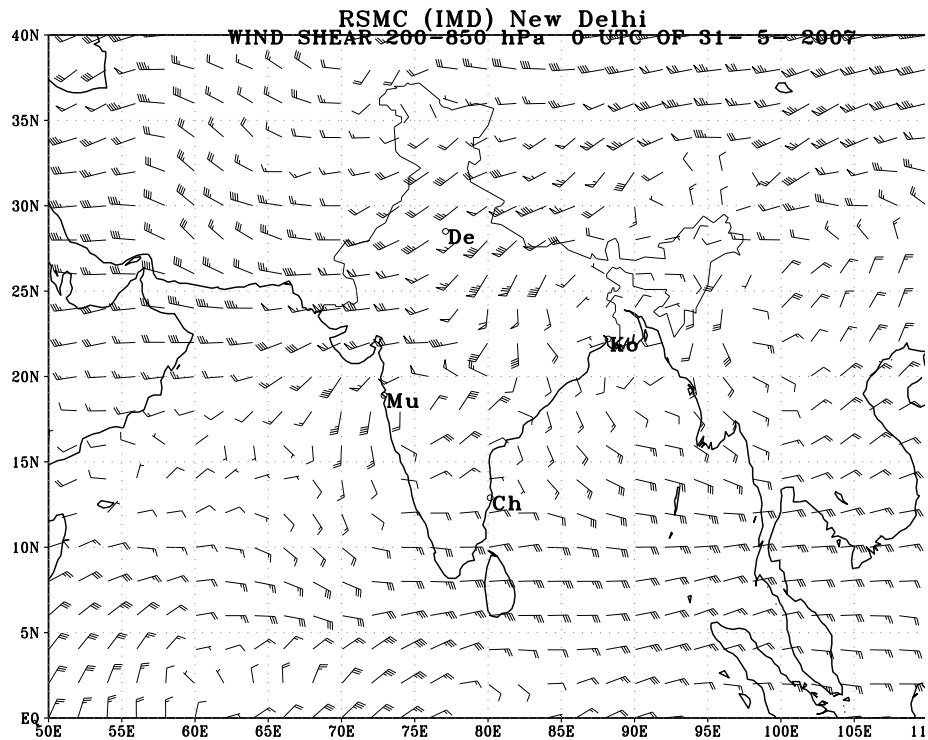
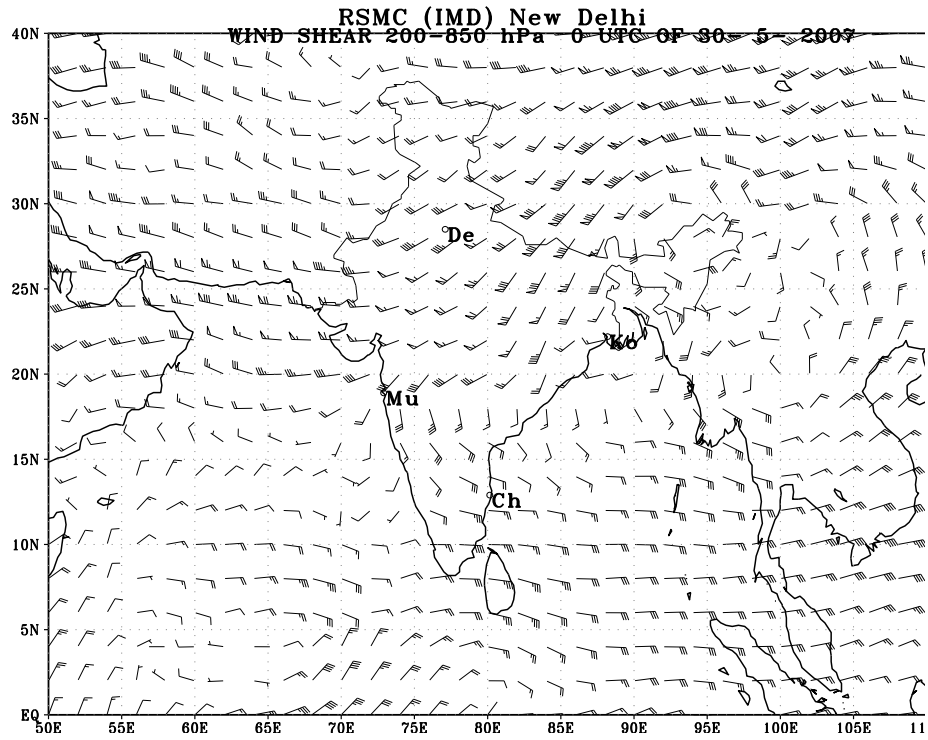


Fig 12. Vertical wind shear between 200 and 850 hPa level according to LAM analysis during genesis phase (30-31 May) of cyclone GONU.

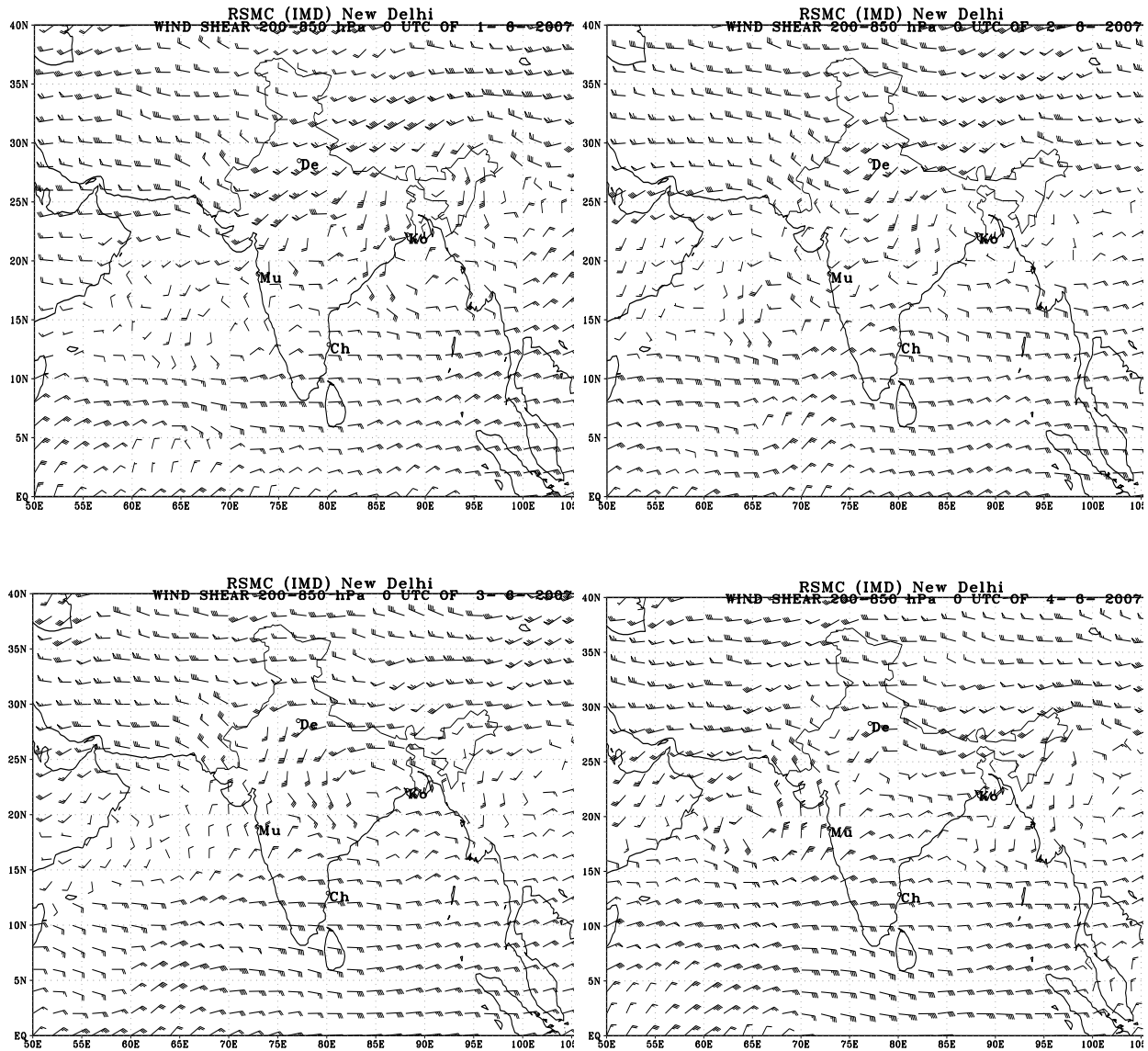


Fig 13. Vertical wind shear between 200 and 850 hPa level according to LAM analysis during intensification phase (1-4 June) of cyclone GONU.

5.2.3. Vertical velocity

The middle level vertical velocity at 500 hPa levels according to LAM analysis based on 0000 UTC observations during genesis period (30-31 May) and intensification phase (1-4 June) are shown in Fig.14 & 15 respectively. Analysis shows upward vertical motion over the storm region on 30 May, 1, 2 and 4 June. The upward vertical velocity was maximum as on 4 June which might have led to intensification of the system to super cyclone stage. The surface friction in the presence of low level vorticity produces upward motion in region of positive vorticity. Hence, the regions of low level positive vorticity are associated with enhanced upward motion, cumulus convection and release of latent heat. The increased heating leads to increase in horizontal convergence, which in turn

increases the relative vorticity and upward vertical motion. Hence, the upward vertical motion as seen in Fig.14 & 15 was in agreement with the low level relative vorticity distribution. The distribution of vertical velocity also indicated the north-northwestward movement of the velocity maxima towards Makran coast. It confirmed the earlier findings that the system moves in the direction of increasing vertical velocity, increasing positive vorticity and increasing convection (Krishna Rao, 1997). The vertical velocity at 500 hPa suggested two maxima, the primary maxima to the north-northwest of the system centre and the secondary maxima to the south of the system centre.

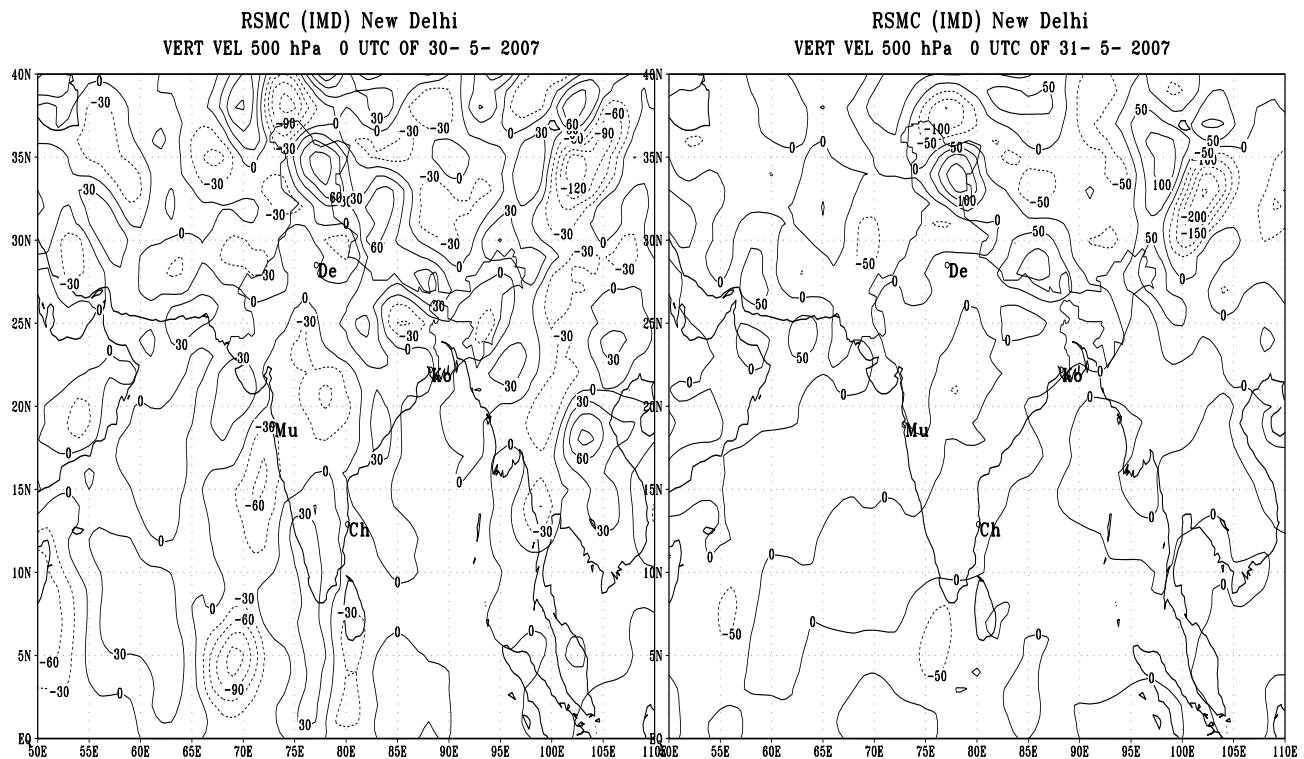


Fig 14. Vertical velocity at 500 hPa level according to LAM analysis during genesis phase (30-31 May) of cyclone GONU.

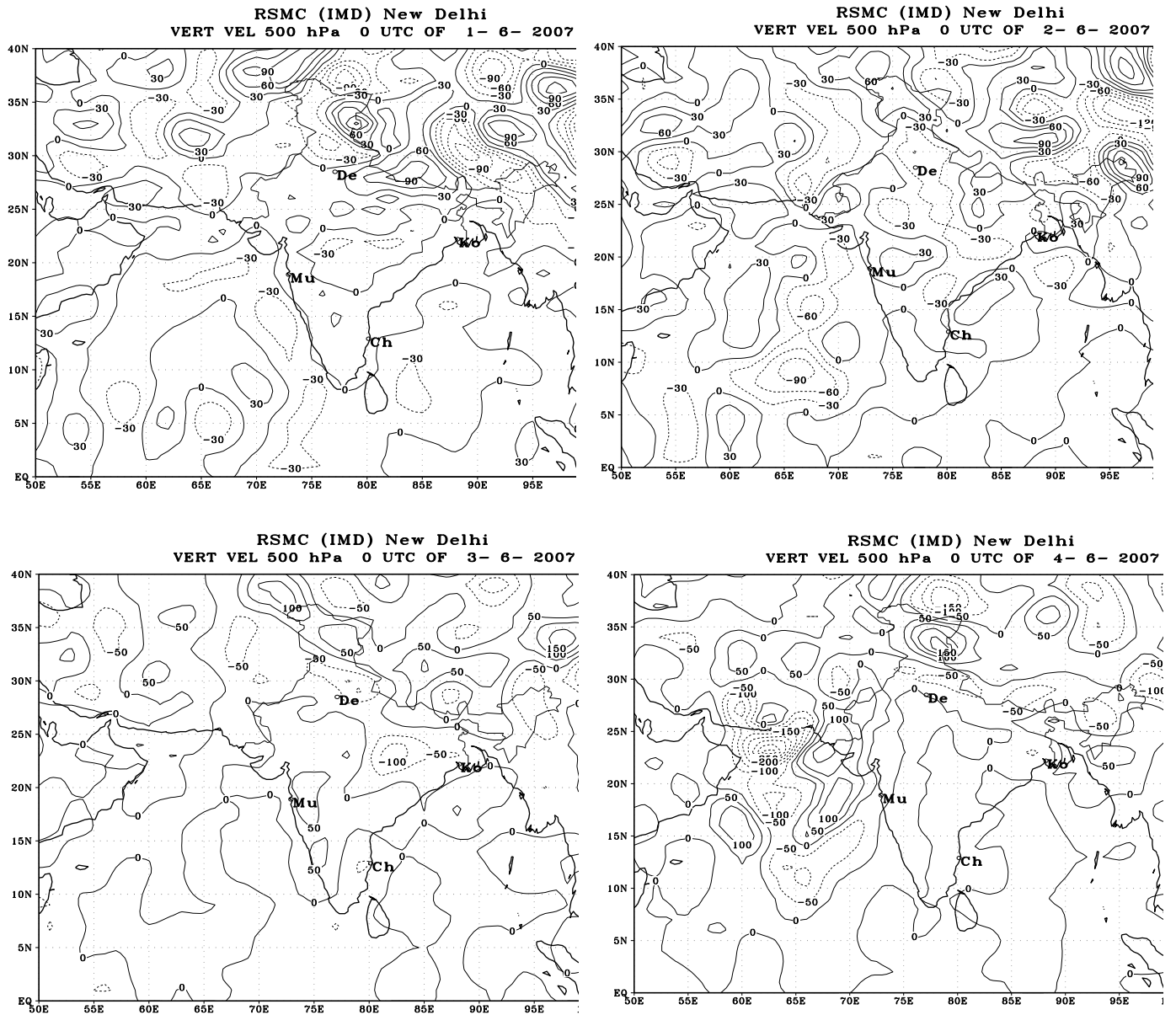


Fig. 15: Vertical velocity at 500 hPa level according to LAM analysis during intensification phase (1-4 June) of cyclone GONU.

5.3 Thermodynamic Parameters:

The spatio-temporal distribution of relative humidity, precipitable water content and moisture flux over Indian region during genesis and intensification phase are analysed and presented in section 5.3.1 to 5.3.4.

5.3.1 Relative humidity

The relative humidity (RH) over Indian region at representative levels of 850 and 500 hPa based on 0000 UTC observations during genesis and intensification

phase, as per LAM analysis are shown in Fig.16 and Fig. 17 respectively. According to Gray (1968), the large value of RH in lower and middle troposphere is an important parameter for cyclone genesis. The RH was more than 90% upto mid-tropospheric levels over the area of the storm through out the life period. McBride and Gray (1979) have shown that though the RH is important for tropical cyclone genesis, this does not differ significantly in convective systems which intensify into tropical cyclones and those which do not. The RH was more than 70% at 500 hPa on both 3rd & 4th June over the cyclone region without much differentiation. It hence endorsed the earlier findings.

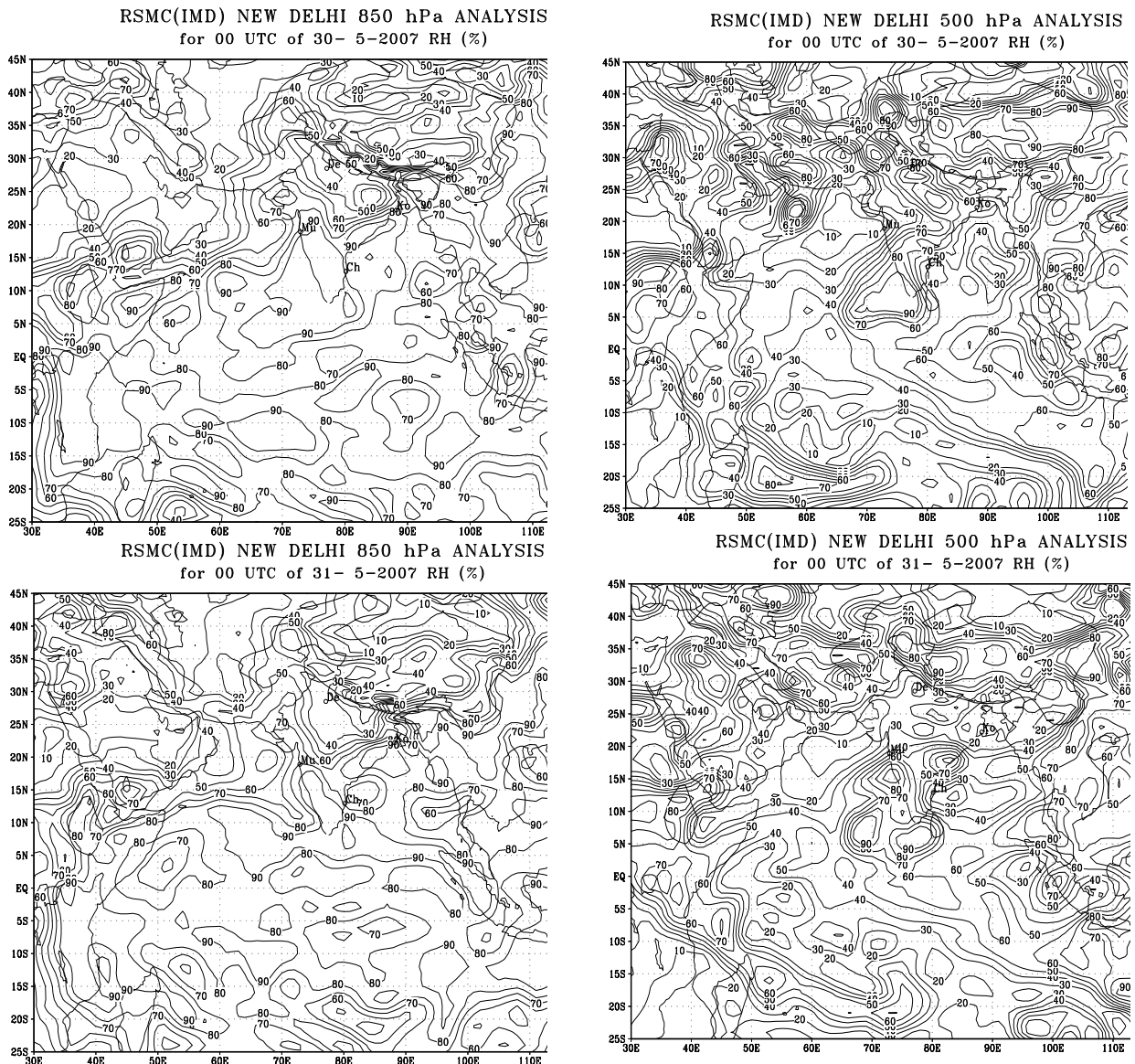
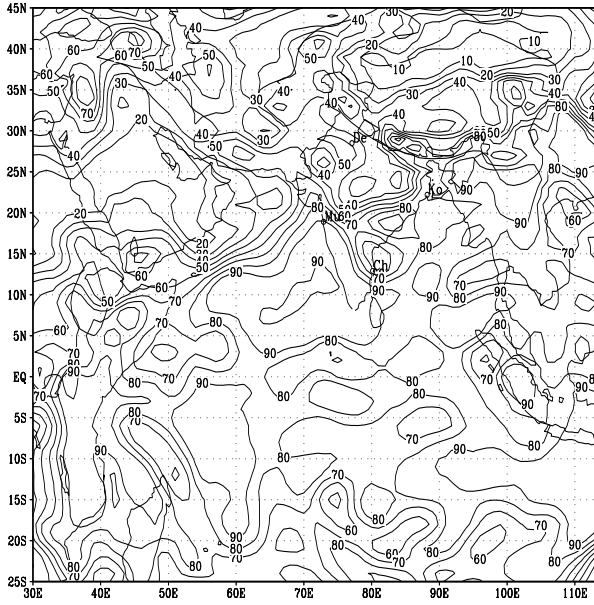
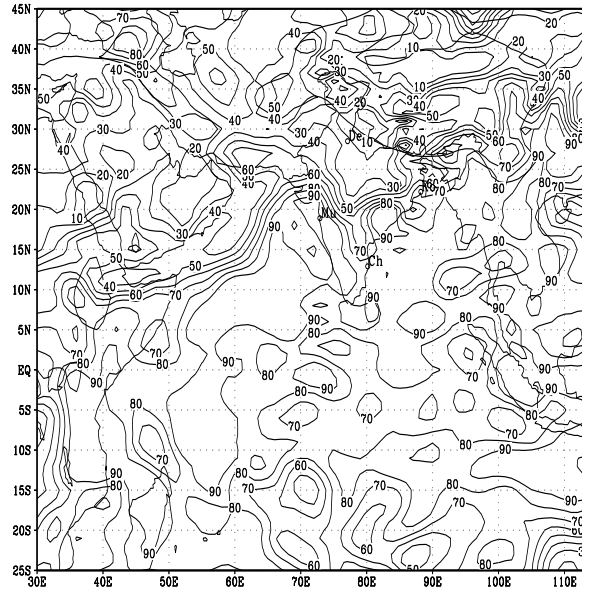


Fig. 16. Relative humidity at 850 and 500 hPa levels according to LAM analysis during genesis phase of the system

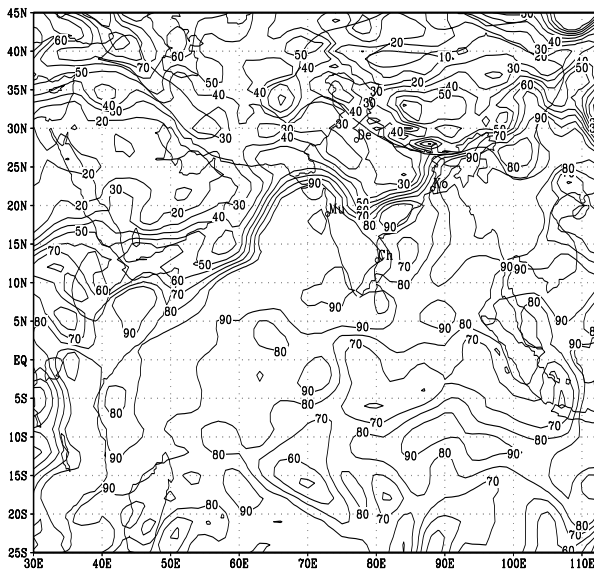
RSMC(IMD) NEW DELHI 850 hPa ANALYSIS
for 00 UTC of 1- 6-2007 RH (%)



RSMC(IMD) NEW DELHI 850 hPa ANALYSIS
for 00 UTC of 2- 6-2007 RH (%)



RSMC(IMD) NEW DELHI 850 hPa ANALYSIS
for 00 UTC of 3- 6-2007 RH (%)



RSMC(IMD) NEW DELHI 850 hPa ANALYSIS
for 00 UTC of 4- 6-2007 RH (%)

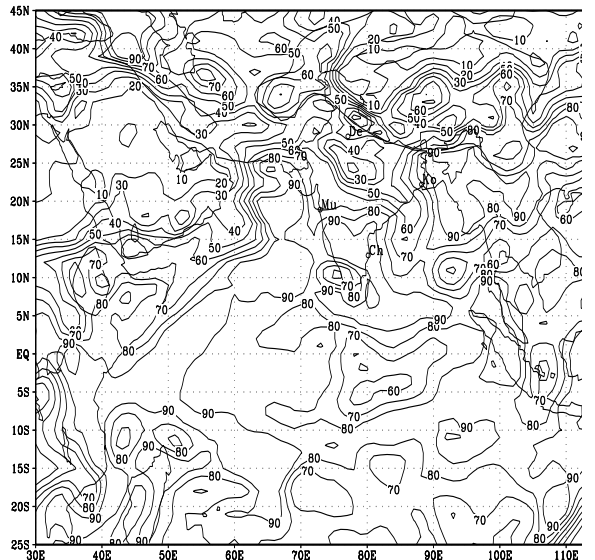
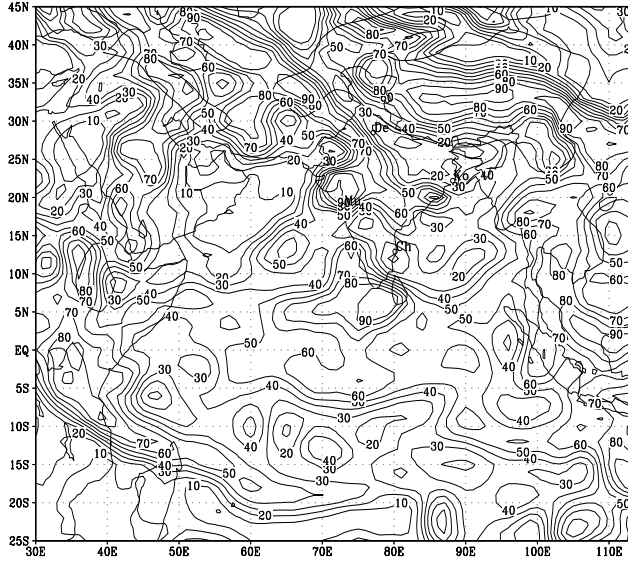
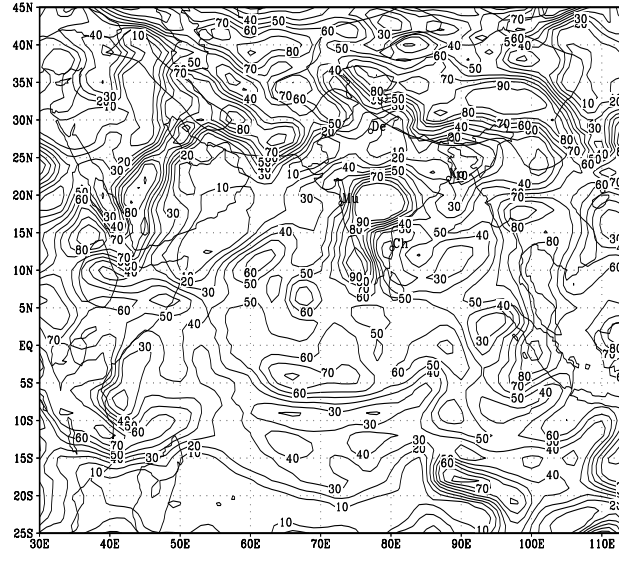


Fig. 17(a). Relative humidity at 500 hPa levels according to LAM analysis during intensification phase of the system.

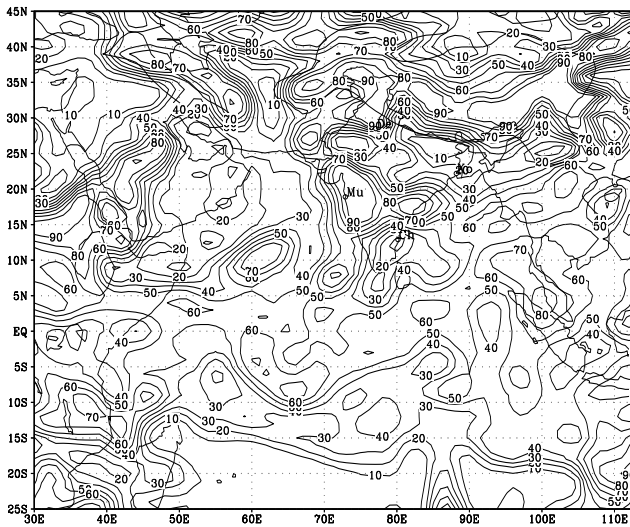
RSMC(IMD) NEW DELHI 500 hPa ANALYSIS
for 00 UTC of 1- 6-2007 RH (%)



RSMC(IMD) NEW DELHI 500 hPa ANALYSIS
for 00 UTC of 2- 6-2007 RH (%)



RSMC(IMD) NEW DELHI 500 hPa ANALYSIS
for 00 UTC of 3- 6-2007 RH (%)



RSMC(IMD) NEW DELHI 500 hPa ANALYSIS
for 00 UTC of 4- 6-2007 RH (%)

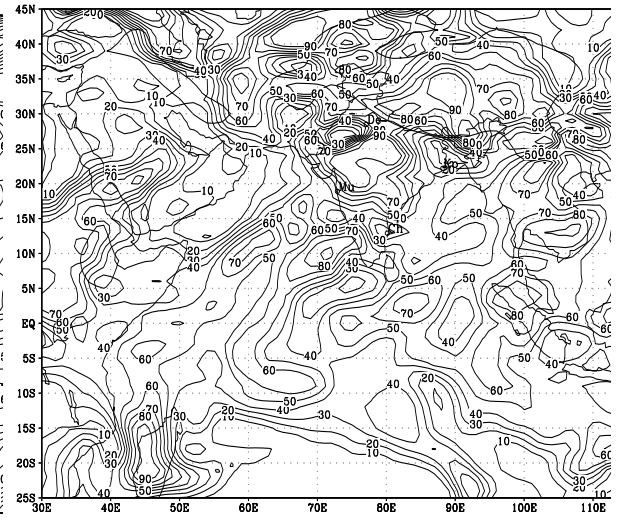


Fig. 17(b). Relative humidity at 850 hPa levels according to LAM analysis during intensification phase of the system.

5.3.2 Precipitable Water Content

The Precipitable water content (PWC) values of the atmosphere according to LAM analysis during genesis and intensification phase are shown in Fig.18 & 19 respectively. The centre of maxima in PWC lay to the southwest of the centre

of the system on 30 and 31 May. Comparing the PWC distribution and the rainfall distribution on the subsequent days during the storm period, though the pattern was similar to a large extent, the region of maxima in PWC was dislocated with respect to the centre of maximum rainfall. Also there was slight increase in the PWC over the region of maxima from 30 to 31 May and remained same there after (about 5 cm).

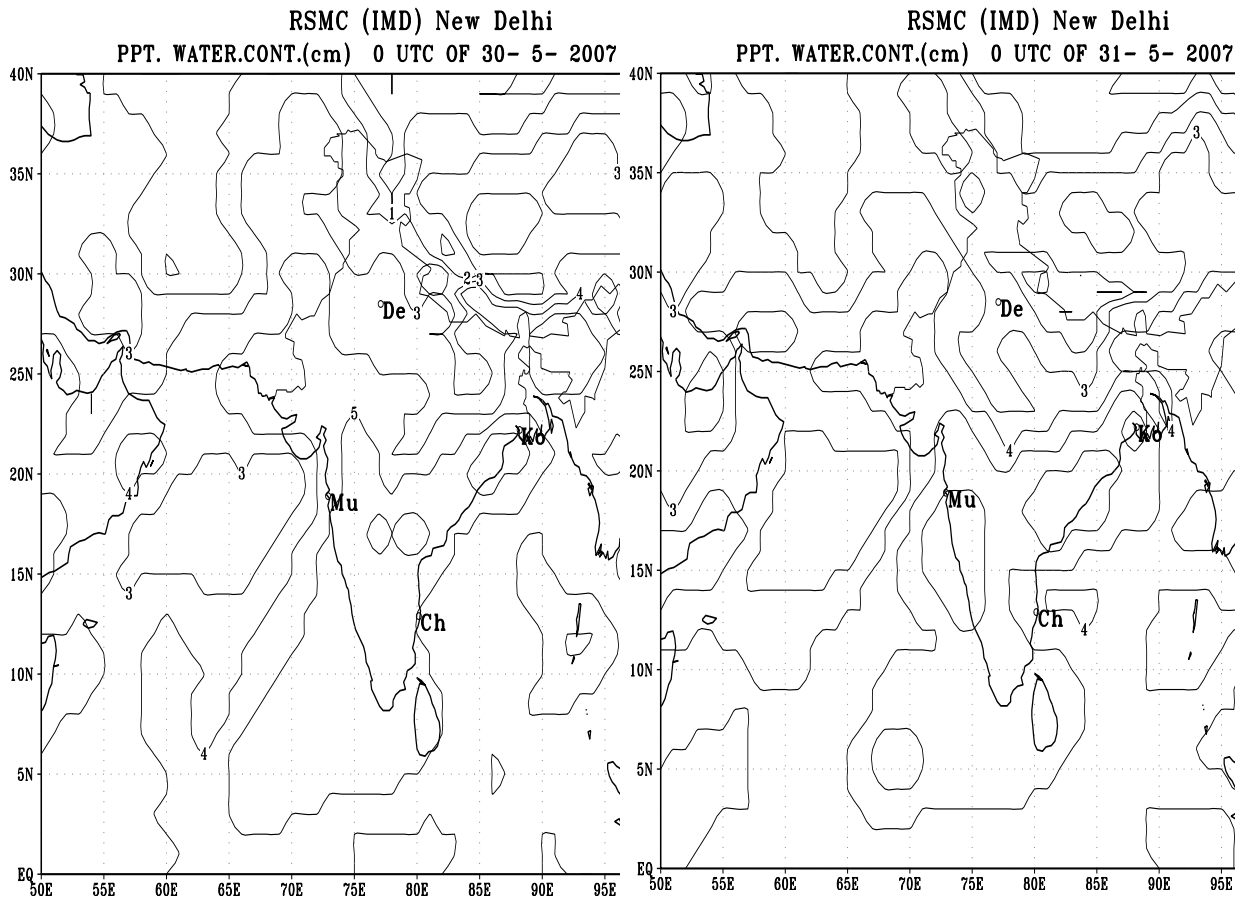


Fig. 18. Precipitable water content at 0000 UTC according to LAM analysis, during genesis phase of the system.

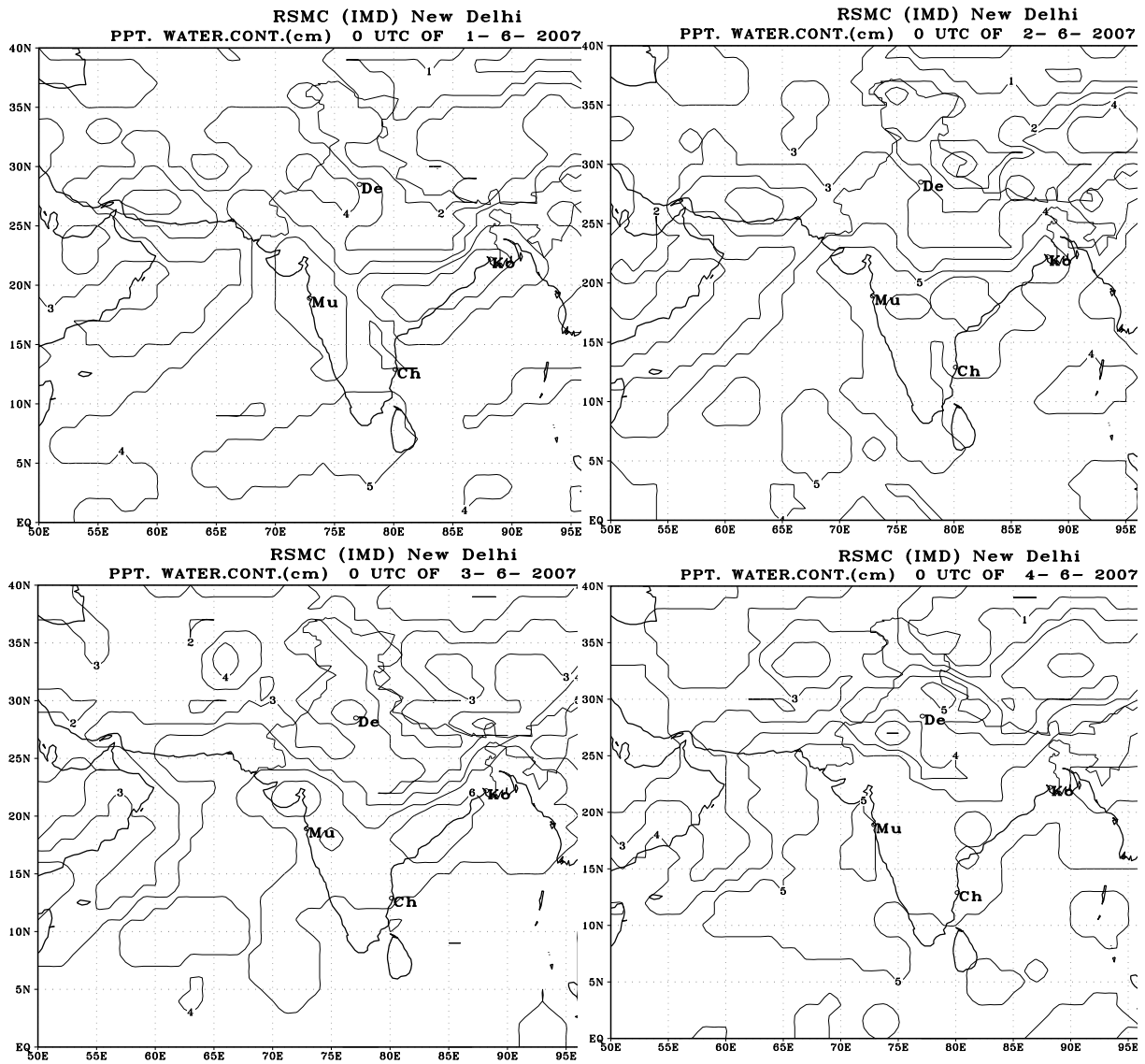


Fig. 19. Precipitable water content at 0000 UTC according to LAM analysis, during intensification phase of the system.

5.3.3 Moisture Flux

The moisture flux at 0000 UTC during genesis and intensification phase are shown in Fig.20 and 21 respectively. There was moisture advection towards the centre of the system during the life period of storm. The moisture advection over the region increased from 30 May onwards and became maximum on 4 June ($>250 \times 10^{-5} \text{ gm/cm}^2/\text{sec}$). The region of maxima moved in a north-northwesterly direction. Hence, the moisture flux also indicated the system to move north-northwestwards. Further, it could depict the trend in intensification unlike the PWC.

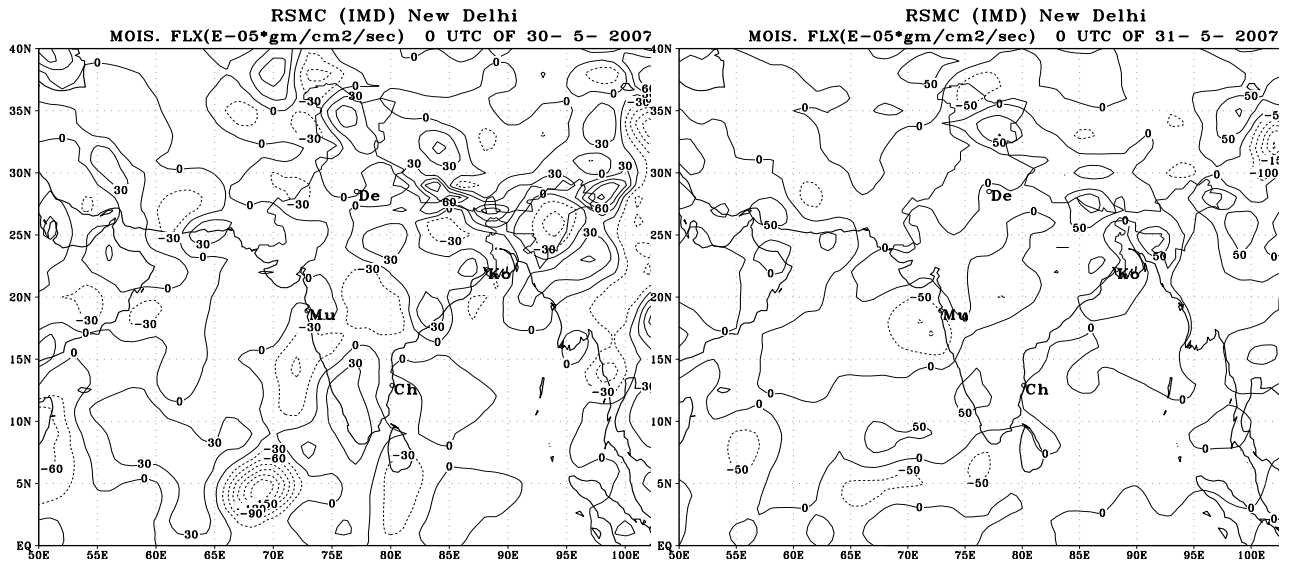


Fig. 20. Moisture flux at 0000 UTC during genesis phase of cyclone GONU.

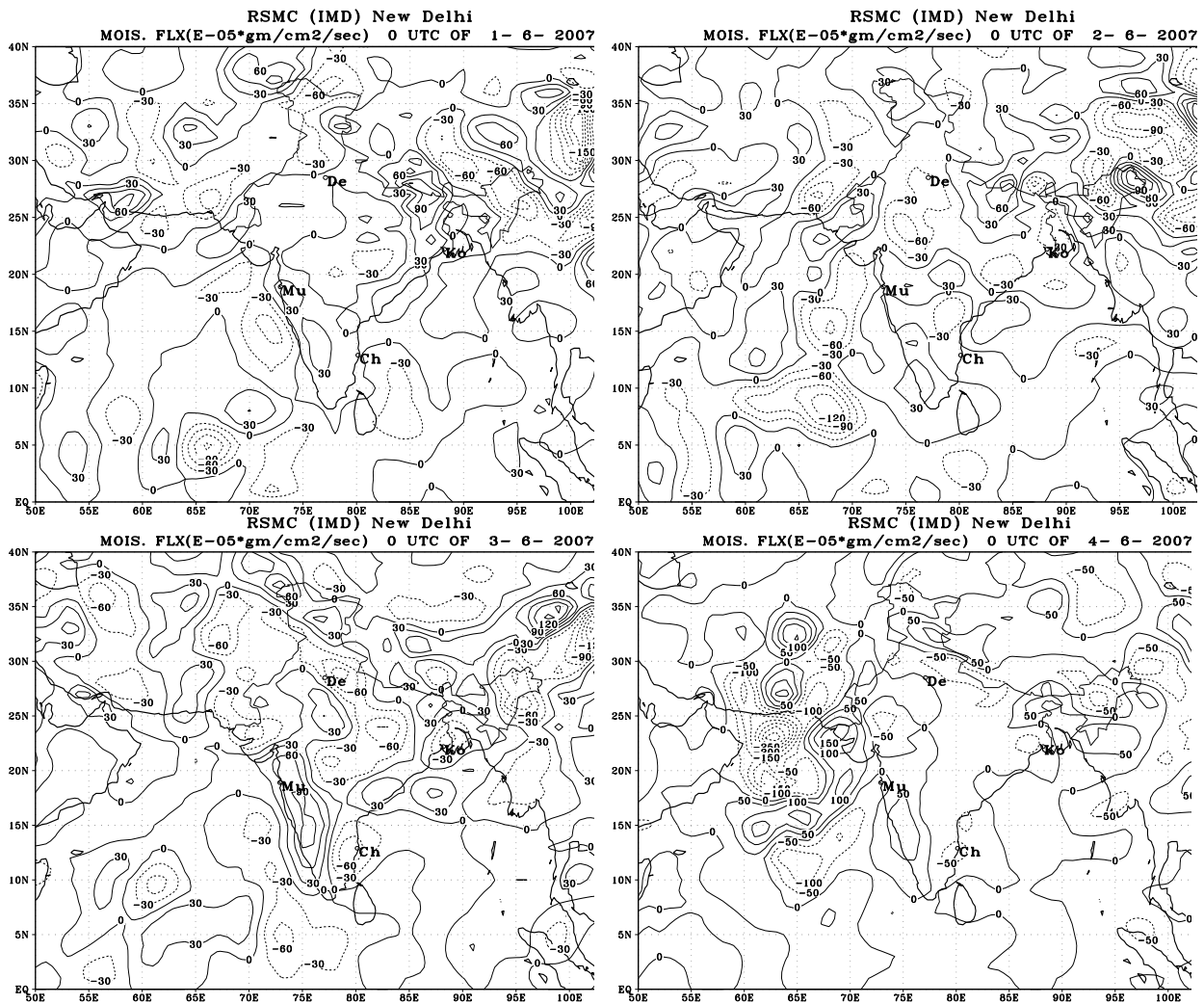


Fig. 21. Moisture flux at 0000 UTC during intensification phase of cyclone GONU.

5.4 Satellite observed features

The position and intensity analysis of tropical cyclones over Indian Ocean are being carried out by IMD following the Dvorak Technique (Dvorak 1984). The analysis of Satellite observed cloud features and estimation of position and intensity of Super Cyclone **GONU** over Arabian Sea are described in section.5.4.1. Sea Surface Temperature derived from satellite observations pertaining to this system is presented in section 5.4.2. The INSAT derived OLR distribution over Arabian Sea has been analysed and presented in section.5.4.3. Utility of Satellite derived Water Vapour Wind (WVW) vectors for monitoring and prediction of the movement of the system have been discussed in section.5.4.4. Satellite derived QPE associated with the system is analysed in section.5.4.5.

5.4.1. Genesis and intensification:

Broken cluster of intense convective clouds with Cloud Top Temperature (CTT) of -40°C or less was observed over southeast Arabian Sea on 30 May, 2007 and it yielded a low level circulation over the same area at 0900UTC on that Day. The convective cloud clusters associated with low level circulation became more intense (CTT about -70°C) and organised into a vortex at 0300 UTC of 31 May with intensity T1.0 near $12.5^{\circ}\text{N} / 73.5^{\circ}\text{E}$. As the vortex moved northwest-wards, cloud clusters became more organised. It developed into a band type structure and intensity was estimated as T1.5 with centre at $14.5^{\circ}\text{N}/69.0^{\circ}\text{E}$ at 1200 UTC of 1 June.

Gradually band structure of the cloud system improved and the system further intensified with intensity T2.0 and centred near $15.0^{\circ}\text{N}/68.0^{\circ}\text{E}$ at 00UTC of 2 June. As the vortex moved westward during next six hours, spiralling of cloud band around the centre increased. The intensity was estimated as T2.5 at 0700UTC of 2 June. The position of the system centre at that time was $15.0^{\circ}\text{N}/67.0^{\circ}\text{E}$. Thereafter, both cloud band and convection around the system centre showed continuous improvement over next 36 hrs period. Accordingly, T-number also increased over this period and at 1800UTC of 3 June the estimated T-number was T4.0 with centre at $18.0^{\circ}\text{N}/66.5^{\circ}\text{E}$. The cloud pattern evolved into an eye pattern during next six hours and at 00UTC of 4 June eye was visible with system centre at $18.4^{\circ}\text{N}/65.1^{\circ}\text{E}$ and intensity T4.5. Very rapid intensification was observed during next 12 hours and the system gained its maximum intensity at 1500 UTC of 4 June. At this time, the eye temperature was 9.0°C with surrounding gray shade temperature of around -70.0°C and overall intensity was estimated as T6.5 corresponding to the intensity of Super Cyclonic Storm. The same intensity was observed till 1900 UTC of 4 June and weakening sign noticed from 2000 UTC of 4 June. The vortex centred at $20.7^{\circ}\text{N}/62.8^{\circ}\text{E}$ with intensity T6.0, CI 6.5 at 0000 UTC of 5 June. Moving in a north-westerly direction, the vortex gradually weakened during next 48 hours and it crossed the coast of Iran near $25.5^{\circ}\text{N}/58.2^{\circ}\text{E}$ with intensity T2.5 at 0400UTC of 7 June. Thus, contrary to synoptic observations, the satellite observations indicated no landfall over Oman

and hence the system had only one landfall over Iran. Visible and IR imageries of different observation times are depicted in Fig.22. The tropical IR imageries with CTT contour analysis of 30 May to 7 June are shown in Fig.23. The satellite observed position and intensity of the vortex are depicted in Table 3.

Table.3. Position and intensity of the cyclone „GONU’ as observed from INSAT imageries.

Date	Time (UTC)	Position (Lat / Long)	Intensity
31-05-07	0300	12.5N/73.5E	T 1.0
	0600	13.0N/73.0E	T 1.0
	1200	13.5N/73.0E	T 1.0
	1800	13.5N/73.0E	T 1.0
01-06-07	0000	14.0N/72.0E	T 1.0
	0600	14.0N/71.0E	T 1.0
	1200	14.5N/69.0E	T 1.5
	1800	15.0N/68.0E	T 1.5
02-06-07	0000	15.0N/68.0E	T 2.0
	0700	15.0N/67.0E	T 2.5
	1200	15.1N/66.8E	T 3.0
	1800	15.3N/66.7E	T 3.0
03-06-07	0000	15.4N/66.6E	T 3.5
	0600	16.1N/66.7E	T 3.5
	1200	17.5N/66.7E	T 3.5
	1800	18.0N/66.5E	T 4.0
04-06-07	0000	18.4N/65.1E	T 4.5
	0300	18.6N/64.9E	T 5.0
	0600	19.1N/64.7E	T 5.5
	0900	19.4N/64.4E	T 6.0
	1200	19.9N/64.1E	T 6.0
	1800	20.4N/63.6E	T 6.5
	2000	20.5N/63.5E	T 6.0 C.I. 6.5
05-06-07	0000	20.7N/62.8E	T 6.0 C.I. 6.5
	0400	21.0N/62.0E	T 5.5 C.I. 6.0
	0600	21.2N/61.7E	T 5.5 C.I. 6.0
	1200	21.7N/61.0E	T 5.0 C.I. 5.5
	1500	22.0N/60.9E	T 4.5 C.I. 5.0
	1800	22.1N/60.8E	T 4.5 C.I. 5.0
06-06-07	0000	22.7N/60.0E	T 4.5 C.I. 5.0
	0600	23.0N/59.5E	T 4.5 C.I. 5.0
	1200	23.5N/59.3E	T 4.5 C.I. 5.0
	1500	24.1N/59.2E	T 4.0 C.I. 4.5
	1800	24.2N/59.2E	T 4.0 C.I. 4.5
	2100	24.8N/58.8E	T 3.5 C.I. 4.0
07-06-07	0000	25.2N/58.4E	T 3.0 C.I. 3.5
	0300	25.4N/58.2E	T 2.5 C.I. 3.0
	0400	25.5N/58.1E	OVER LAND

5.4.2 SST:

The SST as observed by MODIS+TMI+AMSR-E during 4-7 June 2007 are shown in Fig. 24. It is observed that the Gulf of Oman was most warm ($>30^{\circ}\text{C}$) during the period. This warmer Gulf might have contributed to maintain the intensity of the system leading to a landfalling cyclone over Iran.

The warmer SST ($>30^{\circ}\text{C}$) around the system centre on 4 June 2007 (near 18.5°N and 65°E at 0000 UTC of 4 June 2007) might have contributed to maintain the intensification of the system in super cyclone stage. The subsequent fall in SST during 5-7 June contributed to gradually weakening of system even over the sea.

5.4.3. OLR and convection

The mean daily OLR distribution over Arabian Sea and neighbourhood area for 30 and 31 May, 2007 are shown in Fig. 25. The OLR distribution suggested persistence of convection on 30 May with OLR value less than 160 Wm^{-2} over an area of about $5^{\circ}\text{Lat} \times 5^{\circ}\text{Long}$ of southeast Arabian Sea. Further, it was observed that the area of intense convection with OLR values less than 140 Wm^{-2} increased over southeast Arabian Sea on 31 May. OLR distribution over Arabian Sea at 0600 UTC of 1 to 6 June, 2007 is shown in Fig. 26. The regions of low OLR with core value less than 100 Wm^{-2} were observed mostly on the western sector of the system and gradually moved north-northwest wards with the movement of the system during this period. The intense convection gradually increased upto 4 June night and minimum core value of OLR less than 80 Wm^{-2} was observed at 1800 UTC of 4 June near the system centre (Fig.26).

5.4.4 Water Vapour derived Wind Vectors (WVWV)

With the availability of Water Vapour derived Wind Vectors (WVWV) over the Indian region from Meteosat satellite of EUMETSAT and the Indian Satellite (Kalpana-1 and INSAT 3A), new possibility arises for application of this product in Cyclone tracking. Kelkar (1997) made a detailed review of satellite based techniques including (a) use of satellite derived mean wind flow, (b) animation of sequence of satellite imageries and extrapolation of the apparent motion of the cloud systems and (c) monitoring changes in the upper level moisture pattern using the Water Vapour (WV) absorption channel imagery. He had suggested that further refinements in the satellite based techniques could improve the cyclone track prediction. The WV channel does not show any features on the earth's surface, as the radiations emitted by the surface at these wavelengths are entirely absorbed by the low level atmospheric water vapour. Rather, the channel indicates the changes in water vapour in the middle and upper tropospheric levels as depicted by the successive half hourly images obtained from geostationary satellites. In addition, the wind vectors derived from WV imagery can be treated as representative of upper air wind fields. Due to the absence of upper air observations over the oceanic regions, WVWVs help considerably to understand the middle and upper tropospheric flow pattern, particularly over the

data sparse oceanic regions. Bhatia et al. (2006) have reported the use of WVVVs derived from METEOSAT-5 satellite for improving the track prediction of depressions that formed over Bay of Bengal in the monsoon season of 2005. Thus WVVVs can also be used for monitoring the TCs and prediction of their movement of TCs on real time basis. Velden et.al. (1992,1997) have summarized a number of applications of WVVV produced from GOES satellite of USA.

The WVVVs derived operationally from satellite (METEOSAT-7) data at every synoptic hour by the Co-operative Institute for Meteorological Satellite Studies (CIMSS), University of Wisconsin-Madison have been used in the study. WVVVs are produced from water vapour drift motions using WV imagery by identifying and tracking targets to obtain approximations of layer-mean motions, with a height assignment of the target using the radiometric signal. The basic steps of WVVV production are (a) selecting a feature to track a target (b) tracking the target in a time sequence of images to obtain a relative motion (c) assigning a pressure height (altitude) to the vector and (d) assessing the quality of the vector. Heights are assigned from the water vapour brightness temperature in clear sky conditions and from radiative transfer techniques in cloudy regions. The clear sky WVVVs are representative of layer mean motion while cloudy sky WVVVs are cloud top motion. The middle- and upper- level winds derived from geostationary satellites are one of the most practical products in cyclone operations. As WVVVs represent the middle and upper tropospheric (500 hPa – 100 hPa) flow pattern, so it is the equivalent of having a large number of upper-air stations over oceanic regions at all times to supplement the conventional upper air observations. Use of this additional data helps in assessing the prevailing synoptic pattern, which is important for the diagnosis and the forecast of all tropical systems.

Meteosat water vapour winds of 00UTC for the period 1 to 7 June, 2007 are depicted in Fig.27. The actual position of the system, prevailing wind pattern, suggested movement of the system based on WVVV products and actual movement of the system are shown in Table-4. During 1-2 June, an anti-cyclonic circulation at 100-250 hPa lay over east central Arabian Sea with ridge line passing around lat 15-16 ° N over the Arabian Sea and the system was south of the ridge line. Northwest movement of the system was suggested by the prevailing steering wind of 100-250 hPa. This was found to be consistent with the observed movement of the system. On 4 June morning, the ridge was located along lat. 20 ° N and the anticyclone lay over north-east Arabian Sea. As the system lay south of the ridge line, the steering WVVV wind suggested west-northwesterly movement of the system, when the system showed northwesterly movement. In the evening when the system was intensifying into a super cyclonic storm, WVVV showed northwesterly movement of the system. The environmental flow at this level got modified marginally by the storm. On 5 June morning, the ridge line lay along 20.5 ° N , suggesting west-northwesterly movement of the system. The observed movement was also west-northwesterly. During 5 June evening to 6 June morning, WVVV suggested northwesterly movement of the system when the observed movement was also in a

northwesterly direction. On 6 June evening WVVV suggested northerly movement at the time of landfall and then north-northeasterly movement of the system. It was in agreement with the observed movement of the system. The system moved north-northeasterly after the landfall under the influence of an upper tropospheric trough in westerly lying to the west of the system centre.

Thus, it was observed that WVVVs are very useful in real time monitoring and tracking of super cyclone 'GONU' and more research efforts are required to generate more accurate and reliable WVVVs in real time.

Table 4: Features observed in WVVV in association with the Super Cyclone 'GONU'

System location			Winds over the storm centre	Suggested movement	Actual movement
Time (UTC)	Lat . (°N)	Long (°E)			
010000	14.0	72.0	SE	NW	NW
011200	14.5	69.0	SE	NW	NW
020000	15.0	68.0	ESE	WNW	WNW
040000	18.5	65.0	ESE	WNW	W
041200	20.0	64.0	SE	NW	W
050000	20.5	63.0	E	W	WNW
051200	21.5	61.0	ESE	WNW	NW
060000	22.5	60.0	SE	NW	NW
061200	23.5	59.5	SSW	NNE	N

5.4.5. QPE analysis associated with the vortex GONU

Analysis of daily Quantative Precipitation Estimation (QPE) associated with the system for the period 4 to 7 June is shown in Fig. 28. The maximum value of QPE (less than 65 mm) on the southwest sector of the system was observed on 4 June which is in agreement with the distribution of maximum convective cloud zone. On the date of landfall over Iran i.e, 7 June, the maximum QPE value was about 45mm over coastal area of Iran. Arkins method (Arkin, 1983) has the limitation to estimate the heavy rainfall.

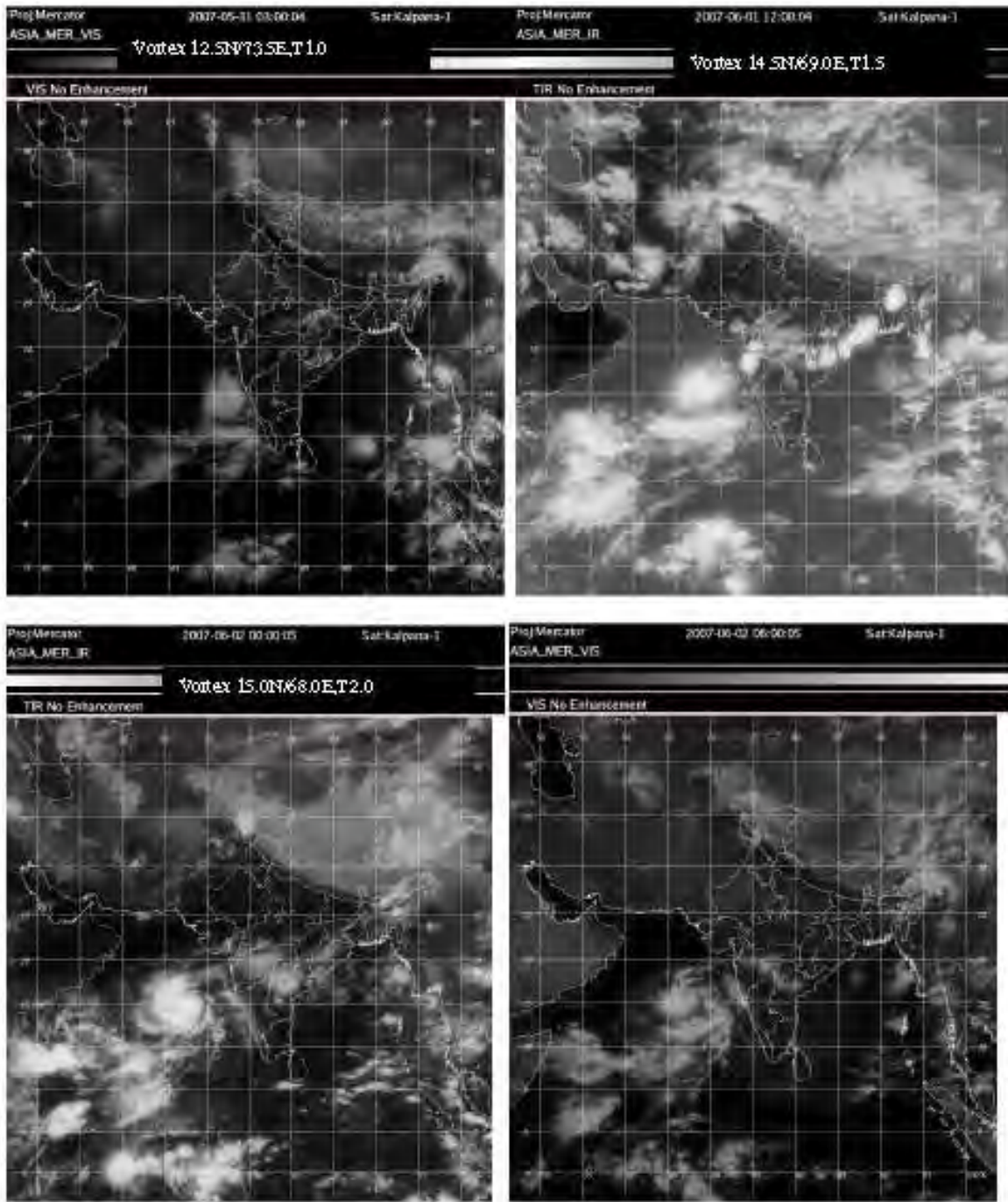


Fig. 22(a) Satellite imageries (Visible/IR) of different time of observation and dates associated with the cyclone GONU.

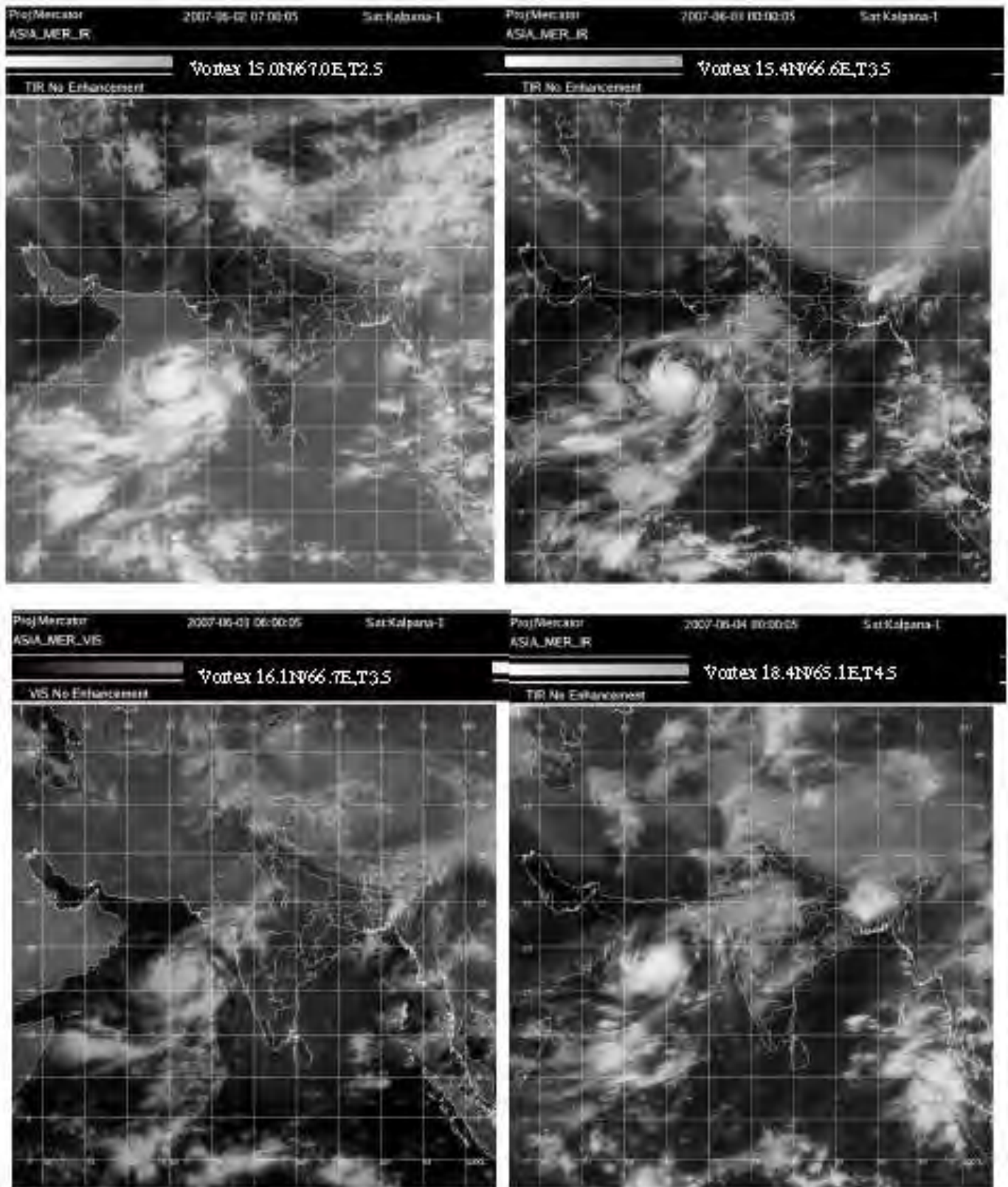


Fig. 22(b) Satellite imageries (Visible/IR) of different time of observation and dates associated with the cyclone GONU.

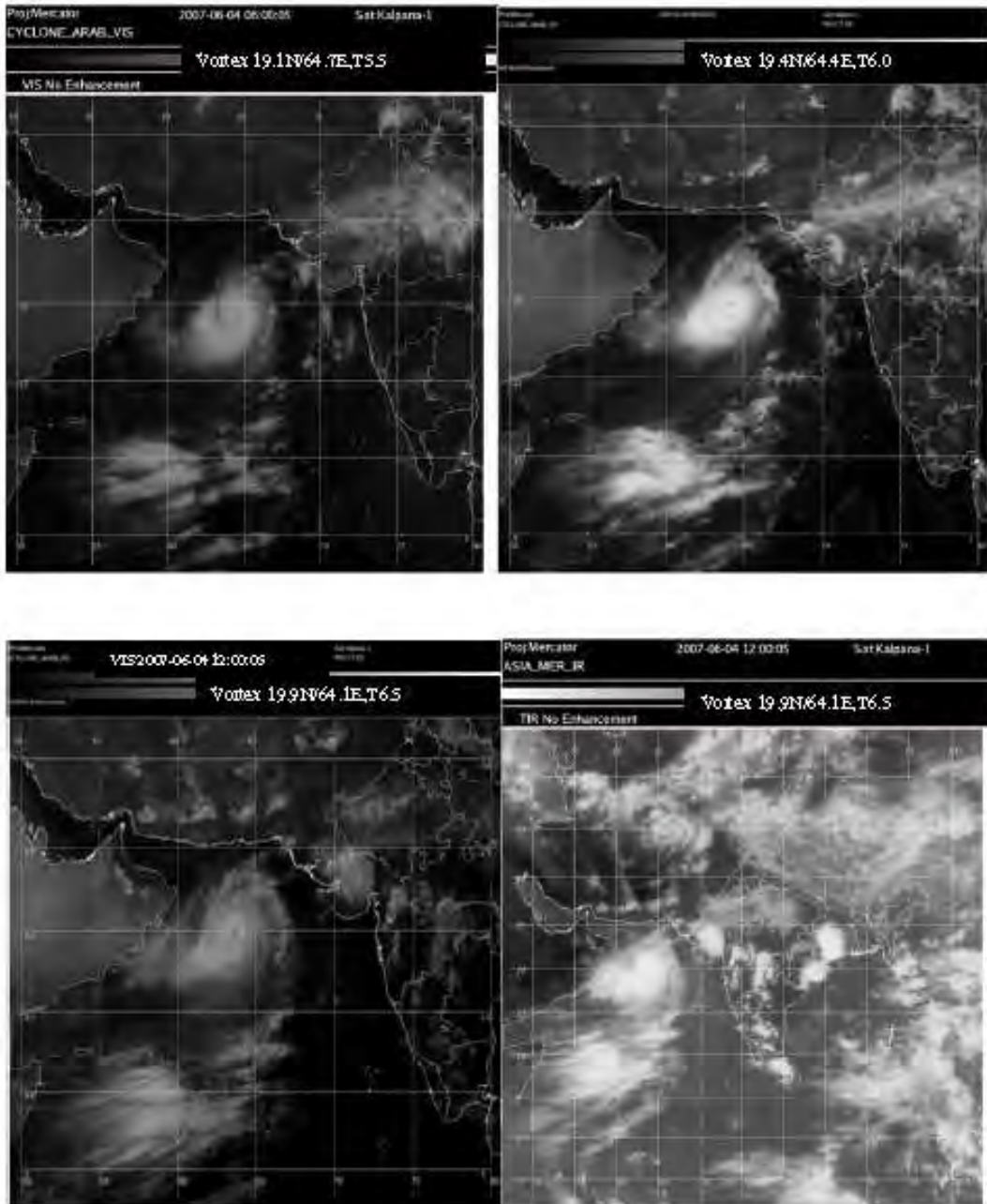


Fig. 22(c) Satellite imageries (Visible/IR) of different time of observation and dates associated with the cyclone GONU.

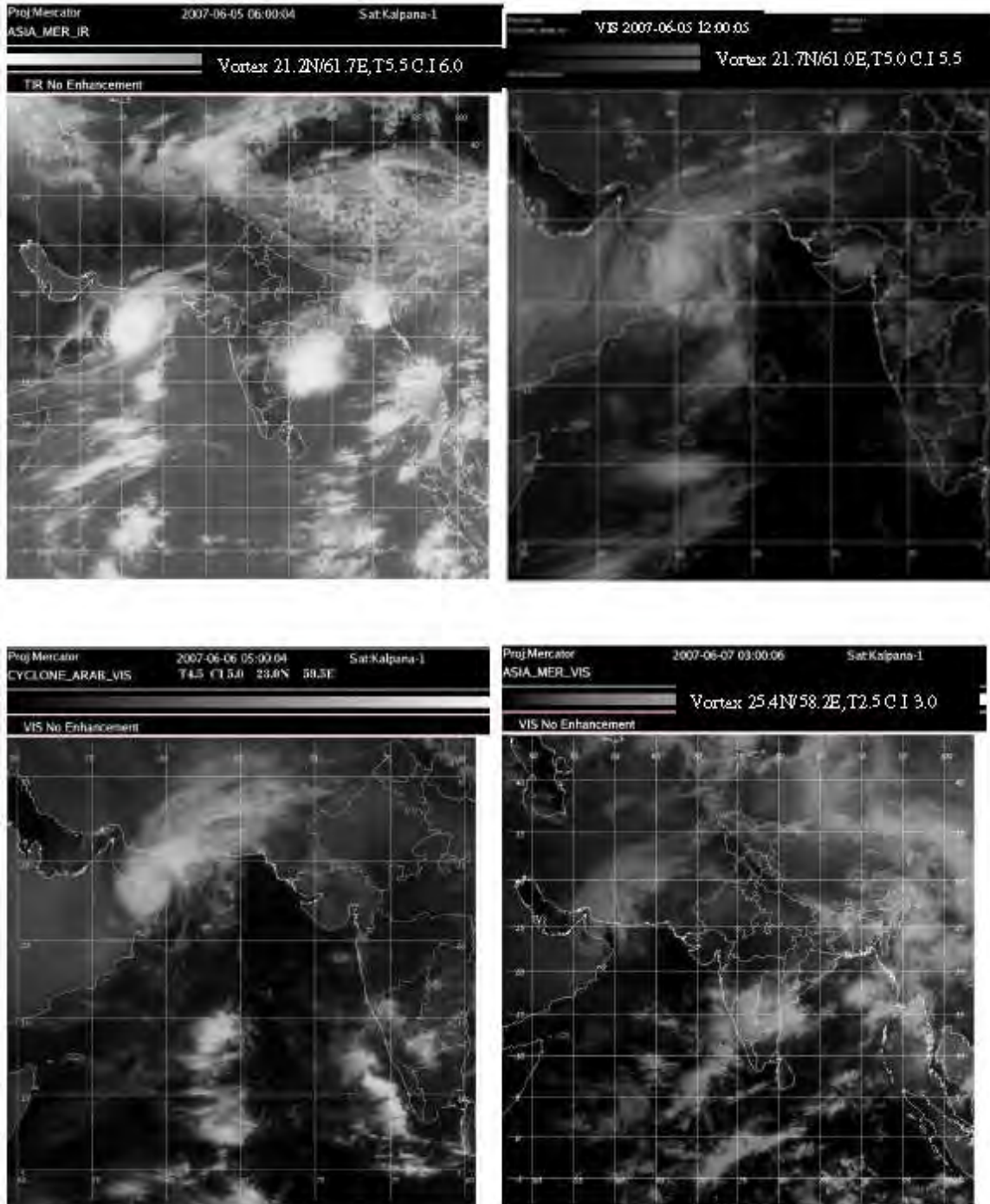


Fig. 22(d) Satellite imageries (Visible/IR) of different time of observation and dates associated with the cyclone GONU.

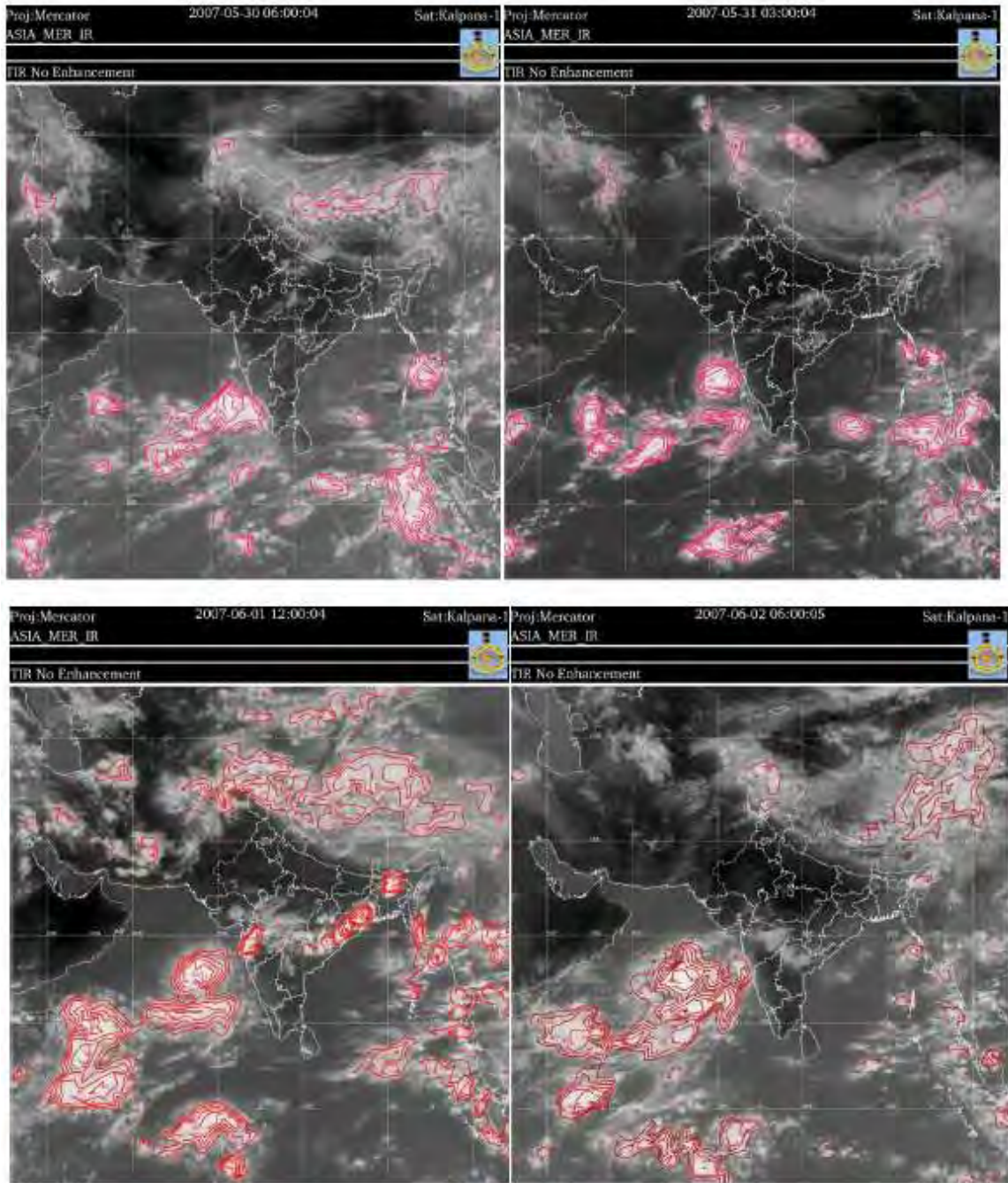


Fig. 23(a) IR imageries with CTT contour analysis of different time of observation and dates associated with the cyclone GONU'.

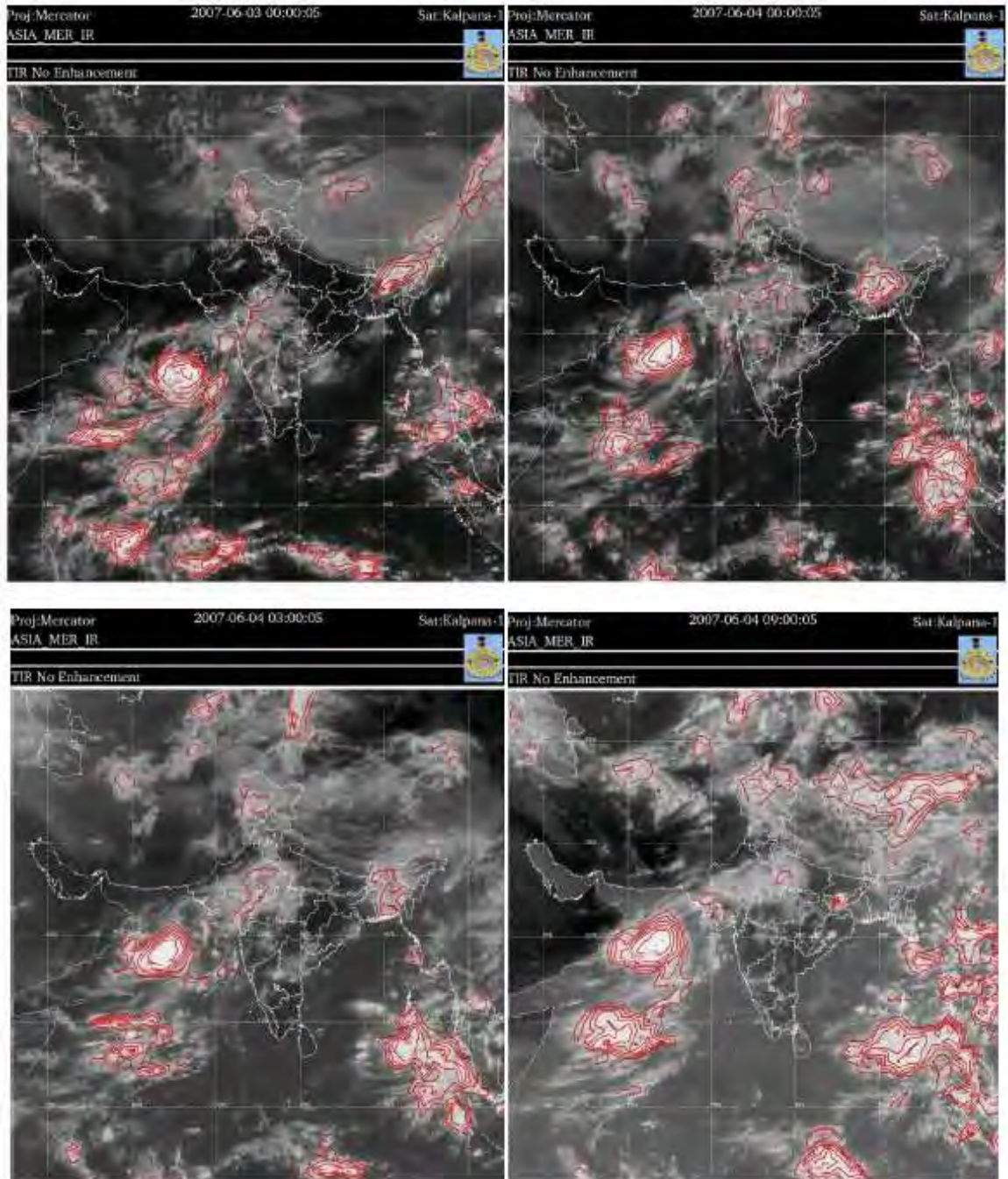


Fig. 23(b) IR imageries with CTT contour analysis of different time of observation and dates associated with the cyclone GONU.

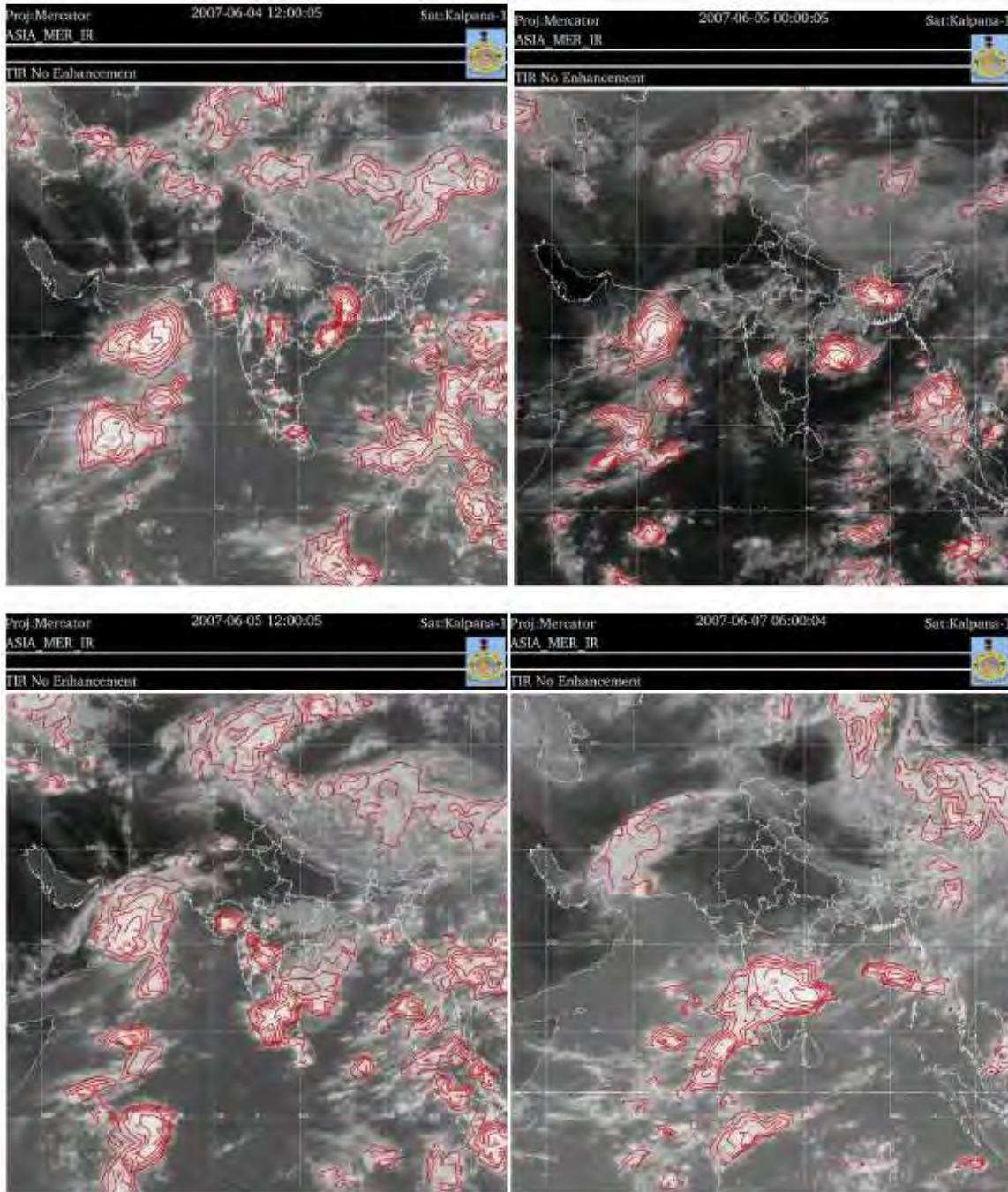


Fig. 23(c) IR imageries with CTTcontour analysis of different time of observation and dates associated with the cyclone 'GONU'.

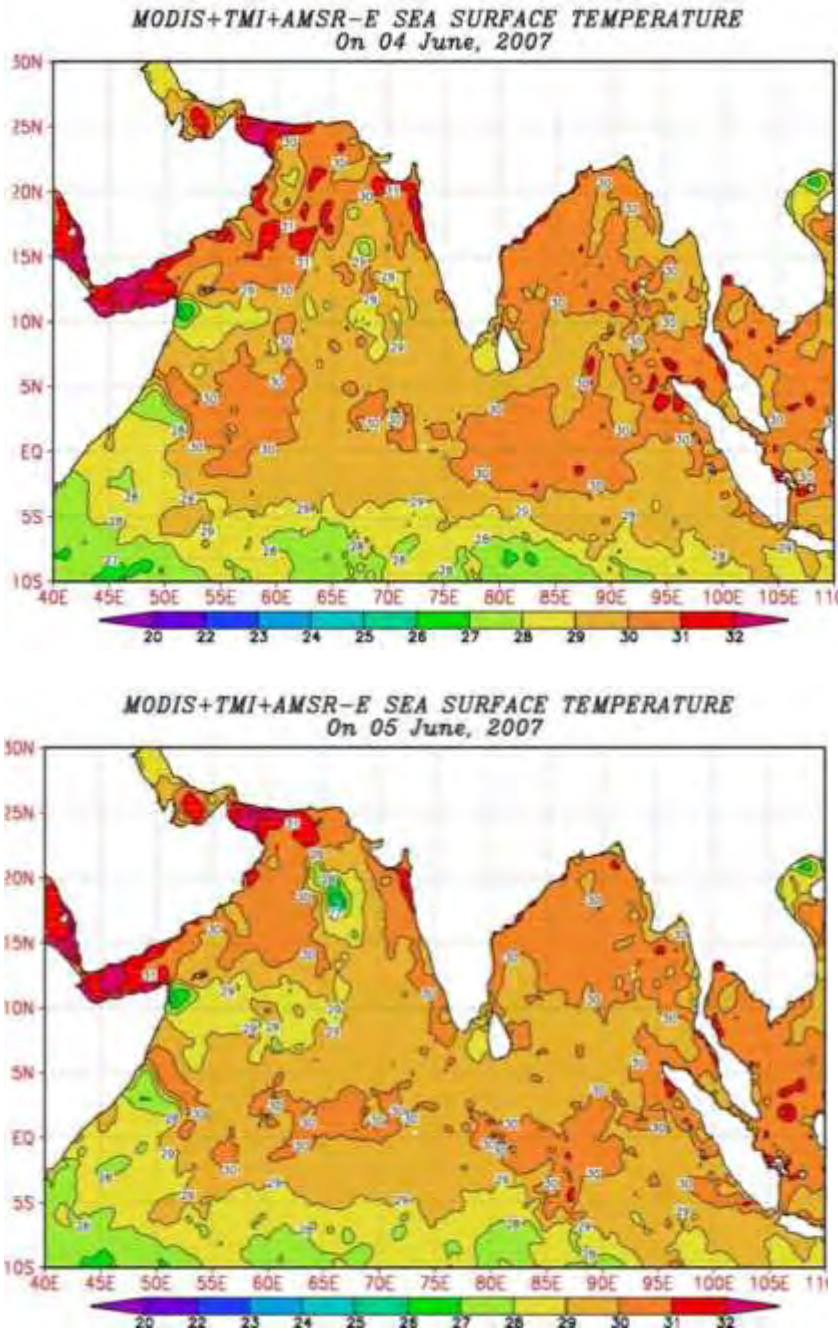


Fig. 24. Sea surface temperature (SST) over the north Indian Ocean during 4-7 June 2007.

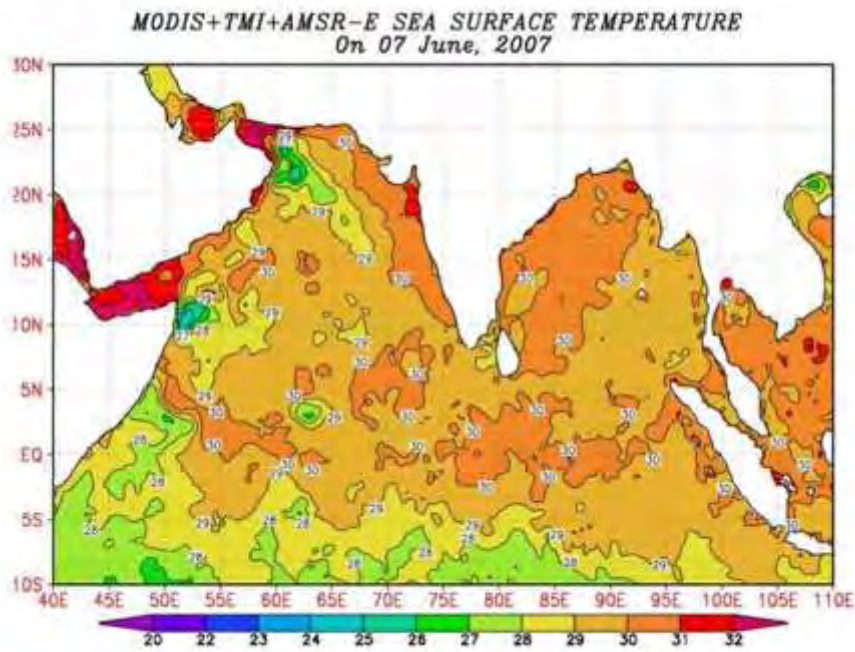
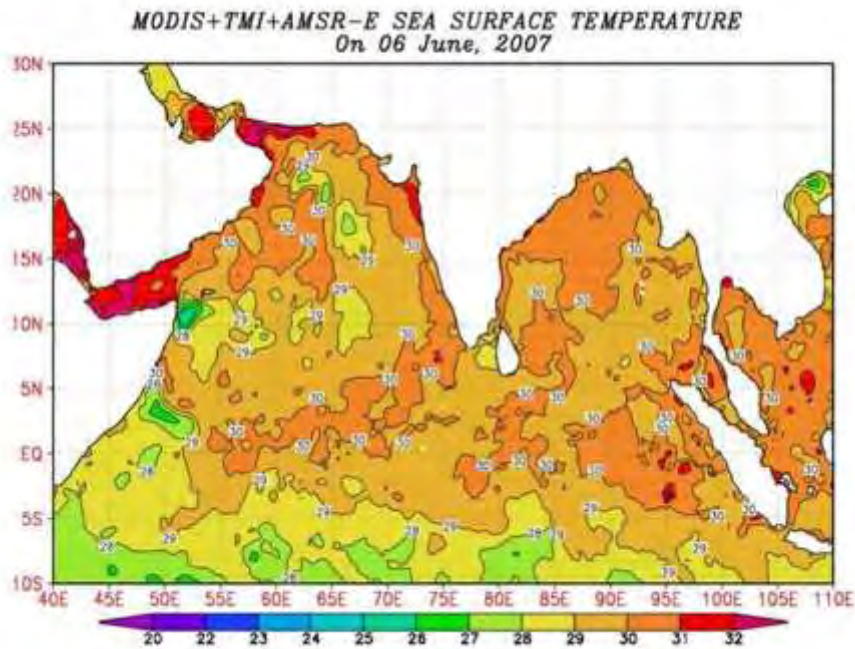


Fig. 24(contd.). Sea surface temperature (SST) over the north Indian Ocean during 4-7 June 2007.

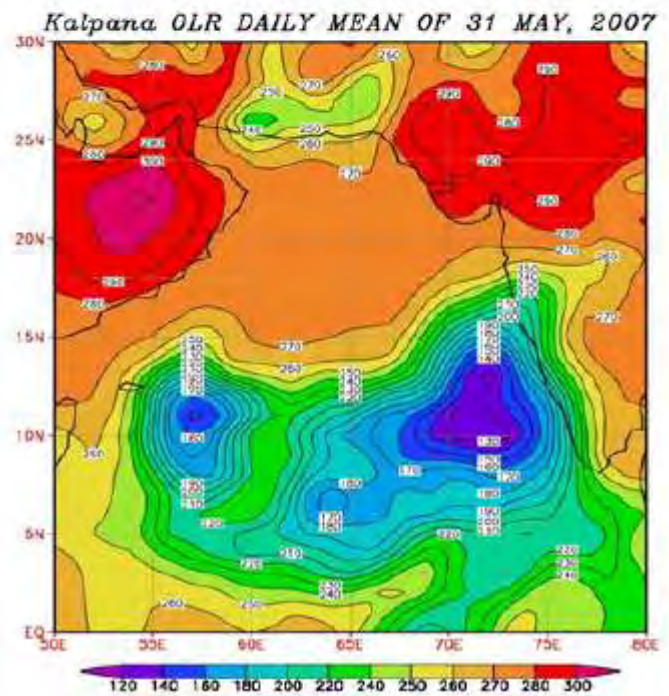
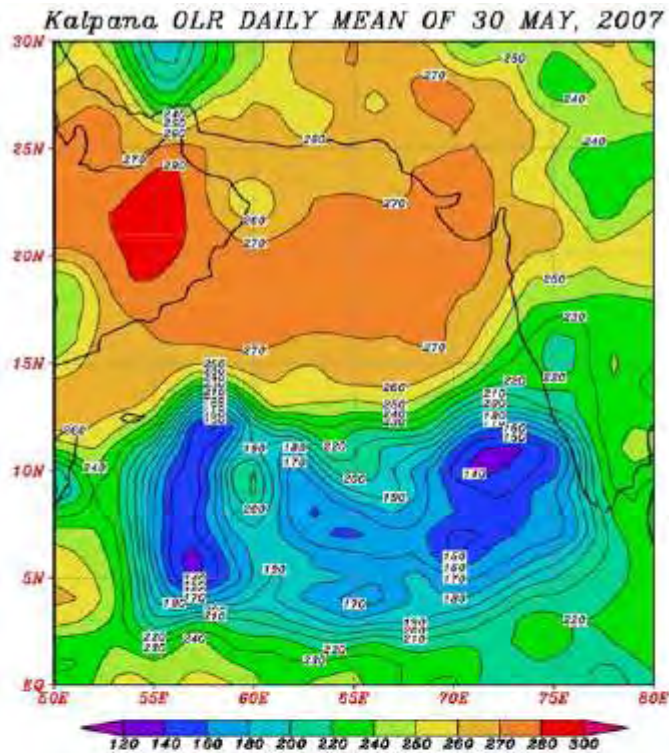


Fig.25. The mean daily OLR distribution over Arabian Sea and neighbourhood area for 30 and 31 May, 2007

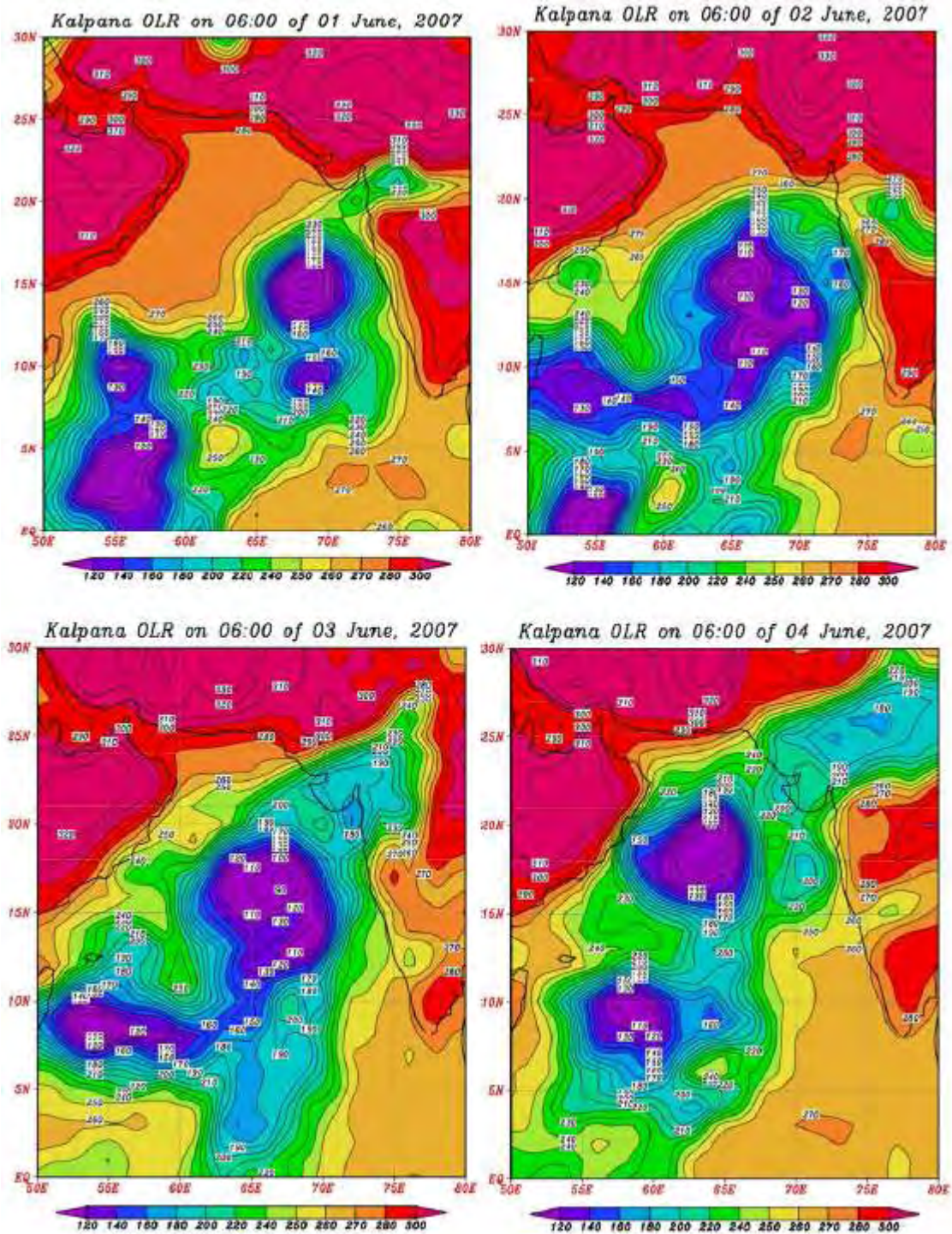


Fig.26(a).The OLR distribution at 0600 UTC associated with cyclone ‘GONU’ area for 1- 4 June, 2007

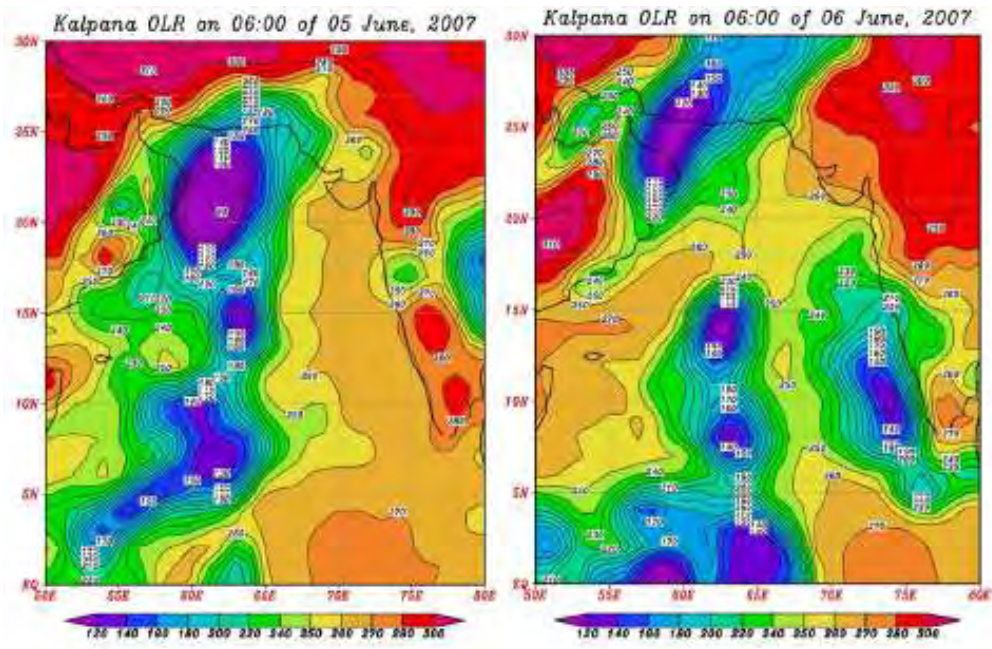


Fig.26(b).The OLR distribution at 0600 UTC associated with cyclone GONU' area for 5 & 6 June, 2007

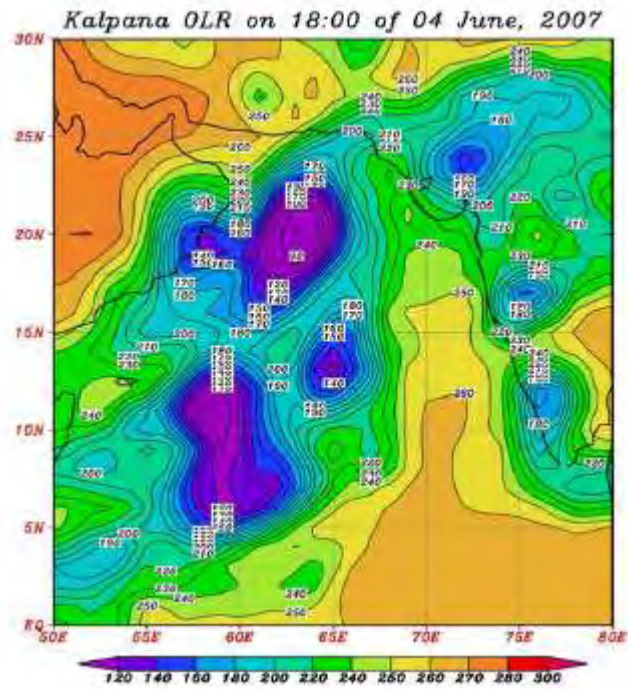
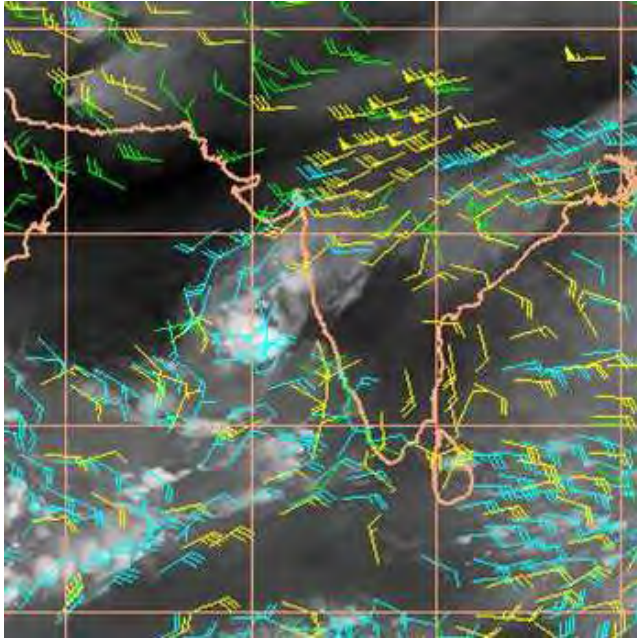
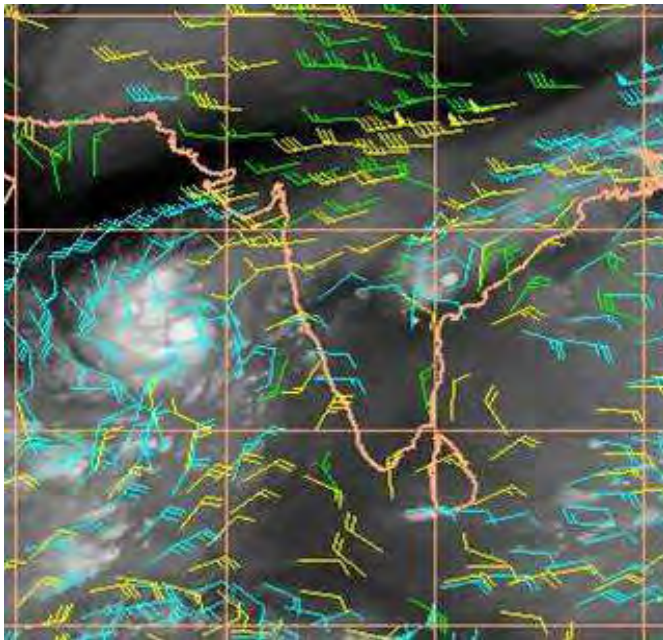


Fig. 26 (c). The OLR distribution at 1800 UTC of 4June,2007 associated with cyclone GONU'

(a) 1 June, 2007



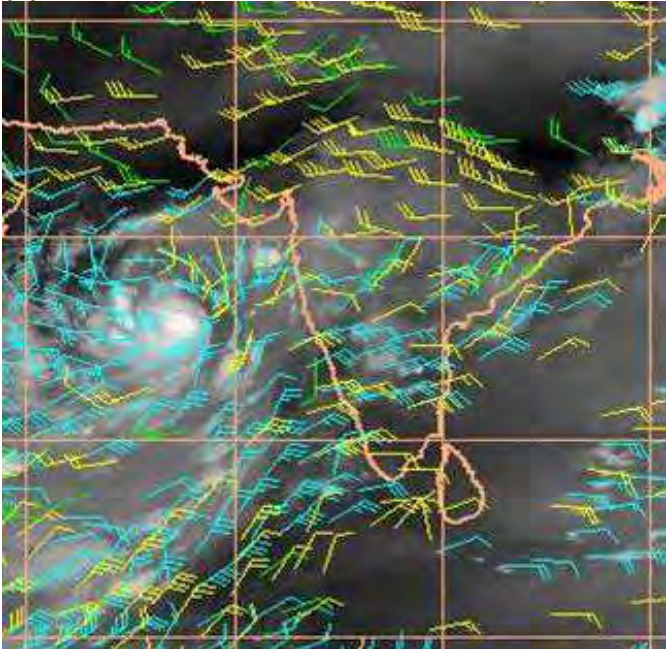
(b) 2 June, 2007



Blue: 100-250 hPa, Yellow: 251-350 hPa, Green 351-500 hPa

Fig .27(a-f) Meteosat Water Vapour winds of various layers at 00UTC for the period 1-6 June, 2007

(c) 3 June, 2007



(d) 4 June, 2007

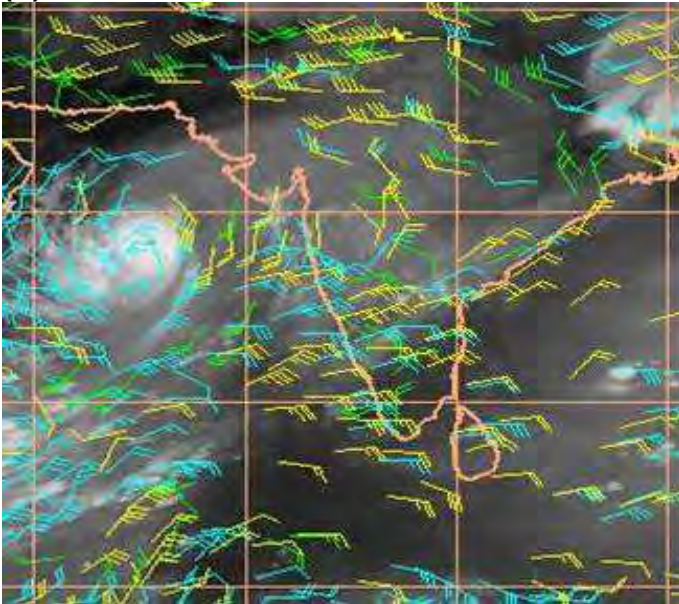
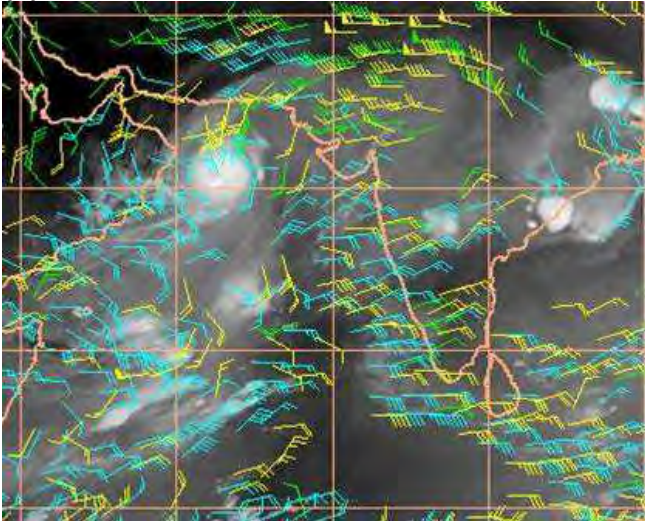


Fig .27(Contd). Meteosat Water Vapour winds of various layers at 00UTC for the period 1- 6 June, 2007

(e) 5 June, 2007



(f) 6 June, 2007

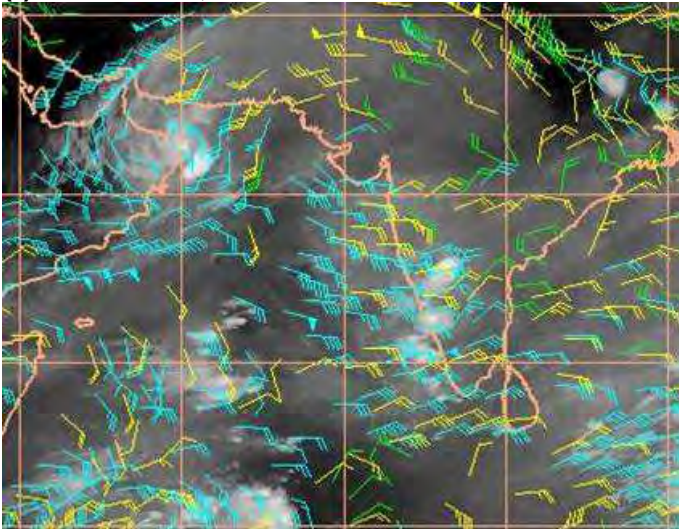
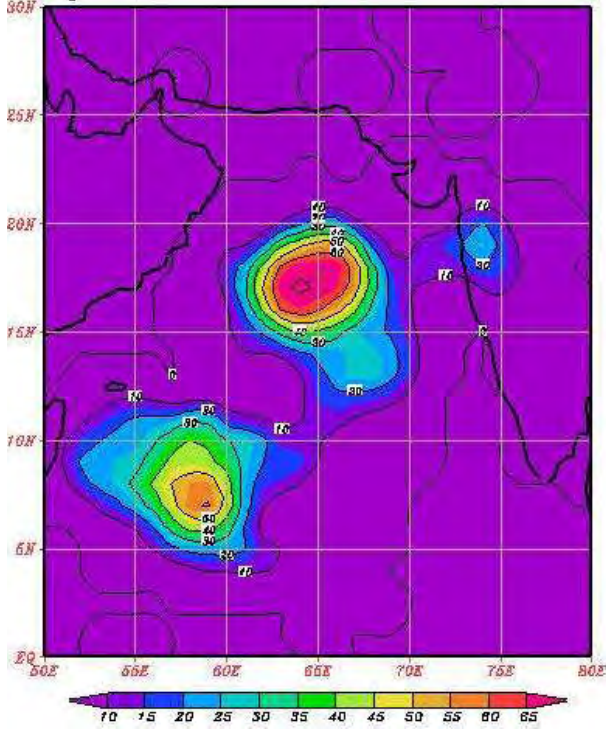


Fig. 27 (Contd). Meteosat Water Vapour winds of various layers at 00UTC for the period 1-6 June, 2007

(a) 4 June, 2007



(b) 5 June, 2007

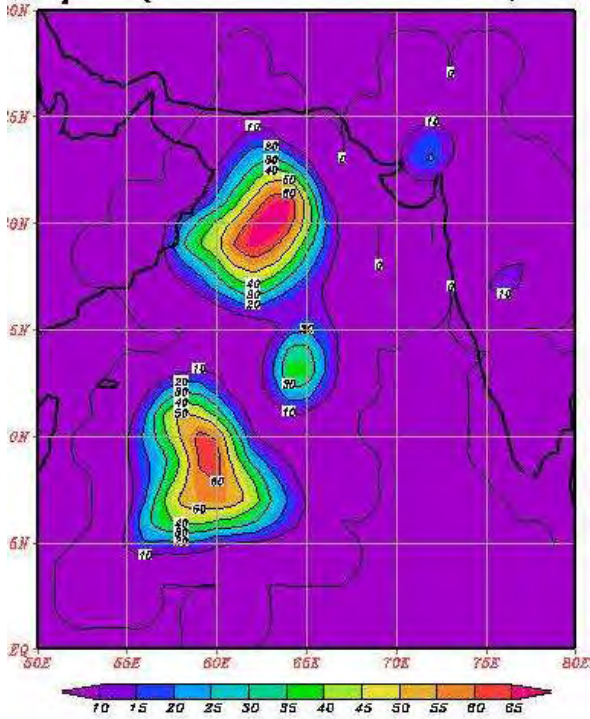
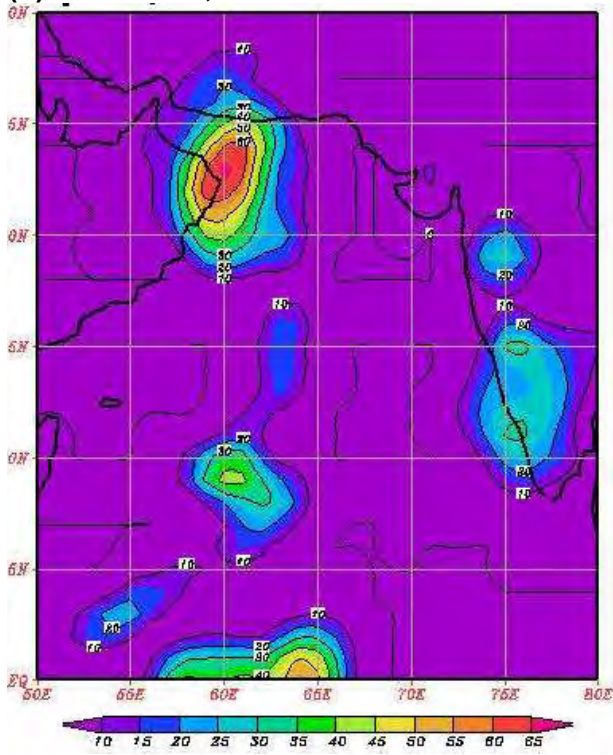


Fig. 28(a-d) Daily QPE analysis for the period of 4- 7June, 2007

(c) 6 June, 2007



(d) 7 June, 2007

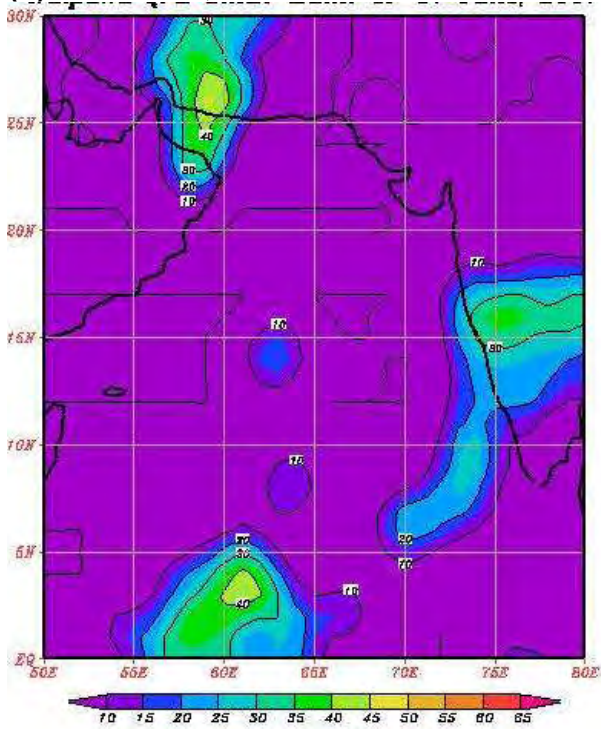


Fig. 28(a-d)(contd.) Daily QPE analysis for the period of 4-7 June, 2007

6. Features observed through other satellites

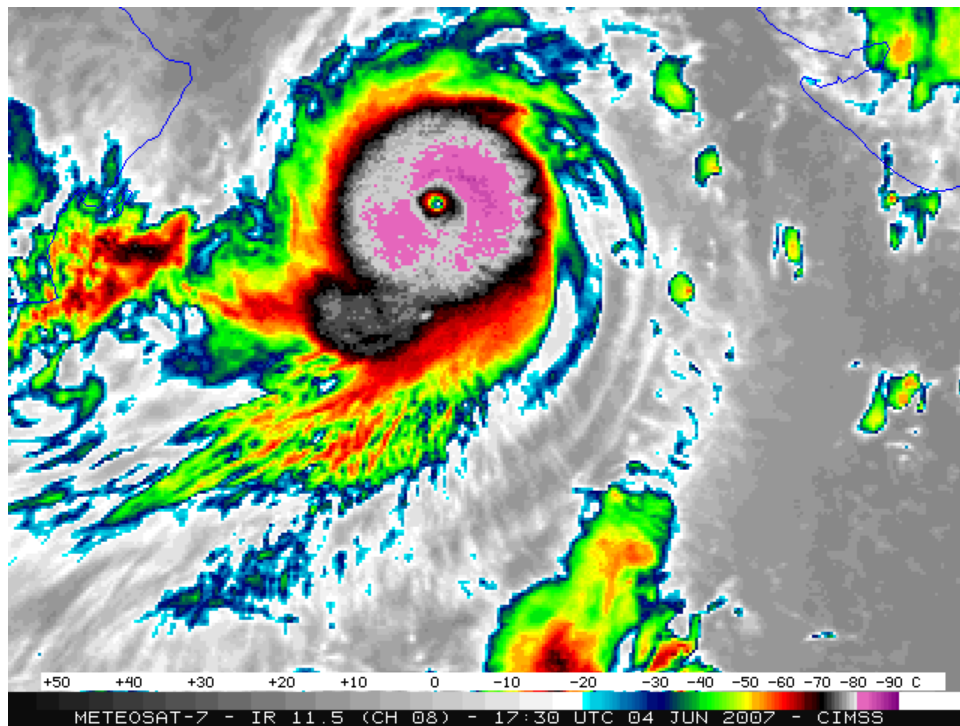


Fig. 31 Meteosat -7 IR imageries of cyclone GONU at 1730 UTC of 4 June.

According to METEOSAT-7, the system also intensified rapidly during 03-04 June 2007. METEOSAT-7 InfraRed (IR) imagery showed very cold brightness temperature values (-80° to -88° C, violet to purple enhancement) in the eyewall region during much of the 2-day period. A distinct eye was apparent on the METEOSAT-7 IR images, as well as on the METEOSAT-7 visible images on 04 June, 2007. A typical imagery is shown in Fig. 29

An overpass of the NOAA-17 satellite occurred at 17:33 UTC on 04 June; the IR image (Fig. 30) depicted a detailed “banded structure” to the cold brightness temperature field, with a minimum temperature of -89° C (darker purple enhancement). Also the area of gravity waves south of the eye (within the gray-to-white enhanced area of -75° to -79° C brightness temperatures) were observed.

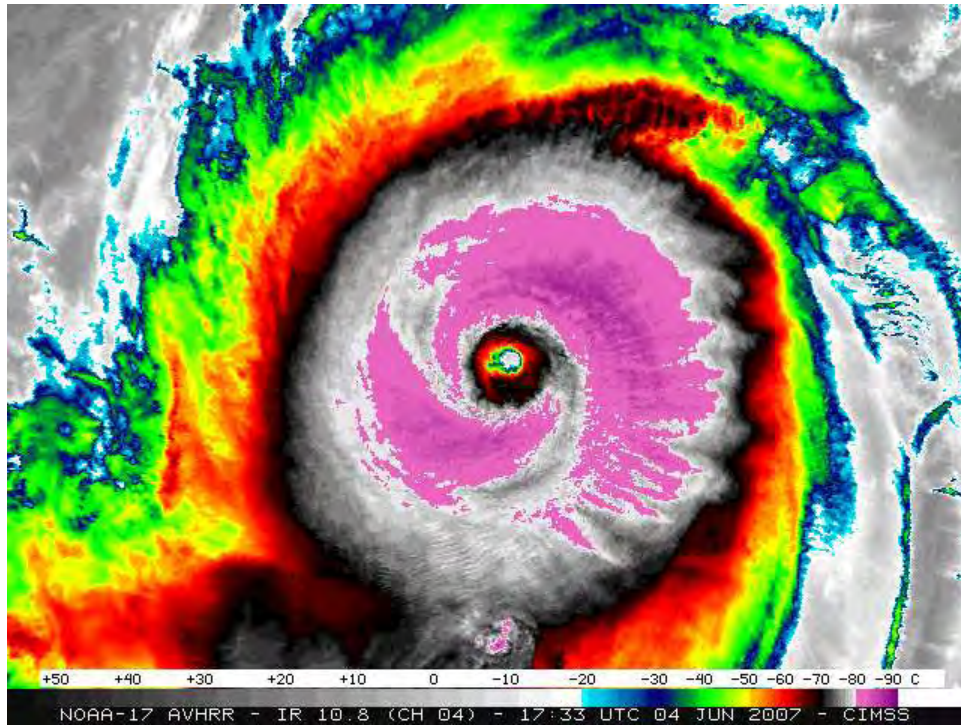


Fig. 30. Meteosat -17 AVHRR-IR imageries at 1733 UTC of 4 June 2007.

The CIMSS Advanced Dvorak Technique (ADT) is a satellite-based method of estimating tropical cyclone intensity — the ADT plot (*Fig. 31*) indicated that **GONU** intensified very rapidly from late in the day on 03 June (day 2007154) to early in the day on 04 June (day 2007155), reaching Category 5 intensity (with 140 knot wind speed). This was the first tropical cyclone of Category 5 strength on record in the Arabian Sea.

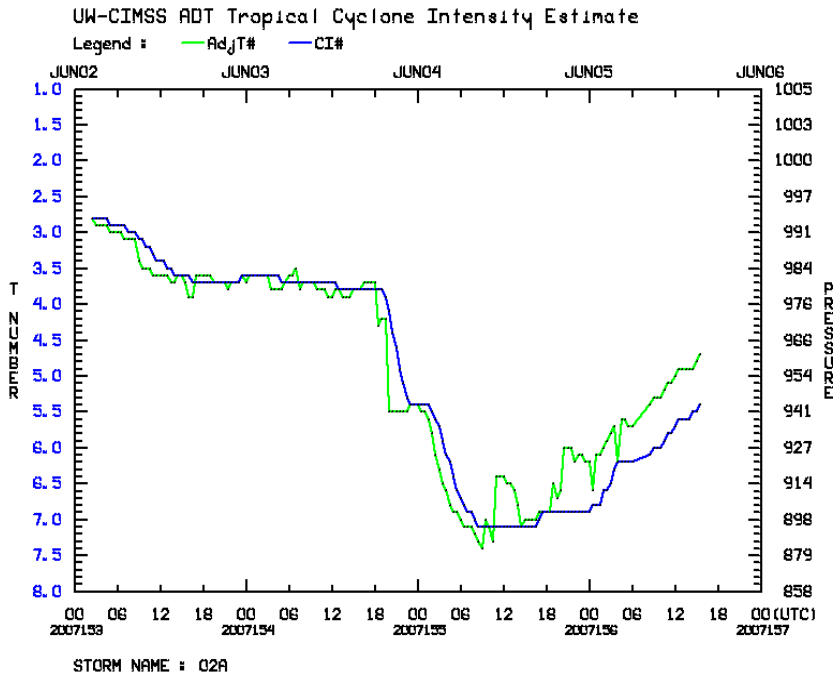


Fig. 31. Relation between ADT T number and lowest MSLP of cyclone GONU according to CIMSS ADT

7. Performance of dynamical and statistical models

Fig. 32 presents the forecast tracks of the system based on initial condition of 00 UTC of 4 June by operational NWP models along with the observed track. In this case, the T254 forecast track showed southwesterly movement when the system moved north northwest wards. QLM and ECMWF both could capture the northwesterly movement of the system relatively better than T-254. In this case (Table 5), T-254 showed landfall position error of 930 km in the 72 hours forecast. ECMWF showed landfall position errors of 400 to 500 km in the 24 hours to 72 hours forecast period. QLM showed landfall position errors of 395 km in the 72 hours forecast and 505 km in the 24 hours forecast. Out of the three models (ECMWF, NCMRWF T-254 and QLM) compared here for the prediction of cyclone track, ECMWF is found to be the best one, followed by QLM. However, the intensity of the system was under-estimated by all the models. Again ECMWF model performance was relatively better.

A major problem in the use of NWP model over the tropics is the near absence of data over the large oceanic region. In view of the importance of these data in the tropical numerical weather prediction, IMD has been in the process of implementing a massive modernization programme for upgrading and enhancing its observational system. From this modernization programme, good quality observations (both conventional and non conventional) are expected to be available on the mesoscale both in space and time by means of Doppler Weather Radar (DWR), Satellites (INSAT-3D Radiance), wind profilers, meso-network (Automatic Weather Stations), buoys and aircrafts in the real time mode to ingest into the assimilation cycle of global, regional and mesoscale NWP models.

Table 5: NWP model performance of Arabian Sea Super Cyclone GONU during June 2007

Models	Initial Date/time (UTC)	Landfall Fcst point Lat. /long.	Landfall Fcst time Date/ Time (IST)	Landfall Error (km)	Landfall time error (hours)
T254	03/00 04/00 05/00	17.5/56.0 ---- ----	07/0530	930	3 hrs delay
ECMWF	04/00 05/00 06/00	21.0/58.5 22.0/60.0 22.2/60.0	06/1730 06/2230 06/2030	500 425 410	15 hrs early 4 hrs early 6 hrs early
QLM	04/00 05/00 06/00	21.8/60.1 24.0/58.9 21.1/59.8	06/1730 ---- 06/2300	395 ---- 505	18 hrs early no landfall 4 hr early

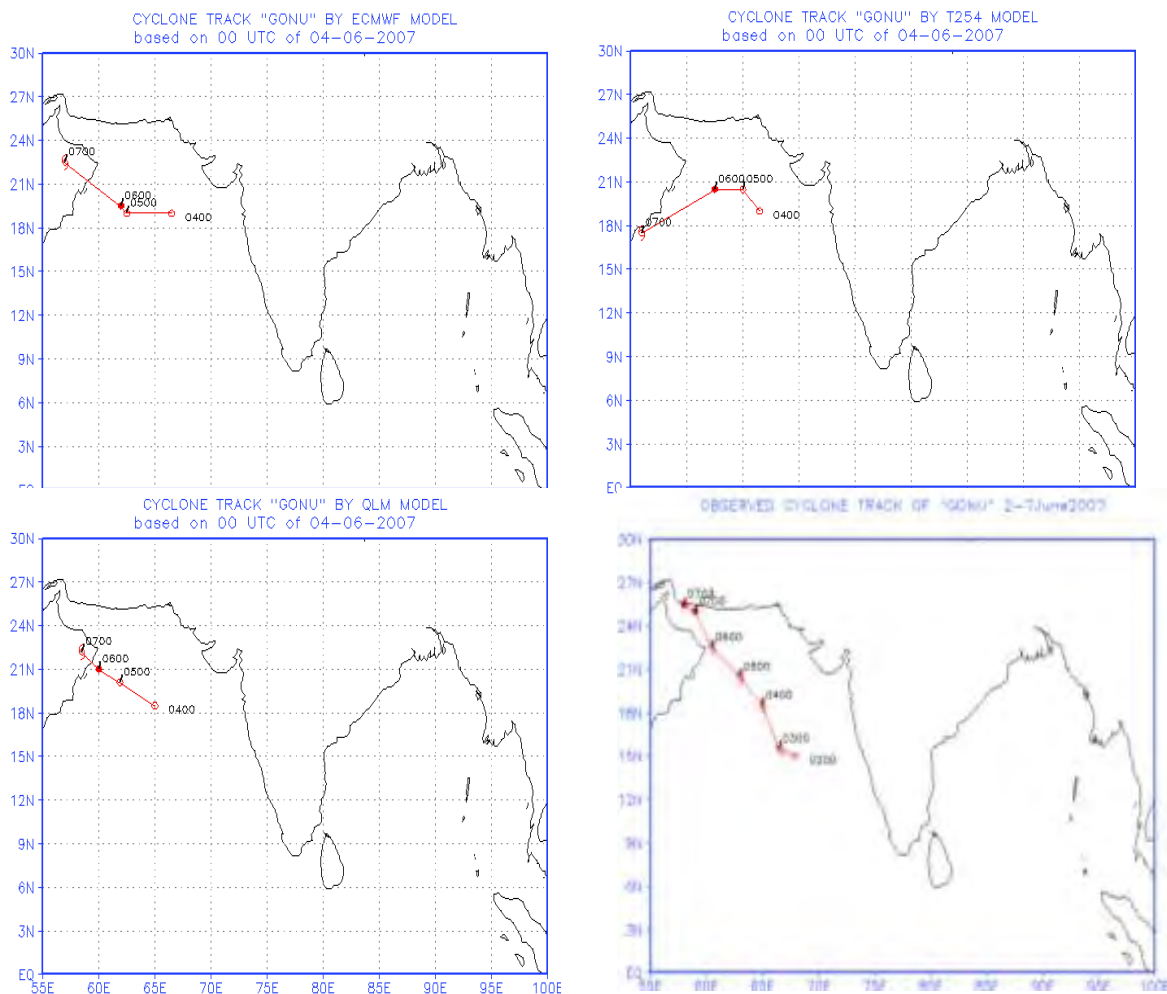


Fig. 32 Predicted Track of NWP models for the Cyclone, „GONU’

The performance of CLIPER model during cyclone **GONU** is given in Table6.

Table 6: Performance of CLIPER model during **GONU**

Based Time	Forecast period (hrs)	
	12	24
02.06.2007/1200	47	235
03.06.2007/0000	182	209
03.06.2007/1200	112	164
04.06.2007/0000	32	86
04.06.2007/1200	51	146
05.06.2007/0000	110	165
05.06.2007/1200	51	211
06.06.2007/0000	148	333
Average	91	193

As seen in previous cases, in this case also, the CLIPER model performance was good only for very short range forecast (up to 12 hrs).

8. Performance of RSMC, New Delhi

The system was monitored by IMD and warnings were issued to various national and international agencies including Oman and Iran and to public through its cyclone warning organizations. The statistics of warnings issued by RSMC, New Delhi are given below:

Special Tropical Weather Outlook – 02
Tropical cyclone advisories – 39
Tropical Cyclone Advisories for international civil aviation – 18

8.1 Intensity forecast

The intensity forecast issued by RSMC, New Delhi has also been verified and the results are shown in Table 7. The intensity has been predicted for subsequent 24 hrs and mentioned in terms of Dvorak's T number. For this purpose the bulletins issued by RSMC, New Delhi and the best track parameters published by RSMC, New Delhi (RSMC-2008) have been referred. It is found that the average intensity forecast error of RSMC, New Delhi has been T 0.85 in case of **GONU**. However, the maximum intensity of the system was predicted to be T 6.5 which was found to be correct with of course a difference in time of occurrence.

Table 7: 24 hrs Intensity forecast verification of cyclone GONU during the period 2.6.07 to 7.6.07

Based on Chart	Present Intensity	Forecast Time	Forecast Intensity	Actual Intensity	Error
020900	2.5	030900	3.5	3.5	00
021200	3.0	031200	4.0	3.5	0.5
021500	3.0	031500	4.0	3.5	0.5
021800	3.0	031800	4.0	4.0	00
022100	3.0	032100	4.0	4.0	00
030000	3.5	040000	4.5	4.5	00
030300	3.5	040300	4.5	5.0	0.5
030600	3.5	040600	4.5	5.5	1.0
030900	3.5	040900	4.5	6.0	1.5
031200	3.5	041200	4.5	6.0	1.5
031500	3.5	041500	4.5	6.5	2.0
031800	4.0	041800	5.0	6.5	1.5
032100	4.0	042100	5.0	6.0	1.0
040000	4.5	050000	5.0	6.0	1.0
040300	5.0	050300	6.0	6.0	00
040600	5.5	050600	6.5	5.5	1.0
040900	6.0	050900	6.5	5.5	1.0
041200	6.0	051200	6.5	5.0	1.5
041500	6.5	051500	6.5	4.5	2.0
041800	6.5	051800	6.5	4.5	2.0
042100	6.0	052100	5.5	4.5	1.0
050000	6.0	060000	5.5	4.5	1.0
050300	6.0	060300	5.5	4.5	1.0
050600	5.5	060600	5.0	4.5	0.5
050900	5.5	060900	5.0	4.5	0.5
051200	5.0	061200	4.5	4.5	00
051500	4.5	061500	3.5	4.5	1.0
051800	4.5	061800	3.5	4.0	0.5
052100	4.5	062100	2.5	3.5	1.0
060000	4.5	070000	2.5	3.0	0.5
060300	4.5	070300	3.5		
060600	4.5	070600	3.5		
060900	4.5	070900	4.0		
061200	4.5	071200	4.0		
061500	4.5	071500	3.5		
061800	4.0	071800	3.0		
062100	3.5	072100	2.5		
070000	3.0	080000	2.0		
Total					25.5
Average					0.85
Total no. of observations verified					30

8.2 Track and land forecast

First Landfall Forecast for Oman was issued at 1200 UTC of 4 June, 2007 (36 hrs in advance of landfall over Oman). It was stated in the bulletin that system would cross Oman coast close to Lat. 22.5⁰N around 0000 UTC of 6 June. The system also crossed Oman coast near Lat. 22.5⁰N between 0200-0300 UTC of 6 June.

First Landfall Forecast for Iran was issued at 1500 UTC of 6 June. The bulletin stated that the system would cross Iran coast near Long. 58.0⁰E by 1200 UTC of 7 June, 2007. The system crossed Iran coast near Long. 58.8⁰E between 0300 & 0400 UTC of 7 June, 2007.

The 12 and 24 hrs landfall forecast errors are shown in Table 8. They were about 11 km in each case.

Table 8: 12 and 24 hrs landfall forecast errors of RSMC, New Delhi in case of GONU

Name Of cyclone	Life Period	Maximum intensity (Category)	24 hours Landfall error		12 hours Landfall error	
			Position (km)	Time (hr)	Position (km)	Time (hr)
GONU (ARS)	1-7 June 2007	SuCS	11	2.5	11	0.0

The 12 and 24 hrs track forecast error are shown in Table 9. The average 12 and 24 hrs track error of RSMC, New Delhi were 94 and 137 kms respectively. The performance was better than CLIPER indicating better skill of RSMC forecast.

Table 9: 12 and 24 hrs track forecast error of RSMC, New Delhi in case of GONU

Time of issue	Base timet	Present position (°N/°S)	FCST verification of 12 hrs				FCST verification of 24 hrs			
			Time	FCST (°N/°S)	Actual (°N/°S)	Error(km)	Time	FCST (°N/°S)	Actual (°N/°S)	Error (km)
02/2100	02/1200	15.0/67.0	03/0000	15.5/66.0	15.5/66.5	53	03/1200	16.0/65.0	17.5/66.5	231
03/0300	02/1800	15.0/67.0	03/0600	15.5/66.0	16.0/66.5	77	06/1800	16.0/65.0	18.0/66.0	246
03/0740	03/0000	15.5/66.5	03/1200	15.5/66.0	17.5/66.5	229	04/0000	16.5/65.0	18.5/65.0	222
03/1330	03/0600	16.0/66.5	03/1800	16.5/66.0	18.0/66.0	167	04/0600	17.0/65.0	19.0/64.5	228
03/2100	03/1200	17.5/66.5	04/0000	18.5/66.0	18.5/65.0	105	04/1200	19.5/64.5	20.0/64.0	76
04/0350	03/1800	18.0/66.0	04/0600	18.5/65.5	19.0/64.5	119	04/1800	19.5/64.5	20.5/63.5	152
04/0750	04/0000	18.5/65.0	04/1200	19.5/64.0	20.0/64.0	56	05/0000	20.5/63.0	20.5/63.0	00
04/1330	04/0600	19.0/64.5	04/1800	19.5/63.5	20.5/63.5	111	05/0600	20.5/62.0	21.5/61.5	123
04/2040	04/1200	20.0/64.0	05/0000	20.5/63.0	20.5/63.0	00	05/1200	21.5/61.0	21.5/61.0	00
05/0250	04/1800	20.5/63.5	05/0600	21.0/63.0	21.5/61.5	165	05/1800	22.0/62.0	22.0/60.5	154
05/0930	05/0000	20.5/63.0	05/1200	21.0/62.0	21.5/61.0	117	06/0000	22.0/60.0	22.5/59.5	76
05/1330	05/0600	21.5/61.5	05/1800	22.0/60.5	22.0/60.5	00	06/1200	O/L	-	-
05/2035	05/1200	21.5/61.0	06/0000	22.0/59.5	22.5/59.5	55	06/1800	-	25.0/59.0	-
06/0235	05/1800	22.0/60.5	06/0600	O/L	-	-	07/0000	-	24.5/59.0	-
06/0845	06/0000	22.5/59.5	06/1200	O/L	24.0/59.0	1254	07/0600	-	25.0/58.5	-
06/2100	06/1200	24.0/59.0	07/0000	24.5/58.5	25.0/58.5	56	07/1200	25.5/58.0	-	-
07/0430	06/1800	24.5/59.0	07/0600	25.0/58.5	O/L	-	-	-	-	-
07/0730	07/0000	25.0/58.5	07/1200	O/L	O/L	-	-	-	-	-
Total						1310				1508
Average						94				137
Total No. of observations verified						14				11
O/L : Over Land										

9. Climate Change aspects

For the purpose of analysis, depression and deep depression have been considered as a single category. Similarly severe cyclonic storm, very severe cyclonic storm and super cyclonic storm have been considered as a single category. Hence, the frequencies of cyclonic disturbances have been analyzed in three categories, viz (1) depression/deep depression (D), (2) cyclonic storm (C) and (3) severe cyclonic storm and above (S). The annual and decadal average, coefficient of variation (CV) and linear trend coefficients of the frequencies of above categories of cyclonic disturbances have been calculated and analyzed. Also the annual average and linear trend coefficients of the cyclonic storms cyclonic disturbances have been analyzed. As the average annual frequencies of cyclonic disturbances crossing Oman coast are very less, only the results of decadal frequencies are presented and discussed. The detailed classification of cyclonic disturbances over the north Indian Ocean are given in cyclone manual (IMD, 2003).

9.1 Cyclonic disturbances landfalling over Arabia-Africa:

The monthly frequencies of cyclonic disturbances crossing Arabia-Africa are shown in Table 10.

Table 10. Monthly frequency of cyclonic disturbances crossing Arabia-Africa. (Intensity at the time of landfall)

Months	D	C	S	C+S	D+C+S
January	0	0	0	0	0
February	0	0	0	0	0
March	0	0	0	0	0
April	0	0	0	0	0
May	4	4	3	7	11
June	1	2	1	3	4
July	2	0	0	0	2
August	1	0	0	0	1
September	4	0	0	0	4
October	1	2	2	4	5
November	1	0	0	0	1
December	2	0	0	0	2
Total	16	8	6	14	30

Source: e-Atlas

Only 30 cyclonic disturbances had landfall over Arabia-Africa during 1891-2007. It included 16 depressions, 8 cyclonic storms and 6 severe cyclones (wind speed ≥ 48 kts). Hence the landfalling disturbances are not frequent for Arabia-Africa.

Out of these 30 disturbances, 20 cyclonic disturbances (depression and above) including 13 systems with cyclonic storm and higher intensity crossed Oman coast during 1891-2007 (Table 11). Hence on an average, one cyclonic storm has crossed Oman coast per decade (Table 12) with the coefficient of variation of 83%. It suggests that the land falling cyclonic storm are very rare for Oman coast and they exhibit large interannual and interdecadal variabilities. Due to colder SST, many cyclonic disturbances dissipated over the Arabian Sea before landfall.

Table 11. Cyclonic disturbances crossing Oman coast during 1891-2007
Table 2. Cyclonic disturbances crossing Oman coast during 1891-2007

S.NO.	Intensity at the time of land fall	Point of land fall		Date of land fall		
		Lat	Long.	Date	Month	Year
1	CS	26	58.5	4	5	1898
2	SCS	19.5	57	26	5	1911
3	CS	18	55	27	5	1916
4	CS	18.5	55.5	2	6	1919
5	CS	19.3	54.5	13	10	1921
6	D	20	56	1	10	1929
7	CS	24.8	54.5	26	10	1948
8	CS	17.2	52.7	24	5	1959
9	D	23.5	58	18	7	1959
10	D	19.2	57.8	30	5	1962
11	CS	18.5	56.5	7	12	1963
12	D	20	57.8	2	6	1970
13	D	22	58.5	2	7	1972
14	SCS	20.8	57.8	13	6	1977
15	CS	19	56.5	20	6	1979
16	D	19.6	57	24	9	1979
17	D	21.5	59	10	8	1983
18	CS	20.5	55	3	10	1992
19	CS	17.5	54	10	6	2002
20	VSCS	22.6	59.4	7	6	2007

D : D: Depression/ deep depression, CS: cyclonic storm, SCS: severe cyclonic storm, VSCS: very severe cyclonic storm

Table 12. Mean and coefficient of variability (CV) of decadal frequencies of cyclonic disturbances crossing Oman coast

Cyclonic disturbances	Mean	CV (%)
Depression (D)	0.58	136
Cyclonic storm (C)	0.83	69
Severe cyclonic storm(S)	0.25	181
Total cyclonic storm (C+S)	1.08	83
Total cyclonic disturbances (D+C+S)	1.67	74

9.2 Interannual and Interdecadal variation

The annual and decadal frequencies of different categories of cyclonic disturbances crossing Iran-Arabia-Africa and Oman coast are shown in Fig. 33 and 34 respectively. It is found that there is no significant trend at 1% level in the decadal frequencies of different categories of cyclonic disturbances crossing these coasts during 1891-2007. On the other hand, the decadal frequencies of total cyclonic disturbances show epochal nature with three epochs during 1891-1930, 1941-1980 and 1991-2007. To verify the characteristics changes in track of the disturbances crossing the Arabia- Africa over the years, the tracks of different decades are shown in Fig. 35. It is found that the disturbances crossing Arabia-

Africa mostly developed over southeast or east central Arabian Sea and they moved north-westwards. The frequency of such disturbances was maximum in 1971-80. Further, there is no significant trend over the years.

Inter-annual variation in frequency of cyclonic disturbances crossing Iran-Arabia-Africa

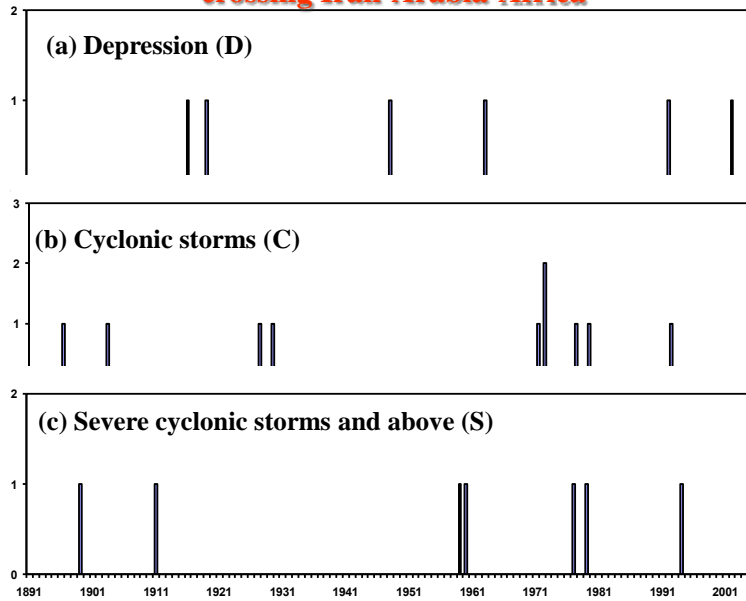


Fig. 33(a). Decadal frequency of cyclonic disturbances crossing Iran-Arabia-Africa.

Inter-annual variation in frequency of cyclonic disturbances crossing Iran-Arabia-Africa

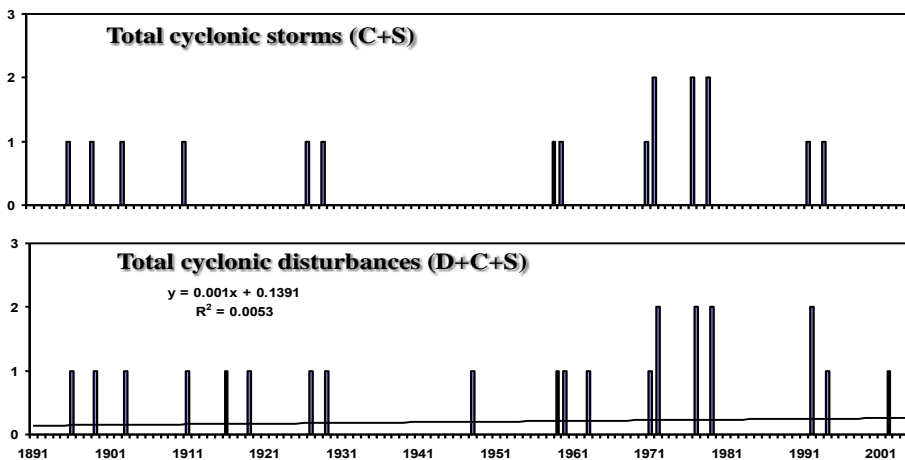
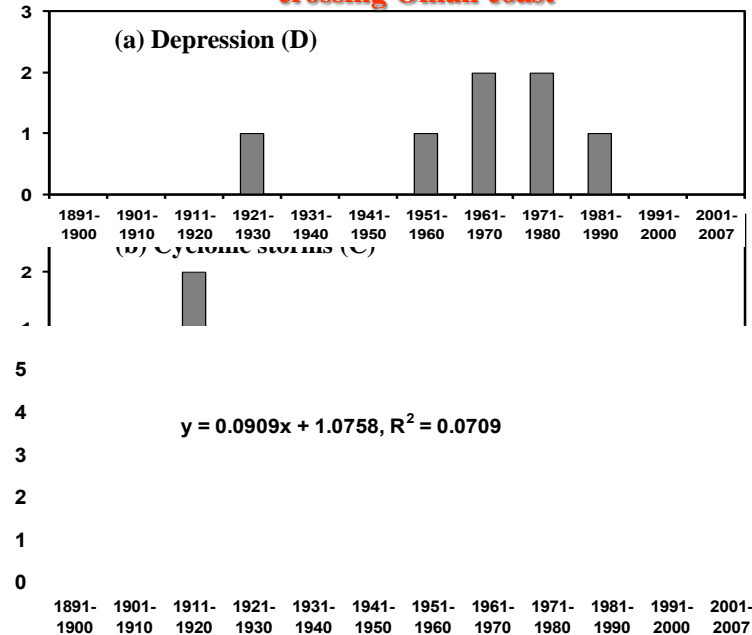
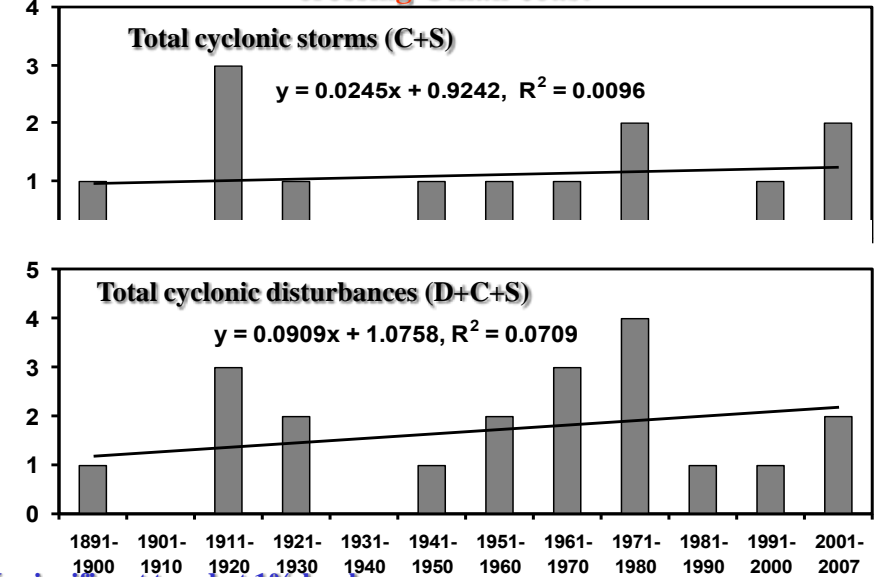


Fig. 33(b). Decadal frequency of cyclonic disturbances crossing Iran-Arabia- Africa.

Inter-decadal variation in frequency of cyclonic disturbances crossing Oman coast



Inter-decadal variation in frequency of cyclonic disturbances crossing Oman coast



No significant trend at 1% level.

Shows epochal nature with three epochs during 1891-1930, 1941-1980 and 1991-2007

Fig. 34. Decadal frequency of cyclonic disturbances crossing Oman coast.

Thus, the study shows that the land falling cyclones for Arabia-Africa coast are random in nature. They do not exhibit any significant long term trend. They may have the epochal nature of variations and the present epoch has set in since 1990's.

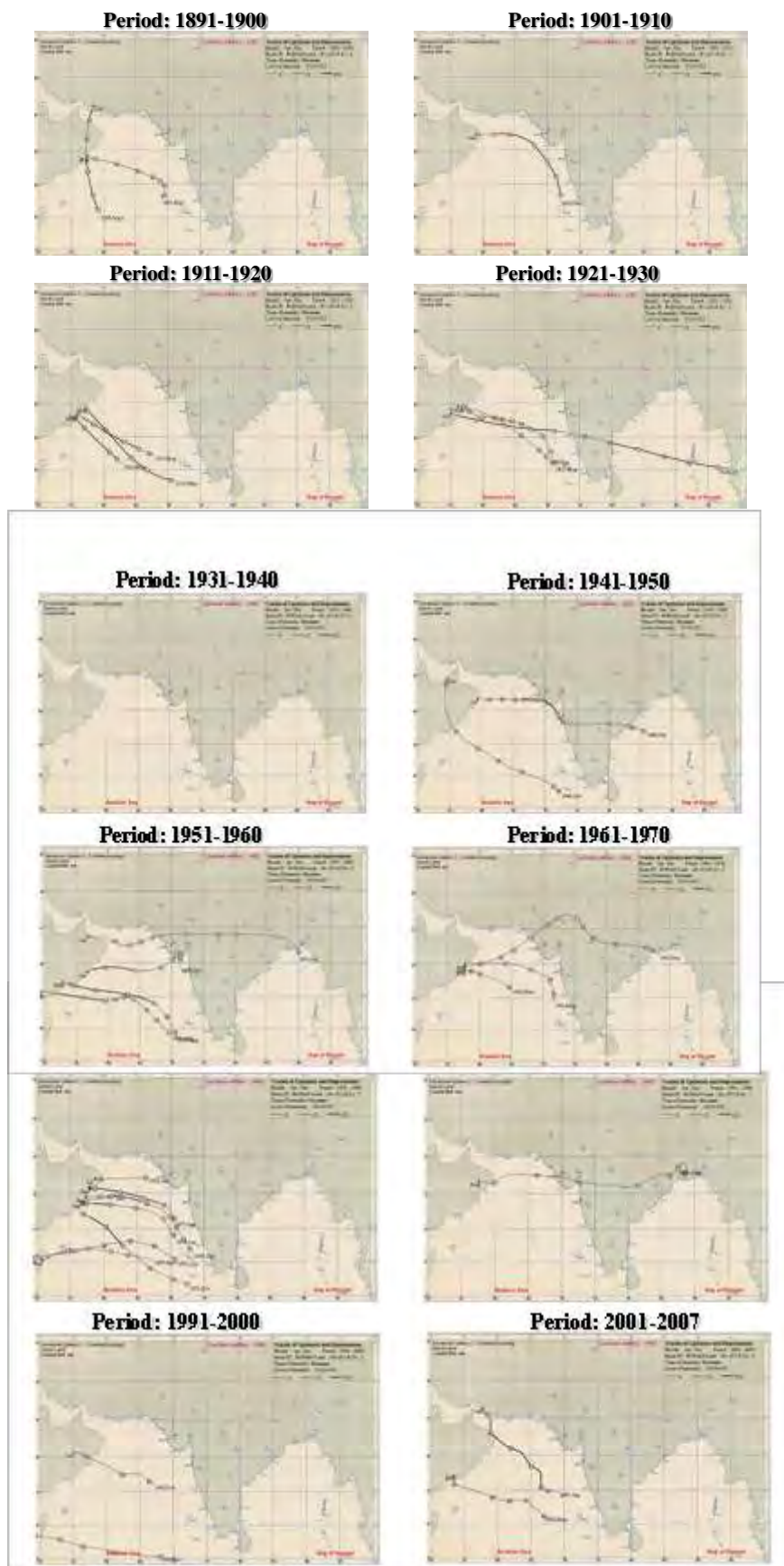


Fig. 35. Decadal track of disturbances crossing Arabia- Africa

9.3 Current Understanding of the Impact of Climate Change on Tropical Cyclone Activity

The climatological conditions under which tropical cyclones occur have been well established over decades of research. These include a requirement for warm sea surface temperatures, low vertical wind shear and high values of large scale relative vorticity in the lower layers of the troposphere (Gray, 1968, 1975; McBride, 1995). It is also well established observationally that over the past several decades the sea surface temperatures over most tropical ocean basins have increased in magnitude by between 0.25 – 0.5 degrees C (e.g., Webster et al. 2005; Santer et al., 2006).

Globally the major factor affecting tropical cyclone frequency and tracks on an interannual (e.g., 2-7 year) time scale is the ENSO phenomenon. This has been shown to affect the genesis regions and the subsequent motion in all tropical cyclone basins (Nicholls, 1979, 1984; Chan, 1985, 2000; Gray and Sheaffer, 1991; Landsea et al., 1999; Irwin and Davis, 1999; Chia and Ropelewski, 2002; Wang and Chan 2002; Chu, 2005;). On the interannual time-scale, there is no established insitu positive relationship between sea surface temperature and tropical cyclone frequency (Nicholls, 1984; Chan and Liu, 2004). The exception to this is the North Atlantic, where it is well established that sea surface temperature is one of the factors impacting on the number and severity of cyclones (Raper 1992, Shapiro and Goldenberg, 1998, Landsea et al., 1998).

Emanuel (2005) has produced evidence for a substantial increase in the power of tropical cyclones (denoted by the integral of the cube of the maximum winds over time) for the West Pacific and Atlantic basins during the last 50 years. This result is supported by the findings of Webster et al (2005) that there has been a substantial global increase (nearly 100%) in the proportion of the most severe tropical cyclones (category 4 and 5 on the Saffir-Simpson scale), for the period from 1975 to 2004, which has been accompanied by a similar decrease in weaker systems. Mann and Emanuel (2006) reported that tropical cyclone counts in the Atlantic closely track low-frequency variations in tropical Atlantic SSTs, including a long-term increase since the late 1800s and early 1900s.

A number of authors attribute the reported increase as being due primarily to data reliability issues, in that the strong tropical cyclones are more accurately monitored in the recent years. Numerous tropical cyclones may have been missed and not counted even in the Atlantic basin, especially prior to 1910 (Landsea et al. , 2004, 2006 and Landsea, 2005). The historical record of tropical cyclone tracks and intensities is a byproduct of real-time operations. Thus its accuracy and completeness changes continuously through the record as a result of the continuous changes and improvements in data density and quality, changes in satellite remote sensing retrieval and dissemination, and changes in training. Current estimates of tropical cyclone intensity are highly dependent on a satellite imagery interpretation technique, known as the Dvorak technique (Velden et al, 2006). Consistent with this, a step-function change in methodologies for determination of satellite intensity around the globe occurred with the introduction of geosynchronous satellites in the mid to late 1970's.

Further changes in methodologies occurred through the 1980's as satellite instrumentation changed and as the technique evolved. Klotzbach (2006) restricted his analysis to the last 20 years when there were consistent satellite imagery and found no significant change in global net tropical cyclone activity and a small trend (~+10%) in category 4 and 5 frequencies. Kamahori et al. (2006) – using the Japan Meteorological Agency (JMA) typhoon database – found that there was a substantial drop in the amount of category 4 and 5 typhoon activity between the periods 1977- 1990 and 1991-2004, which is in contrast to the Webster et al. (2005) study that utilized the Joint Typhoon Warning Center (JTWC) typhoon database. Undoubtedly, this discrepancy relates to JMA vs JTWC satellite treatment of tropical cyclone intensities once aircraft reconnaissance was discontinued there in 1987. Chan (2006) extended the analysis of Webster et al. for the Northwest Pacific basin back to earlier years and argued that the trend in that basin is part of a large inter-decadal variation, similar to what Goldenberg et al. (2001) argue for the Atlantic basin.

In the Atlantic basin, where the most reliable historical hurricane records are believed to exist, the causes of the pronounced multidecadal variability of major hurricane activity in recent decades is currently being debated. Goldenberg et al. (2001) argue that Atlantic major hurricane activity is oscillatory, being modulated (via vertical wind shear and other circulation changes) by a multidecadal mode of SST variability referred to as the Atlantic Multidecadal Oscillation. Mann and Emanuel (2006) dispute this claim, attributing decadal changes in tropical Atlantic sea surface temperature to variations in radioactive forcing caused by varying solar activity, volcanic and manmade aerosols, and greenhouse gases. Expectations about future trends vs cyclical variations of Atlantic hurricane activity would be quite different depending upon the relative importance of these two proposed factors in explaining Atlantic tropical cyclone variations in recent decades. Currently published theory and numerical modelling results are inconsistent with the observational studies of Emanuel (2005) and Webster et al. (2005) by a factor of 5 to 8 (for the Emanuel study).

Concerning future changes in tropical cyclone intensity, there is substantial disagreement among recent global and regional climate modelling studies, although the highest resolution models available show evidence for some increase in intensity (Oouchi et al, 2006; Walsh et al., 2004), in support of both potential intensity theory and idealized hurricane model simulations. A limitation of the climate models used thus far is that the simulated tropical cyclones are substantially weaker than observed—and dramatically so for the lower resolution models—and the models have not demonstrated that they can reproduce the observed increase of attainable tropical cyclone intensities with increasing SST. In cases where this relationship has been examined the dependence is much weaker than observed.

This community of international researchers and tropical cyclone forecasters believe that the public perception on impact of cyclonic change are somewhat hampered by a lack of uniform monitoring and recording practices and correctness of historical data. Issues include different averaging periods for surface wind estimates, non-uniform operational gust factors, and multiple tables

used to estimate maximum wind from satellite. These differences can result in a confusing public message as well as non-uniform historical records that produce significantly different tropical cyclone climatologies (Kamahori et al. 2006).

9.4. Scenario over the north Indian Ocean

The north Indian Ocean (NIO) which accounts for about 5% of total global tropical cyclones (TC) produces about five TC per year. Out of five, four TCs form in the Bay of Bengal (BOB) and one forms in the Arabian Sea (AS). Extensive work has been done on the changes in the frequency and intensity of TCs of North Indian Ocean (Bhaskar Rao et al, 2001). Long term cyclone data over the North Indian Ocean show a significant decreasing trend. However, if we remove cyclone data of monsoon season, no significant trend is found. It is well known that during the monsoon season, cyclone formation does not take place, mainly due to large horizontal shear of the vertical winds. Therefore, it is felt that probably there might have been some bias in assessment of cyclonic disturbances during the monsoon season when better monitoring tools / systems (prior to 1960) were not available. Decrease in frequency of cyclonic disturbances in monsoon season has been compensated by increase in weaker systems like low pressure area (Ajaymohan, 2010).

Utilizing the data set of satellite era it has been shown that the stronger TCs with maximum sustained winds (MSW) exceeding 95 nautical miles per hour (knots) and above have become more frequent in the NIO during past three decades (Singh et al, 2000, 2001). When the frequency of all TCs with MSW exceeding 63 knots is considered, the uptrend reduces.

Krishna Kumar et al (2005) examined the influence of global warming on cyclonic storms by analyzing simulations using HadRM2 model forced by control and increased greenhouse gas (GHG) concentrations. Their analyses indicate slight increase in frequency of storms in Bay of Bengal and significant decrease in Arabian Sea in global warming scenario. The intensity under enhanced greenhouse gas conditions is greater than that of the current climate.

Based on observations, Rajeevan et al (2000) pointed out that in spite of increase in SST over Bay of Bengal, the frequency of storms (depressions and above) during monsoon season have been decreasing at a rate of 1 storm per decade since 1980.

Considering different coastal states of India, about 68% of the disturbances developing over the Bay of Bengal have landfall over east coast and about 30% of the disturbances developing over the Arabian Sea have landfall over west coast. The trends in the frequencies of cyclonic disturbances over east and west coasts of India are shown in Fig.1. There is no significant change in the frequency of different categories of cyclonic disturbances crossing

west coast of India. There is decreasing trend in the frequency of total cyclonic storms landfalling over the east coast of India. It may be due to the fact that the number of low intensity cyclonic storms and depressions has reduced significantly during the monsoon season. However there is no significant change in the frequency of severe cyclonic storms landfalling over the east coast of India.

Considering individual states of India, while the frequency of severe cyclonic storms crossing Andhra Pradesh coast shows significant increasing trend, the frequencies of cyclonic storms crossing Orissa, West Bengal and Gujarat coasts show significant decreasing trends. The quasi-biennial oscillation (QBO) is significantly observed in the frequency of cyclonic storms crossing Orissa coast. The cyclonic storms crossing Andhra Pradesh and Tamil Nadu coasts show significant cycles of 5-6 years similar to ENSO cycle. The severe cyclonic storms crossing Andhra Pradesh coast exhibits QBO and that crossing West Bengal coast shows QBO as well as 4-5 years cycle of oscillation. There is no periodicity in the frequency of disturbances landfalling over other coastal states of India (Tyagi et al, 2010).

10. Conclusions and suggestions

The following broad conclusions are drawn from the analysis of various features of the Super cyclone, **GONU**.

- (i) The super cyclonic storm **GONU** could be mainly detected and tracked by the Satellites due to lack of sufficient buoy observations over the Arabian Sea and absence of DWR along Oman and Iran coast. Hence, the deployment and networking of DWRs, and utilisation of their outputs alongwith satellite imagery and surface and upper air data along Arabian coast and ocean data buoys can improve the monitoring and prediction of cyclones crossing these coasts.
- (ii) According to ADT technique followed by CIMSS, the maximum intensity of the system was estimated to be T 7.0 (140 knots) at around 0900 UTC of 4 June and the same intensity persisted for about 9 hours till 1800 UTC of 4 June, 2007. According to INSAT imageries and manual Dvorak's technique, the maximum intensity was estimated to be T 6.5 at 1500 UTC of 4 June and the same intensity persisted (for about six hours) till 2100 UTC of the same day. The lowest ECP was 912 hPa based on INSAT imageries and manual Dvorak's technique against 894 hPa estimated by CIMSS using ADT. This difference in intensity estimation needs further investigation. Though the inputs from satellite imageries provide the confidence to estimate the intensity of the system, there is a need to suitably modify Dvorak's technique (1984) for the cyclonic storms over the north Indian Ocean.

- (iii) The intensification of the system to super cyclone stage at 1500 UTC of 4 June was associated with significantly higher upward vertical velocity (> 250 units) at 500 hPa level and relative vorticity at 850 hPa level ($.35 \times 10^{-5}$) at 0000 UTC of 4 June 2007 to the north of the system centre. Also the positive vorticity advection was significantly higher (>150 unit) to the north of the system at 0000 UTC of 4 June. Like the above, the moisture flux was significantly higher ($>250 \times 10^{-5}$ gm/cm²/sec) at 0000 UTC of 04 June 2007 to the north of the system centre suggesting maximum intensification of the system on 4 June. However, the PWC could not depict the trend in intensification.
- (iv) The analysis further suggests that the system intensified into super cyclone stage inspite of high vertical wind shear (20-30 knots) between 200 and 850 hPa levels at 0000 UTC of 4 June 2007. Hence the rate of vertical wind shear needs further investigation.
- (v) The warmer SST ($>30^{\circ}\text{C}$) around the system centre on 4 June 2007 (near 18.5° N and 65° E at 0000 UTC of 4 June 2007) might have contributed to the intensification of the system into super cyclone stage. The subsequent fall in SST during 5-7 June contributed to gradually weakening of system even over the sea. The warmer Gulf of Oman ($>30^{\circ}\text{C}$) during 4-7 June 2007 might have contributed to maintain the intensity of the system leading to a landfalling cyclone over Iran.
- (vi) Most of the models including QLM run by IMD, T-80 and MM5 run by NCMRWF, UKMO and ECMWF could not identify and predict the intensification of the cyclone, **GONU**, into super cyclonic storm though they could visualize the cyclonic circulation at lower tropospheric levels with location varying from actual centre of the system. The intensity was under-estimated in all the models.
- (vii) Water vapour derived wind vectors based on METEOSAT-7 satellite could be very helpful to analyse the steering current and hence in predicting the movement of the cyclone in short range.
- (viii) The landfalling cyclones for Arabia-Africa coasts are random in nature. They do not exhibit any significant long term trend. They may have the epochal nature of variations and the present epoch has set in since 1990's.

Acknowledgements

The authors are thankful to Deputy Director General of Meteorology, Satellite Meteorology Division, Director NCMRWF, UKMO/ECMWF for their valuable inputs. We thank Shri Kalu Ram, Shri R.P. Sharma , Shri D.P. Nayak, Sh M.G. Mittal and Mrs.Monica Sharma for designing, type setting and printing this publication. We thank Dr H. R. Hatwar, ADGM (Research), Pune for facilitating publication of this Monograph.

References:

- Ajayamohan, R. S., William J. Merryfield, and Viatcheslav V. Kharin, 2010, Increasing Trend of Synoptic Activity and Its Relationship with Extreme Rain Events over Central India, *Journal of Climate*, 23, 1004-1013
- Arkin, P A 1983 , —Diagnostic precipitation index from IR satellite imagery, *Trop. Ocean-Atoms. News letter*. 17: 5-7.
- Bengtsson, L., K. Hodges, and E. Roeckner, 2006: Storm tracks and climate change. *J. Climate*, 19, 3518-3543.
- Bhaskar Rao, D. V., Naidu, C. V. and Srinivasa Rao, B. R., 2001, Trends and fluctuations of cyclonic systems over north Indian Ocean, *Mausam*, 52, 37-46
- Bhatia R.C. and Singh Devendra and Giri, R.K., 2006, —Use of METEOSAT-5 derived winds for operational weather forecasting”, Eighth International Winds Workshop, Beijing, China, 24-28 April 2006.
- Chan, J. C. L., 2000: Tropical cyclone activity over the western North Pacific associated with El Niño and La Niña events. *J. Climate*, 13, 2960-2972.
- Chan, J.C.L., 1985: Tropical cyclone activity in the Northwest Pacific in relation to the El Nino/Southern Oscillation Phenomenon. *Mon.Wea.Rev.*, 113, 599-606
- Chan, J.C.L., 2006: Comment on —Changes in tropical cyclone number, duration and intensity in a warming environment, *Science*, 311, p1713.
- Chan, J.C.L., and K.S. Liu, 2004: Global Warming and Western North Pacific Typhoon Activity from an Observational Perspective. *J. Clim.*, 17, 4590-4602.
- Chia, H.H., and C.F. Ropelewski, 2002: The interannual variability in the genesis location of Tropical Cyclones in the northwest Pacific. *J.Climate*, 15, 2934-2944.
- Chu., P.S, 2005: ENSO and tropical cyclone activity, in *Hurricanes and Typhoons: Past, Present, and Potential*, edited by R.J. Murnane and K.B. Liu, pp297-332, Columbia University press, New York.
- Dvorak, V. F., 1975: Tropical cyclone intensity analysis and forecasting from satellite imagery. *Mon. Wea. Rev.*, 103, 420-430.
- Dvorak, V.F., 1984, —Topical Cyclone Intensity Analysis Using Satellite Data’, *NOAA Technical Report*, NESDIS 11.
- Emanuel, K., 2005: Increasing destructiveness of tropical cyclones over the past 30 years. *Nature*, 436, 686-688.
- Goldenberg, S. B., C. W. Landsea, A.M. Mesta-Nuñez, and W. M. Gray, 2001: The recent increase in Atlantic hurricane activity: causes and implications. *Science*, 293, 474-479.
- Gray, W. M., 1968, —Global View of the Origin of Tropical Disturbances and Storms” *Mon. Wea. Rev.*, 96, pp-669-700.
- Gray, W.M., 1975: Tropical cyclone genesis. Dept. of Atmospheric Science Paper No. 234, Colorado State University, Fort Collins, CO, 121 pp.
- Gray, W.M., and J.D. Sheaffer, 1991: El Nino and QBO influences on tropical cyclone activity. In *Teleconnections linking worldwide climate anomalies*,

- edited by M.H. Glantz, R.W. Katz, and N. Nicholls, 257-284, Cambridge University Press, New York.
- Holton, J.R., 1979, "An Introduction to Dynamic Meteorology" academic press, 1979
- IMD, 2003, "Cyclone manual," Published by India Meteorological Department.
- IMD, 2008, Cyclone e-Atlas published by India Meteorological department.
- Irwin, R.P., and R.E. Davis, 1999: The relationship between the Southern Oscillation Index and tropical cyclone tracks in the eastern North Pacific. *Geophys. Res. Lett.*, 20, 2251-2254.
- Kalsi, S. R., 1993 INSAT image analysis of Tropical Cyclone development in the Bay of Bengal, in *Advance in Tropical Meteorology* (Eds. Keshvamurty, R. N and Joshi, PC), Tata McGraw Hill, pp. 289-300.
- Kamahori, H., N. Yamazaki, N. Mannoji, and K. Takahashi, 2006: Variability in intense tropical cyclone days in the western North Pacific. *SOLA*, 2, 104-107, doi:10.2151/sola.2006-027.
- Kelkar, R.R., 1997, "Satellite based monitoring and prediction of tropical cyclone intensity and movement", *Mausam*, 48, 157-168
- Klotzbach, P. J., 2006: Trends in global tropical cyclone activity over the past twenty years (1986-2005), *Geophys. Res. Lett.*, 33, L10805, DOI:10.1029/2006GL025881.
- Krishna Kumar K., Hoerling M., Rajagopalan B., Advancing dynamical prediction of Indian monsoon rainfall, *Geophysical Research Letters*, 32, 2005, 1-4
- Krishna Rao, A.V.R.K, 1997, "Tropical Cyclone- synoptic methods of forecasting", *Mausam*, 48, 239-256
- Landsea, C. W., 2005: Hurricanes and global warming. *Nature*, 438, doi:10.1038/nature04477.
- Landsea, C. W., C. Anderson, N. Charles, G. Clark, J. Dunion, J. Fernandez-Partagas, P. Hungerford, C. Neumann, and M. Zimmer, 2004: The Atlantic hurricane database re-analysis project: Documentation for the 1851-1910 alterations and additions to the HURDAT database. In: *Hurricanes and Typhoons: Past, Present and Future*, R. J. Murname and K.-B. Liu, Eds., Columbia University Press, p. 177-221.
- Landsea, C.W., G.D. Bell, W.M. Gray, S.B. Goldenberg, 1998: The extremely active 1995 Atlantic hurricane season: environmental conditions and verification of seasonal forecasts. *Mon. Wea. Rev.*, 126, 1174-1193.
- Landsea, C.W., R.A. Pielke, Jr., A.M. Mestas-Nuñez, and J. A. Knaff, 1999: Atlantic basin hurricanes: Indices of climatic changes. *Climatic Change*, 42, 82-129.
- Landsea, C.W., B.A. Harper, K. Hoarau, and J.A. Knaff, 2006: Can we detect trends in extreme tropical cyclones? *Science*. 313, 452-454.
- Mann, M. and K. Emanuel, 2006: Atlantic hurricane trends linked to climate change. *EOS*, 87, 233-241.
- McBride, J. L., 1995: Tropical Cyclone Formation. Global perspectives on tropical cyclones, WMO/TD-No. 693, 289 pp.
- McBride, J.L. and Gray, W.M., 1979, "Observational analysis of tropical cyclone formation", Colorado state University, Atmos. Sci. Paper No. 308.

- Mohanty, U.C. and Gupta Akhilesh, 1997, —“Deterministic method for prediction of tropical cyclone tracks”, *Mausam*, 48, 257-272
- Mohapatra, M., Gupta, D.S., Chanchalani, N.K., And Dastidar, S.K., 2002, —“Orissa super Cyclone, 1999- a case study”, *J. Ind. Geophys. Union*, 6, 93-106.
- Nicholls, N., 1979: Possible method for predicting seasonal tropical cyclone activity in the Australian region. *Mon. Wea. Rev.*, 107, 1221-1224.
- Nicholls, N., 1984: Southern Oscillation, sea surface temperature, and interannual fluctuations in Australian tropical cyclone activity *J. Climatol.*, 4, 661-670.
- Oouchi, K., J.Yoshimura, H. Yoshimura, R. Mizuta, S. Kusunoki, and A. Noda, 2006: Tropical cyclone climatology in a global-warming climate as simulated in a 20km-mesh global atmospheric model: frequency and wind intensity analysis. *J. Meteorol. Soc. Japan*, , 84, 259-276.
- Prasad, K., 1997, —“Prediction of tropical cyclones by numerical models- a review, 1997”, *Mausam* 48, 225-238
- Rajeevan, M, Medha Khole and De, U. S., 2000, Variability of SST and tropical storms over Indian Ocean in recent decades, Proceedings of TROPMET-2000, National Symposium on Ocean and Atmosphere, pp.234-237.
- Rama Rao Y.V, H.R. Hatwar, Ahmed Kamal Salah, Y. Sudhakar, 2007 —“An experiment using the high resolution ETA & WRF models to forecast heavy precipitation over India” *Pageoh*, 164, 1593-1615.
- Rao, A.V. R.K., Kelkar, R.R., and Arkin, P.A., 1989, —“Estimation of precipitation and outgoing long wave radiation from INSAT-1B radiance data”, *Mausam*, 40, pp. 123-150.
- Raper, S., 1992: Observational data on the relationships between climatic change and the frequency and magnitude of severe tropical storms. In *Climate and Sea Level Change: Observations, projections and implications*, R.A. Warwick, E.M. Barrow, and T.M. L. Wigley (Eds) Cambridge University Press, 192-212.
- RSMC- Tropical Cyclones, New Delhi, 2007, ” A report on cyclonic disturbances over north Indian ocean during 2006”.
- Santer, B.D., T. M. L. Wigley, P. J. Gleckler, C. Bonfils, M. F. Wehner, K. AchutaRao, T. P. Barnett, J. S. Boyle, W. Brüggemann, M. Fiorino, N. Gillett, J. E. Hansen, P. D. Jones, S. A. Klein, G. A. Meehl, S. C. B. Raper, R. W. Reynolds, K. E. Taylor, and W. M. Washington, 2006: Forced and unforced ocean temperature changes in Atlantic and Pacific tropical cyclogenesis regions. *Proc. National Academ. Science*, 103, 13905-13910.
- Shapiro, L.J., and S.B. Goldenberg, 1998: Atlantic sea surface temperatures and tropical cyclone formation. *J. Atmos., Sci.*, 11, 578-590.
- Singh, O. P. , T. M. Ali Khan and Md. S. Rahman, 2000, Changes in the frequency of tropical cyclones over the North Indian Ocean, *Meteorology and Atmospheric Physics*, 75, 11-20

- Singh, O. P. , T. M. Ali Khan and Md. S. Rahman, 2001, Has the frequency of intense tropical cyclones increased in the north Indian Ocean?, *Current Science*, 80, 575-580.
- Tyagi, Ajit, Mohapatra, M., Bandyopadhyay, B. K. and Baresh Kumar, 2010, Interannual variation of frequency of cyclonic disturbances landfalling over WMO/ESCAP Panel member countries, Published in 1st WMO international conference on tropical cyclones and climate change, Muscat, Sultanate of Oman, 8-11 March 2009, Ed. Salim Al-Hatrushi and Yassine Charabi, WMO/TD-No. 1541, pp. 1-7.
- Velden, C., B. Harper, F. Wells, J. L. Beven II, R. Zehr, T. Olander, M. Mayfield, C. Guard, M. Lander, R. Edson, L. Avila, A. Burton, M. Turk, A. Kikuchi, A. Christian, P. Caroff, and P. McCrone, 2006: The Dvorak Tropical Cyclone Intensity Estimation Technique: A Satellite-Based Method that Has Endured for over 30 Years. *Bull. Amer. Meteor. Soc.*, 87, 1195-1210.
- Velden, C.S., C.M. Hayden, S. Nieman, W.P. Menzel, S. Wanzong, and J. Goerss, 1997, —Upper-tropospheric winds derived from geostationary satellite water vapor observations”, *Bull. Amer. Meteor. Soc.*, 78, 73-195.
- Velden, C.S., Hayden, C. M., W.P., Franklin, J.L. and Lynch, J.S., 1992, —The impact of satellite-derived winds on numerical hurricane track forecasting, *Weather. and Forecasting*, 7, pp. 107-118.
- Walsh, K. J. E., K.-C. Nguyen, and J. L. McGregor, 2004: Fine-resolution regional climate model simulations of the impact of climate change on tropical cyclones near Australia. *Clim. Dyn.*, 22, 47-56, DOI: 10.1007/s00382-003-0362-0
- Wang, B. and J. C. L. Chan, 2002: How ENSO regulates tropical storm activity over the western North Pacific. *J. Climate*, 15, 1643-1658.
- Weatherford, C.L., and Gray, W.M., 1988, —Typhoon structure as revealed by aircraft reconnaissance, Part I: Data analysis and climatology, Part II: Structural variability.” *Mon. Wea Rev.*, 116, 1032-1043, 1044-1056.
- Weatherford, C.L., and Gray, W.M., 1988, —Typhoon structure as revealed by aircraft reconnaissance, Part 2: Data analysis and climatology,” *Mon. Wea Rev.*, 116, 1032-1043.
- Webster, P.J., G.J. Holland, J.A. Curry, and H-R. Chang, 2005: Changes in tropical cyclone number, duration and intensity in a warming environment. *Science*, 309, 1844-1846.